Máster
Gestión Forestal basada en Ciencia de Datos/
Forest Management based on Data Science
(DATAFOREST)

Fire severity analysis in Sierra de La Culebra wildfire from hyperspectral satellite data

Student: José Alberto Cipra Rodriguez

Advisors: María del Carmen Quintano Pastor

José Manuel Fernández-Guisuraga

06/2025

INDEX

RESUMEN

La evaluación de las perturbaciones post-incendio en los ecosistemas mediterráneos es esencial para cuantificar el impacto ecológico y guiar la restauración. Este estudio estima la severidad del incendio en la Sierra de la Culebra usando índices de vegetación (VIs) derivados de imágenes de satélite hiperespectrales (PRISMA) y multiespectrales (Sentinel-2). Se calculó una serie de índices de vegetación: índices de banda ancha adaptados a PRISMA, índices específicos de banda estrecha e índices multiespectrales estándar para Sentinel-2. Se identificaron los VIs de mejor desempeño analizando su eficacia en diferentes tipos de ecosistemas (bosque de coníferas, bosque de frondosas y matorral) y tipos del Índice Compuesto de Quemado (CBI; vegetación, suelo y lugar). La elaboración de los mapas se realizó según el tipo de sensor, ecosistema y CBI. Los datos hiperespectrales proporcionaron una caracterización detallada y continua de las propiedades espectrales relacionadas con las clases de severidad de incendio en todos los tipos de ecosistemas en comparación con los datos multiespectrales, mostrando correlaciones más fuertes con los valores de CBI. El CBI de la vegetación mostró mejores correlaciones con los VIs que el CBI del suelo, probablemente debido al diseño enfocado en la vegetación de la mayoría de los VIs. Los ecosistemas de bosque latifoliado y matorral mostraron valores de correlación más altos que los de bosque de coníferas, probablemente debido a las diferencias en la densidad del bosque y la estructura de los fustes, así como a la biomasa remanente y las condiciones del suelo tras un incendio. Entre los índices con mejores desempeños, los basados en las bandas borde rojo, NIR y SWIR fueron los que obtuvieron mejores resultados. En cuanto a los datos hiperespectrales, el índice de vegetación diferencial de borde rojo (DVIRED), el índice de vegetación mejorado (EVI) y el índice de absorción de celulosa (CAI) mostraron su utilidad para evaluar la salud de la vegetación. En cuanto a los datos multiespectrales, la diferencia normalizada del borde rojo (NDRE), el índice de clorofila del borde rojo (CIREDGE), el índice de vegetación de diferencia normalizada mejorada (ENDVI) y el índice de vegetación de diferencia normalizada verde (GNDVI) mostraron un gran rendimiento. En particular, el CAI fue el índice hiperespectral más eficaz, alcanzando la correlación más alta en este estudio (R2 = 0,808). Esta investigación demuestra el importante potencial de las imágenes hiperespectrales para la evaluación detallada post-incendio en los ecosistemas mediterráneos.

PALABRAS CLAVES: Sensores remotos, Impacto ecológico post-incendio, PRISMA, índices hiperespectrales, CBI.

ABSTRACT

Assessing the post-fire disturbance in Mediterranean ecosystems is essential for quantifying ecological impact and guiding restoration. This study estimates the fire severity in the Sierra de la Culebra wildfire using vegetation indices (VIs) derived from hyperspectral (PRISMA) and multispectral (Sentinel-2) satellite imagery. A range of VIs was computed: broadband-based indices adapted for PRISMA, narrowband-specific indices, and standard multispectral indices for Sentinel-2. The best-performing VIs were identified by analyzing their efficacy across different ecosystem types (coniferous forest, broadleaf forest, and shrubland) and Composite Burn Index (CBI) types (vegetation, soil, and site). Mapping was conducted by sensor, ecosystem, and CBI type. Hyperspectral data provided a detailed and continuous characterization of the spectral properties related to fire severity classes across ecosystem types compared to multispectral data, showing stronger correlations with CBI values. Vegetation CBI exhibited better correlations with VIs than soil CBI, likely due to the vegetation-focused design of most VIs. Broadleaf forest and shrubland ecosystems showed higher correlation values than coniferous forest probably owing to differences in forest density and stem structure, and the subsequent remaining biomass and soil conditions after a fire. Among the best-performing indices, those based on red edge, NIR, and SWIR bands performed best. For hyperspectral data, the red edge difference vegetation index (DVIRED), the enhanced vegetation index (EVI), and the cellulose absorption index (CAI) exhibited their usefulness for assessing vegetation health. For multispectral data, the normalized difference red edge (NDRE), the red edge chlorophyll index (CIREDGE), the enhanced normalized difference vegetation index (ENDVI), and the green normalized difference vegetation index (GNDVI) showed strong performance. Notably, CAI was the most effective hyperspectral index, achieving the highest correlation in this study (R^2 = 0.808). This research demonstrates the significant potential of hyperspectral imagery for detailed post-fire assessment across Mediterranean ecosystems.

KEYWORDS: Remote sensing, post-fire ecological impact, PRISMA, hyperspectral indices, CBI.

1. INTRODUCTION

Forest fires are the greatest disturbance in Mediterranean ecosystems worldwide, and even more so in the Mediterranean basin, where large areas have been burned in recent decades due to abrupt changes in fire regimes caused by climate change (Oliveira et al., 2012; M. M. Boer et al., 2017; Gonçalves & Sousa, 2017). Fires play an essential role in shaping the species composition, structure, and dynamics of Mediterranean plant communities (Tessler et al., 2016; Fernández-Guisuraga et al., 2019). Furthermore, fires cause physical, chemical, and biological changes in forest soils (Evangelides & Nobajas, 2020).

In the study of post-fire environments, the terms fire severity and burn severity are frequently used interchangeably, yet they enclose distinct concepts (M. Boer et al., 2008; Keeley, 2009). Fire severity refers to the immediate extent of environmental alteration induce by a fire event, encompassing changes to both biotic and abiotic components of the ecosystem (Lentile et al., 2006; Veraverbeke et al., 2010; Morgan et al., 2014). Unlike, burn severity integrates the magnitude of fire-induced environmental change with the subsequent trajectory of vegetation recovery. Both fire and burn severity collectively describe the impacts of fire on vegetation and soil properties, influencing ecosystem structure and function (Key & Benson, 2006; Parsons et al., 2010; Morgan et al., 2014).

Assessing fire severity is critical for quantifying losses in above- and below-ground biomass (Keeley, 2009), evaluating the ecological and socioeconomic impacts of wildfires, and informing evidence-based decision-making in land management (Fernández-Manso & Quintano, 2020). Fire severity is defined as the magnitude of ecological change in a burned area relative to the pre-fire scenario and is measured qualitatively as the effects of the fire on vegetation and soil (Key & Benson, 2006; Lentile et al., 2009). It is evaluated in the field by analyzing vegetation and soil and integrating indices such as the Composite Burn Index (CBI) (Key & Benson, 2006). It is calculated by assessing across five structural strata: substrates – ranging from inert materials to soil, organic waste, and harvested fuelwood; grasses – herbaceous, low shrubs, and low trees layer of height less than 1 m; shrubs and trees – tall shrub and sapling layer between 1 and 5 m height; intermediate trees – trees with a diameter between 10 and 25 cm, and heights between 5 and 20 m; large trees – dominant trees with crowns receiving direct sunlight with height above 20 m (De Santis & Chuvieco, 2007; De Bonis & Laneve, 2013). In the substrate layer, metrics include fine fuel consumption and charcoal characteristics. For the herbaceous, shrub, and lower tree layers (<5 m), the percentage of foliage consumed is visually estimated. In taller vegetation layers (≥5 m), foliar coloration (green, brown, black) and charcoal deposition depth on tree trunks are recorded. To ensure consistency, each plot assessment is performed by at least two observers, and only scores reached by consensus are recorded (De Santis & Chuvieco, 2007; Quintano et al., 2023). The final CBI score per plot, referred to as site CBI, is calculated as the mean of scores across all assessed strata. Additionally, vegetation CBI derives by averaging scores across vegetation strata only (excluding substrate), and soil CBI is calculated using only the substrate stratum scores. Furthermore, fire severity data are categorized according to the following CBI thresholds: low (CBI < 1.25), moderate (1.25 ≤ CBI ≤ 2.25), and high (CBI > 2.25) (Miller & Thode, 2007; Quintano et al., 2023).

Remote sensing has become a valuable data source for ecological assessment, as it overcomes limitations associated with traditional field-based methods, such as, error-prone, incomplete, limited, and spatially or temporally inconsistent due to irregular data collection, reducing uncertainty in analyses (Chuvieco et al., 2019). In particular, remote sensing is highly effective for assessing fire severity across large burned landscapes, owing to its favorable cost-benefit ratio and synoptic capabilities (Yin et al., 2020).

The multispectral data provided by Sentinel-2 are commonly used in quantitative fire severity assessments (Quintano et al., 2023). It improves the efficiency, speed, and feasibility of identifying and monitoring regions at risk of wildfires (Atun et al., 2020). Satellite images are also used to determine fire severity over large areas, which are validated by the CBI (Holden et al., 2009).

Hyperspectral remote sensing provides hundreds of contiguous, narrow spectral bands with bandwidths of 5 nm to 15 nm (Goetz, 2009; Transon et al., 2018). The availability of these data has great potential to provide fire severity estimates that align with post-fire management needs. These benefits include reduced logistics costs and the elimination of suboptimal sensitivity broadband data (Quintano et al., 2023). Additionally, it enables precise within-pixel fractional cover estimates for various ground cover classes, including charcoal, which serve as key indicators of fire severity (Veraverbeke et al., 2014; Lewis et al., 2017). Vegetation index (VI) calculations from remotely sensed data are critical for post-fire recovery assessments, assisting with spatio-temporal analysis and mapping fire severity (Chrysafis et al., 2019). VI can highlight the subtleties and characteristics of a feature class or a specific feature and can indicate crop development, vegetation and non-vegetation, soil, and other related information (Chen et al., 2024). This can be a linear or nonlinear combination of two or more spectral bands (Wang et al., 2024).

Traditional multispectral VIs are limited to the characteristic red, near-infrared, and mid-infrared bands. These VIs have the disadvantages of a small number of bands, large bandwidths, and restricted wavelength positions, which cannot accurately reflect biomass characteristics (Wang et al., 2024). Hyperspectral remote sensing, on the other hand, has high spectral resolution and spectral information in hundreds of bands (Wang et al., 2024).

Therefore, this study seeks to estimate wildfire severity in arboreal and non-arboreal ecosystems in the Sierra de La Culebra using PRISMA hyperspectral indices. The three CBI types were evaluated in the field: vegetation, soil, and site, to identify the performance of the hyperspectral indices in predicting fire severity at these levels. In addition, multispectral indices were calculated from a Sentinel-2 satellite image for comparison with the hyperspectral indices.

2. OBJECTIVE

The objective of this study is to estimate the fire severity in the Sierra de La Culebra following the 2022 wildfire by obtaining a set of vegetation indices (VIs) from PRISMA hyperspectral imagery and correlating these with the Composite Burn Index (CBI) at vegetation, soil, and site levels. Additionally, the study aims to validate these hyperspectral indices by comparing them with multispectral indices derived from Sentinel-2 imagery. Furthermore, fire severity will be extrapolated across the entire study area at vegetation, soil, and site levels and visualized through mapping.

3. METHODS

3.1. STUDY AREA

The Sierra de La Culebra wildfire, located in Zamora, Castilla y León, Spain, was the second largest and most destructive fire recorded in the country (Figure 1). This event occurred between June 15th and 19th, 2022, affecting a total area of 28 046 ha (Quintano et al., 2023).

The region exhibits diverse topography, characterize by steep slopes and broad valleys, with altitudes ranging from 747 to 1205 meters above sea level. The climate is classified as Mediterranean, with an average annual temperature of 11°C and an average rainfall of 750 mm (Ninyerola et al., 2005).

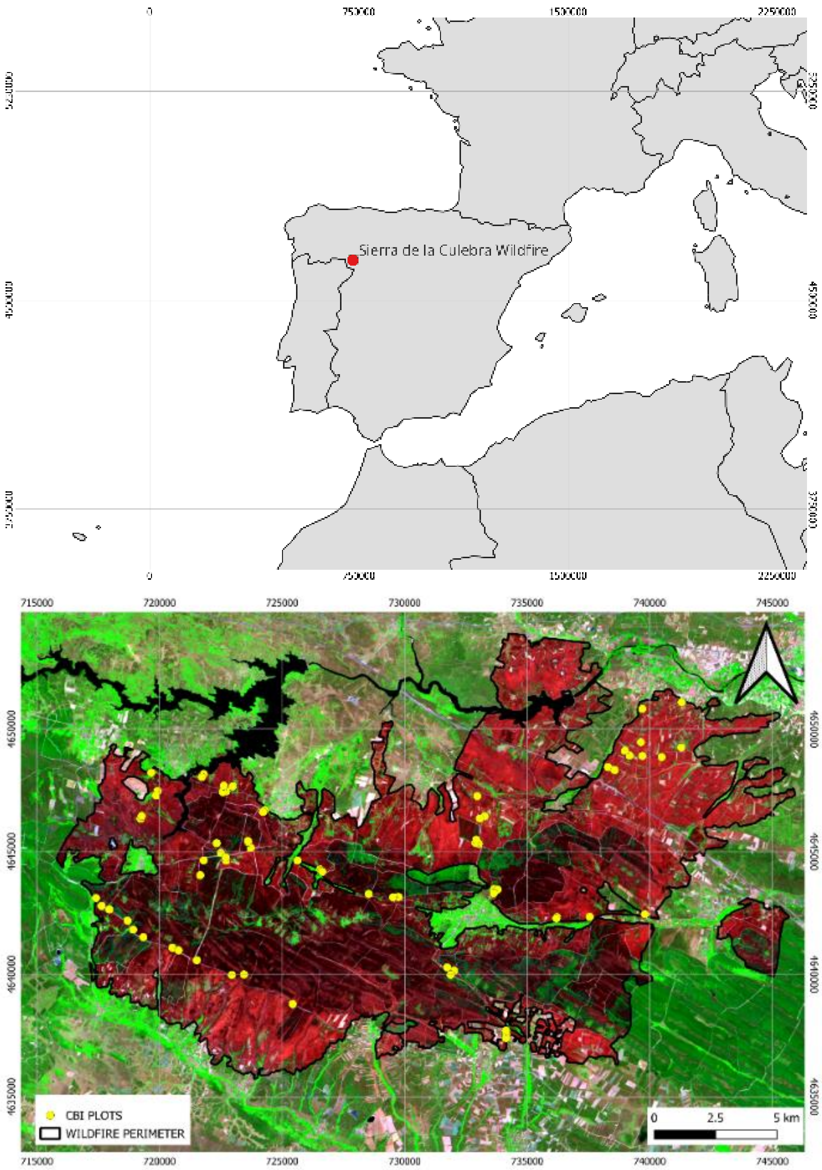

Figure 1. Location map of Sierra de la Culebra wildfire (top) and field plot distribution over a Sentinel-2 false color composite - R: band 12; G: band 8A; B: band 4 (image below).

Based on the vegetation present before the fire, three main ecosystem groups were identified (Figure 2): coniferous forests, dominated by species such as *Pinus sylvestris* L. (Scots pine) and *Pinus pinaster* Ait. (Maritime pine); broadleaf forests, composed of *Quercus ilex* L. (Holm oak) and *Quercus pyrenaica* Willd. (European oak); and shrublands dominated by *Cistus ladanifer* L., *Pterospartum tridentatum* (L.) Willk., *Erica australis* L. and *Halimium lasianthum* subsp. Alyssoides (Lam.) Greuter, as well as Mediterranean grasslands (Quintano et al., 2023).

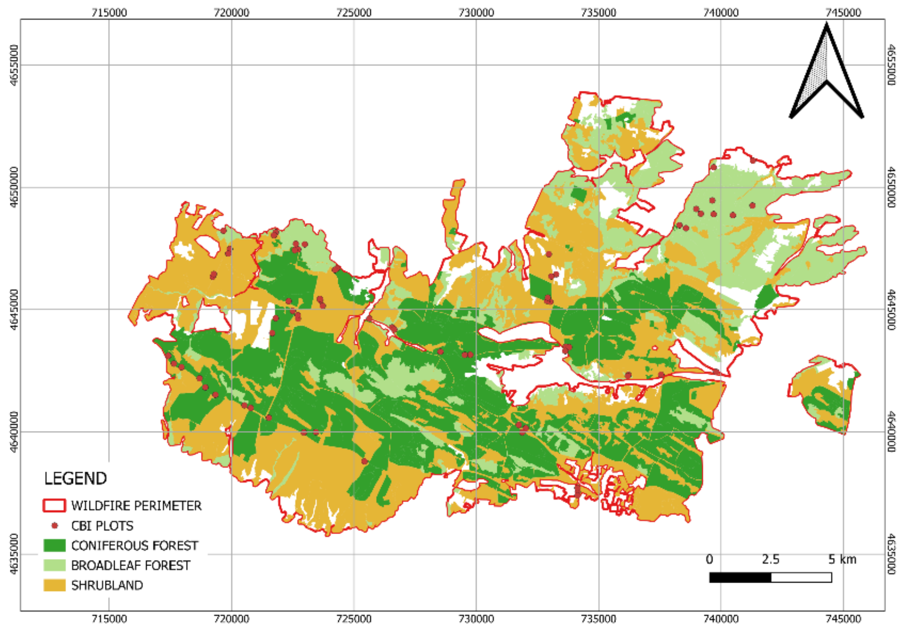

Figure 2. *Map of forestry classification in the Sierra de la Culebra wildfire area.*

Source: Adapted from (Ministerio para la Transición Ecológica y el Reto Demográfico, 2025).

3.2. COMPOSITE BURN INDEX (CBI)

The Composite Burn Index (CBI) is a standardized field measure of fire severity widely used to validate satellite-derived remote sensing products (Holden et al., 2009). It is calculated through visual assessment of post-fire changes across four vegetation and soil strata, providing a general overview of fire damage (Fernández-García et al., 2018). In this study, post-fire attributes, such as changes in species composition or new additions to the soil, were not considered.

A total of 70 field plots, each measuring 30 m × 30 m, were surveyed approximately one month after the wildfire event (Figure 1). Plots were selected using a random stratified sampling design, where strata were defined by the dominant vegetation types, excluding Mediterranean grasslands (Quintano et al., 2023). The distribution of plots by ecosystem category was as follows: 34 plots in coniferous forests, 20 in broadleaved forests, and 16 in shrublands.

Three CBI types were used: vegetation CBI was derived by averaging scores across vegetation strata only (excluding substrate), and soil CBI was calculated using only the substrate stratum scores. Site CBI was also calculated as the mean of both prior CBIs (see Annex A1.1). Fire severity categorization was according to the following CBI thresholds: low (CBI < 1.25), moderate (1.25 <= CBI <= 2.25), and high (CBI > 2.25) (Miller & Thode, 2007).

Severity classes corresponded to distinct post-fire structural patterns: low severity refers to a partial foliage consumption in shrubs and the tree canopy remained almost intact, in other words, minimal canopy damage; moderate severity means substantial understory consumption with incomplete foliage loss in the canopy; and high severity refers to near-total consumption of both understory and overstory foliage (Fernández-Guisuraga et al., 2023).

3.3. HYPERSPECTRAL AND MULTISPECTRAL SATELLITE IMAGERY

To assess post-fire vegetation severity in the Sierra de la Culebra, two types of satellite imagery were employed: hyperspectral and multispectral.

The hyperspectral imagery was acquired from the PRecursore IperSpettrale della Missione Applicativa (PRISMA) mission, developed by the Italian Space Agency (ASI), and downloaded from its platform on July 13th, 2023. PRISMA, launched in March 2019, provides hyperspectral satellite data in a spectral range of 400 to 2500 nm, with a spatial resolution of 30 m, and swath width of 30 km, enabling detailed spectral discrimination of vegetation characteristics. These features make PRISMA a valuable tool for fire severity assessment, particularly due to its sensitivity to post-disturbance spectral changes in vegetation and soil (Amici & Piscini, 2021).

The multispectral imagery was obtained from the Sentinel-2 satellite (level 2A product) on July 15th, 2022, shortly after the fire event. Sentinel-2, belonging to the European Space Agency (ESA) under Copernicus Programme, is equipped with a multispectral sensor that offers 13 bands with spatial resolutions of 10 m, 20 m, and 60 m. These bands span visible (VIS), red-edge, near-infrared (VNIR), and shortwave infrared (SWIR) regions, allowing an assessment of the effects of the fire (Quintano et al., 2023).

3.4. IMAGE PROCESSING

The processing of the hyperspectral and multispectral images was carried out using *Python* in *Visual Studio Code* (see Annexes A5.1 & A5.2). Image handling and computation were carried out with specialized libraries such as *rasterio*, *numpy*, and *pandas* (Gorelick et al., 2017).

3.4.1. QUALITY-BASED BAND EXCLUSION AND COREGISTRATION

To enhance data quality, hyperspectral bands exhibiting low signal-to-noise ratios and sensor artifacts were excluded from the analysis. These bands were identified through visual inspection, following recommendations from prior studies (Tane et al., 2018; Amici & Piscini, 2021). In particular, bands in the 400–434 nm, 1345–1459 nm, 1774–1975 nm, 2010–2035 nm, and 2469–2505 nm regions were discarded (Quintano et al., 2023). To facilitate index calculation and enable comparison with multispectral data, selected hyperspectral bands were aggregated and renamed according to standard wavelength regions: blue (400-500 nm), green (500-600 nm), red (600-700 nm), red edge (700-750 nm), near-infrared (NIR; 750-1050 nm), and shortwave infrared (SWIR; 1050-2500 nm). As a result, the number of hyperspectral bands was reduced from 233 to 191, and these bands were relabeled with both hyperspectral and multispectral names for the vegetation index (VI) computation (see Annex A2.1). Otherwise, Sentinel-2 multispectral imagery bands used in this study included blue (B2), green (B3), red (B4), red edge (B5, B6, & B7), near-infrared (B8, & B8A), shortwave infrared 1 (B11), and shortwave infrared 2 (B12). All other bands were excluded (see Annex A2.2).

In addition, to ensure precise spatial alignment between the PRISMA hyperspectral image and the Sentinel-2 multispectral image, a co-registration process was conducted. This step was essential to allow pixel-by-pixel comparison and accurate VI computation. Ground control points were manually selected and used to geometrically align the images (Gorelick et al., 2017).

3.4.2. VEGETATION INDICES COMPUTATION

Vegetation indices (VIs) were calculated from both hyperspectral and multispectral imagery to quantify post-fire vegetation and soil changes across the study area. A total of 140 spectral indices were computed, 40 multispectral and 100 purely hyperspectral, enabling a comprehensive evaluation of fire severity responses (see Annex A3.1).

Classical broadband indices, such as the Normalized Difference Vegetation Index (NDVI) and the Normalized Burn Ratio (NBR), were calculated using both Sentinel-2 and PRISMA data. These indices are based on reflectance from broad spectral regions and are commonly used for large-scale vegetation monitoring and burn severity assessments.

In contrast, hyperspectral indices, including the Leaf Chlorophyll Index (LCI), Normalized Difference Nitrogen Index (NDNI), and Cellulose Absorption Index (CAI), rely on narrow spectral bands that are available only in hyperspectral datasets. Notably, the computation of these indices involved testing permutations of the VI formula, incorporating two bands immediately below and above the target band for each index. These indices are specifically designed to detect subtle physiological or structural changes in vegetation, such as chlorophyll degradation, nitrogen content variation, or cellulose loss, often linked to fire damage (Clark et al., 2005).

For clarity throughout this study, hyperspectral indices refer to indices calculated exclusively from PRISMA hyperspectral data, regardless of whether their original formulation was for hyperspectral or multispectral use. Multispectral indices refer to indices derived from Sentinel-2 multispectral data. Hyperspectral indices are generally more sensitive than multispectral ones in detecting fine-scale spectral variations, particularly in transition zones between burn severity classes. This increased sensitivity is attributed to the availability of narrow, contiguous bands, which allow for more precise detection of biochemical changes in vegetation and soil properties following fire (Clark et al., 2005).

3.5. STATISTICAL ANALYSIS

All statistical analyses were conducted in R version 4.4.2 (R Development Core Team, 2019; see Annex A5.3). Simple linear regression models were employed to analyze each VI as the independent variable, with CBI values as the dependent variable. This approach allowed for the identification of VIs most strongly associated with fire severity. Prior to VI analysis, raw hyperspectral and multispectral bands were correlated with CBI to identify bands likely to contribute to highly correlated VIs. Two primary performance metrics were used to evaluate model accuracy. The coefficient of determination (R^2) was used to measure the proportion of variability in the CBI data explained by each VI. Values approaching 1 indicate strong explanatory power and high predictive performance. The Pearson correlation coefficient (r) evaluated the strength and direction of the linear relationship between VI and CBI. Additionally, the root mean square error (RMSE) was used to quantify the dispersion of observed values relative to those predicted by the model. Lower RMSE values indicate better model fit and reduced deviation between predicted and actual data (Qiao et al., 2022).

3.6. MAPPING FIRE SEVERITY USING CBI ANALYSIS

Fire severity across the study area was assessed using both PRISMA hyperspectral and Sentinel-2 multispectral imagery by calculating VI tailored to the three ecosystem types (coniferous forest, broadleaf forest, and shrubland). For each ecosystem, the VI with the highest R^2 to CBI type value was selected, based on the prior regression analyses. CBI values were categorized into three severity levels: low (CBI < 1.25), moderate ($1.25 \leq$ CBI ≤ 2.25), and high (CBI > 2.25), following established thresholds. These CBI-VI relationship were then extrapolated to the entire study area by applying the selected VIs to the corresponding spectral imagery, mapping fire severity spatially.

4. RESULTS

4.1. SPECTRAL SIGNATURES

Figure 2 presents the spectral characteristics derived from PRISMA and Sentinel-2 data for three ecosystem types in the Sierra la Culebra wildfire. The spectral signatures are categorized by sensor type and ecosystem type, with mean fire severity classes depicted as colored lines (low severity: green; moderate severity: brown; high severity: red) and the overall mean spectral signature shown as a black line.

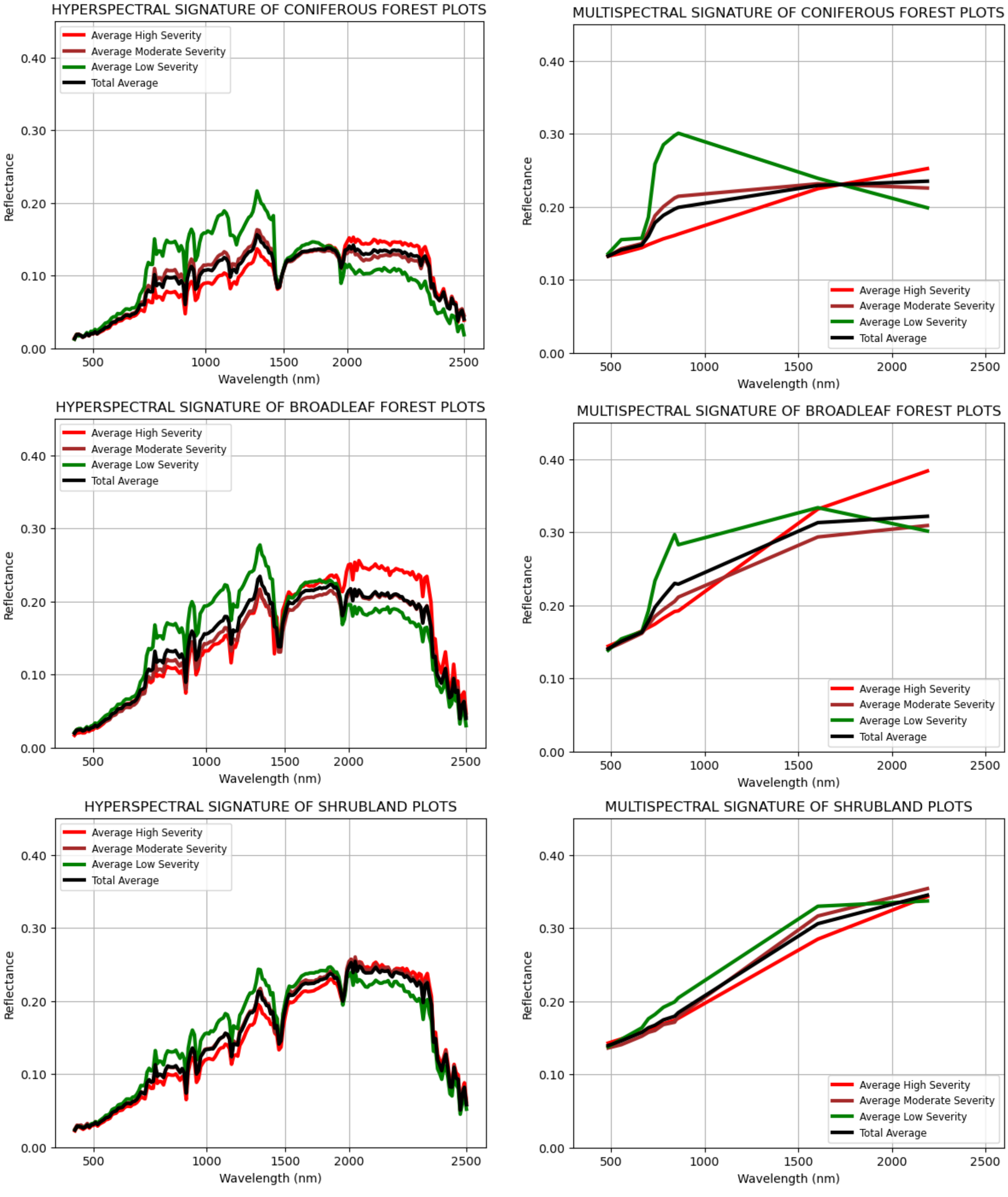

Figure 2. Spectral characteristics of study plots of burned vegetation by ecosystem types derived from PRISMA and Sentinel-2 imagery in the Sierra La Culebra wildfire.

4.2. BEST-PERFORMING SPECTRAL INDICES

A comprehensive set of vegetation indices (VIs) was calculated, comprising 100 purely hyperspectral indices from PRISMA imagery and 40 multispectral indices derived from PRISMA and Sentinel-2 imagery. To determine the optimal index for each sensor, CBI, and ecosystem types, the coefficient of determination (R^2) was employed as the primary evaluation metric. Additionally, the Pearson correlation coefficient (r) was utilized to assess the strength and direction of linear relationships, while the root mean squared error (RMSE) was used to evaluate prediction error and data variability (Figures 3 & 4). All hyperspectral and multispectral indices computed showed diverse fitting (see Annexes A4.1 & A4.2). The best-performing hyperspectral and multispectral indices are exhibited in Table 1 showed varying correlations depending on the CBI type and ecosystem type analyzed. This highlights the importance of selecting indices specific to each ecological context and analysis objective.

Table 1. *Best-performing spectral indices correlated with CBI class and ecosystem type.*

Ecosystem		vegetation CBI		soil CBI		site CBI	
		VI	R^2	VI	R^2	VI	R^2
HYPERSPECTRAL	Coniferous forest	$\mathrm{DVIRED}_{[\rho_{729(VIS)}, \rho_{802(NIR)}]}$	0.739	$\mathrm{EVI}_{[\rho_{485(VIS)}, \rho_{614(VIS)}, \rho_{877(NIR)}]}$	0.443	$\mathrm{EVI}_{[\rho_{485(VIS)}, \rho_{699(VIS)}, \rho_{877(NIR)}]}$	0.611
	Broadleaf forest	$\mathrm{CAI}_{[\rho_{1976(SWIR)}, \rho_{2199(SWIR)}, \rho_{2103(SWIR)}]}$	0.752	$\mathrm{CAI}_{[\rho_{2036(SWIR)}, \rho_{2199(SWIR)}, \rho_{2103(SWIR)}]}$	0.705	$\mathrm{CAI}_{[\rho_{2036(SWIR)}, \rho_{2199(SWIR)}, \rho_{2103(SWIR)}]}$	0.766
	Shrubland	$\mathrm{CAI}_{[\rho_{1993(SWIR)}, \rho_{2199(SWIR)}, \rho_{2086(SWIR)}]}$	0.798	$\mathrm{CAI}_{[\rho_{1993(SWIR)}, \rho_{2199(SWIR)}, \rho_{2086(SWIR)}]}$	0.770	$\mathrm{CAI}_{[\rho_{1993(SWIR)}, \rho_{2199(SWIR)}, \rho_{2086(SWIR)}]}$	0.808
MULTISPECTRAL	Coniferous forest	$\mathrm{NDRE}_{[B5_{(Red\ edge)}, B8_{(NIR)}]}$	0.778	$\mathrm{CIREDGE}_{[B5_{(Red\ edge)}, B8_{(NIR)}]}$	0.309	$\mathrm{CIREDGE}_{[B5_{(Red\ edge)}, B8_{(NIR)}]}$	0.634
	Broadleaf forest	$\mathrm{ENDVI}_{[B5_{(Red\ edge)}, B3_{(Green)}, B2_{(Blue)}]}$	0.509	$\mathrm{ENDVI}_{[B5_{(Red\ edge)}, B3_{(Green)}, B2_{(Blue)}]}$	0.442	$\mathrm{ENDVI}_{[B5_{(Red\ edge)}, B3_{(Green)}, B2_{(Blue)}]}$	0.532
	Shrubland	$\mathrm{GNDVI}\ [B3_{(Green)}, B5_{(Red\ edge)}, B8A_{(NIR\ narrow)}]$	0.738	$\mathrm{GNDVI}\ [B3_{(Green)}, B5_{(Red\ edge)}, B8A_{(NIR\ narrow)}]$	0.624	$\mathrm{GNDVI}\ [B3_{(Green)}, B5_{(Red\ edge)}, B8A_{(NIR\ narrow)}]$	0.705

Regarding the performance of the CBI types, the best correlations were observed with the vegetation CBI. In contrast, the soil CBI showed lower correlations and the site CBI showed intermediate performance, which is consistent with being the average of the other two classes. Otherwise, shrubland ecosystem obtained, on average, the highest correlations with the CBI, followed by the broadleaf forest and the coniferous forest.

The hyperspectral indices that were best correlated with CBI values were the cellulose absorption index (CAI), the red edge difference vegetation index (DVIRED), and the enhanced vegetation index (EVI). Regarding multispectral indices, the vegetation indices that showed the best correlation were the normalized difference red edge (NDRE), the red edge chlorophyll index (CIREDGE), the enhanced normalized difference vegetation index (ENDVI), and the green normalized difference vegetation index (GNDVI).

The hyperspectral index that appeared most frequently as the best performer was CAI, which was most prominent in broadleaf forest and shrubland ecosystems with all CBI classes. Throughout the analysis with hyperspectral data, the VI with the best correlation was the CAI with the site CBI and shrubland ecosystem, obtaining a value of -0.899 (R^2 = 0.808). Regarding the multispectral data, the ENDVI and GDNVI indices were the ones with the highest number of occurrences and the best performer, standing out in the broadleaf forest and shrubland in the vegetation, soil, and site CBI. However, the NDRE index applied to coniferous forests with the vegetation CBI was the one that presented the best correlation among the multispectral indices, with a value of -0.882 (R^2 = 0.778).

4.3. SPECTRAL INDICES CORRELATION

The selected hyperspectral indices exhibited negative Pearson correlation in all cases, as depicted in Figure 3. Pearson correlation between hyperspectral VI values and CBI across coniferous forest, broadleaf forest, and shrubland ecosystems is strongly negative. For coniferous forest, the DVIRED index (729 nm/802 nm) with vegetation CBI yielded the highest correlation (R^2 = 0.739, r = -0.866, RMSE = 0.386), while the EVI index (485 nm/614 nm/877 nm) with soil CBI showed a weaker relationship (R^2 = 443, r = -0.666, RMSE = 0.454). In broadleaf forest, the CAI index (2036 nm/2199 nm/2103 nm) with site CBI performed best (R^2 = 0.766, r = -0.875, RMSE = 0.348). For shrublands, the CAI index (1993 nm/2199 nm/2086 nm) with site CBI exhibited the strongest relationship (R^2 = 0.808, r = -0.899, RMSE = 0.359), followed closely by CAI at 1993 nm/2199 nm/2086 nm (R^2 = 0.798, r = -0.894, RMSE = 0.409) with vegetation CBI. These findings highlight the efficacy of hyperspectral indices in assessing vegetation and site CBI across diverse ecosystem types, with CAI consistently outperforming other indices in broadleaf and shrubland settings.

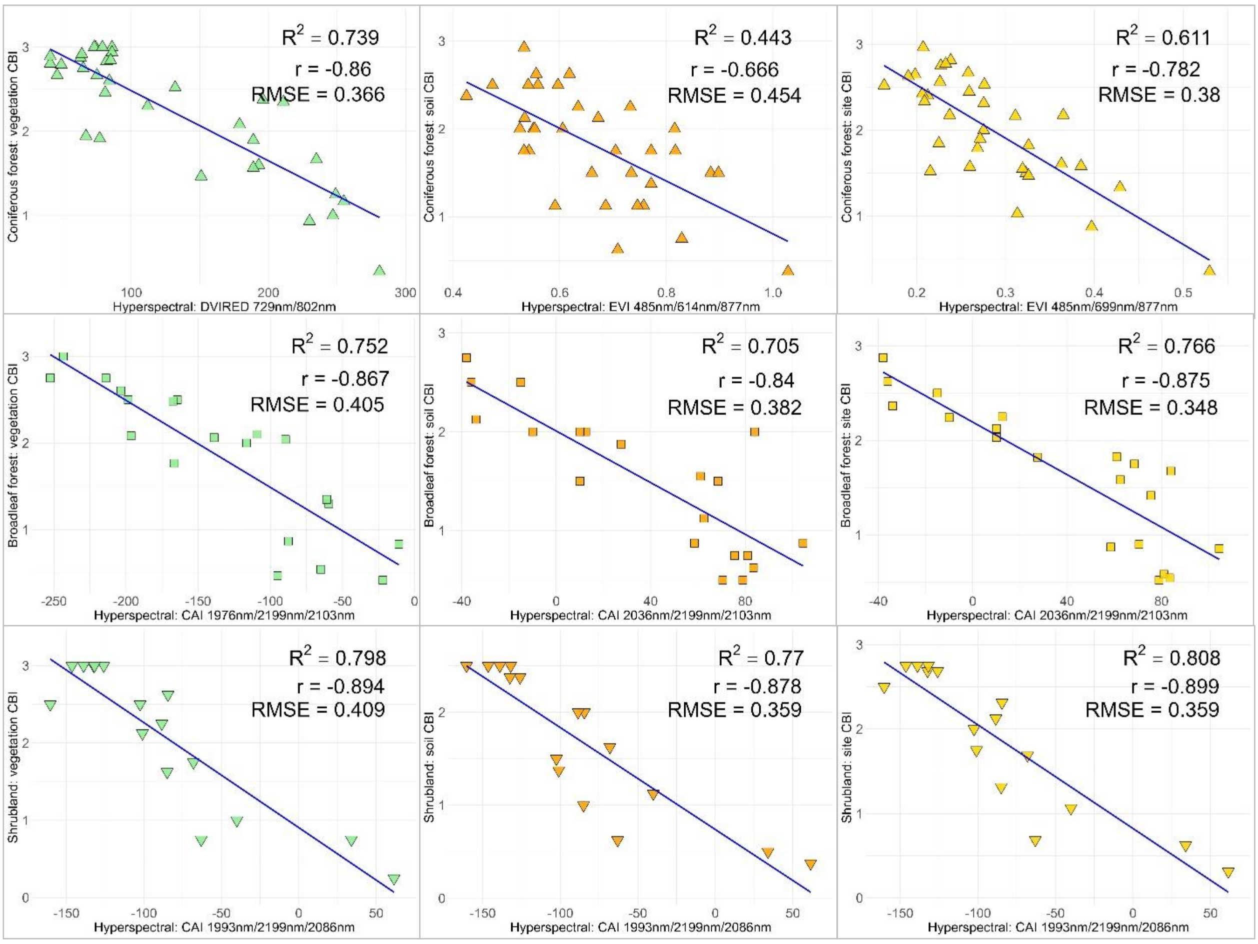

Figure 3. *Relationship between hyperspectral vegetation index values and vegetation, soil, and site CBI across ecosystem types.*

The results presented in Figure 4 reveal the relationship between multispectral VI values and CBI across coniferous forest, broadleaf forest, and shrubland ecosystems. In coniferous forests, the NDRE B5/B8 index with vegetation CBI showed the strongest correlation (R^2 = 0.778, r = -0.882, RMSE = 0.338), while CIREDGE B5/B8 with soil CBI had the weakest fit (R^2 = 0.309, r = -0.556, RMSE = 0.506). For broadleaf forests, ENDVI B5/B3/B2 with site CBI exhibited the highest correlation (R^2 = 0.532, r = -0.729, RMSE = 0.492), with ENDVI B5/B3/B2 with vegetation CBI showing a moderate relationship (R^2 =0.509, r = -0.714, RMSE = 0.569) and ENDVI B5/B3/B2 with soil CBI a slightly weaker one (R^2 =0.442, r = -0.665, RMSE = 0.525). In shrubland, GNDVI B3/B5/B8A with vegetation CBI performed best (R^2 =0.738, r = -0.859, RMSE = 0.466), followed closely by GNDVI B3/B5/B8A with site CBI (R^2 =0.705, r = -0.840, RMSE = 0.445), while GNDVI B3/B5/B8A showed a slightly lower correlation (R^2 =0.624, r = -0.790, RMSE = 0.459). These results indicate that multispectral indices, particularly NDRE B5/B8 and GNDVI B3/B5/B8A, are effective for assessing vegetation and soil CBI, with varying performance across ecosystem types.

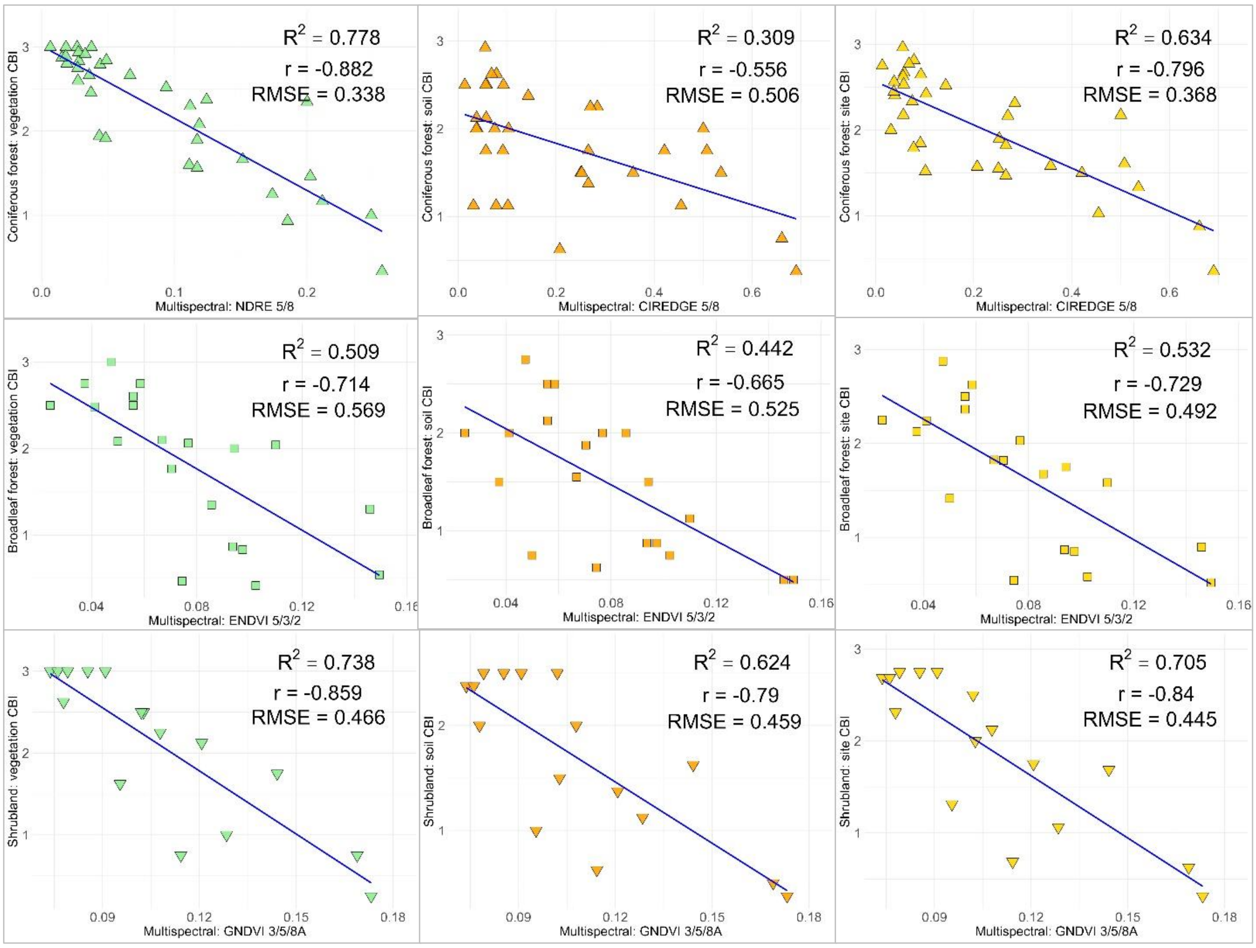

Figure 4. *Relationship between multispectral vegetation index values and vegetation, soil, and site CBI across ecosystem types.*

4.4. SPATIAL DISTRIBUTION OF FIRE SEVERITY

Table 2 shows the vegetation fire severity area by ecosystem type using the hyperspectral (PRISMA) or multispectral (Sentinel-2) indices. For PRISMA, the DVIRED index highlighted a significant high-severity area (6427 ha, 25.6%) in coniferous forests, with moderate (2065 ha, 8.2%) and low (562 ha, 2.2%) severity areas also notable. In broadleaf forests, the CAI index identified high severity at 1693 ha (6.7%), with moderate and low severity areas closely at 1844 ha each (7.3%). Shrubland showed a high-severity area of 4477 ha (17.8%) using CAI, with moderate (3235 ha, 12.9%) and low (2952 ha, 11.8%) severity regions. Sentinel-2 data, using NDRE, ENDVI, and GNDVI indices, corroborated these findings, with coniferous forests exhibiting a high-severity area of 6743 ha (26.9%), broadleaf forests at 1626 ha (6.5%), and shrublands at 3966 ha (15.8%). The spatial distribution maps (Figures 5 & 6) reveal a predominance of high-severity area (red) across all ecosystems, particularly in central regions, with moderate (brown) and low (green) severity patches interspersed, indicating the utility of both data types in mapping fire severity, with hyperspectral data enhancing precision in ecosystem-specific analysis.

Table 2. *Vegetation fire severity areas by ecosystem type using hyperspectral (PRISMA) and multispectral (Sentinel-2) indices*

Ecosystem	Vegetation fire severity	PRISMA (hyperspectral)			SENTINEL-2 (multispectral)		
		VI	Area (ha)	%	VI	Area (ha)	%
Coniferous forest	Low		562	2.2		376	1.5
	Moderate	$\mathrm{DVIRED}_{[\rho_{729(VIS)}, \rho_{802(NIR)}]}$	2065	8.2	$\mathrm{NDRE}_{[B5_{(Red\ edge)}, B8_{(NIR)}]}$	1937	7.7
	High		6427	25.6		6743	26.9
Broadleaf forest	Low		1843	7.3		1233	4.9
	Moderate	$\mathrm{CAI}_{[\rho_{1976(SWIR)}, \rho_{2199(SWIR)}, \rho_{2103(SWIR)}]}$	1844	7.3	$\mathrm{ENDVI}_{[B5_{(Red\ edge)}, B3_{(Green)}, B2_{(Blue)}]}$	2526	10.1
	High		1693	6.7		1626	6.5
Shrubland	Low		2952	11.8		3066	12.2
	Moderate	$\mathrm{CAI}_{[\rho_{1993(SWIR)}, \rho_{2199(SWIR)}, \rho_{2086(SWIR)}]}$	3235	12.9	$\mathrm{GNDVI}\ [B3_{(Green)}, B5_{(Red\ edge)}, B8A_{(NIR\ narrow)}]$	3588	14.3
	High		4477	17.8		3966	15.8

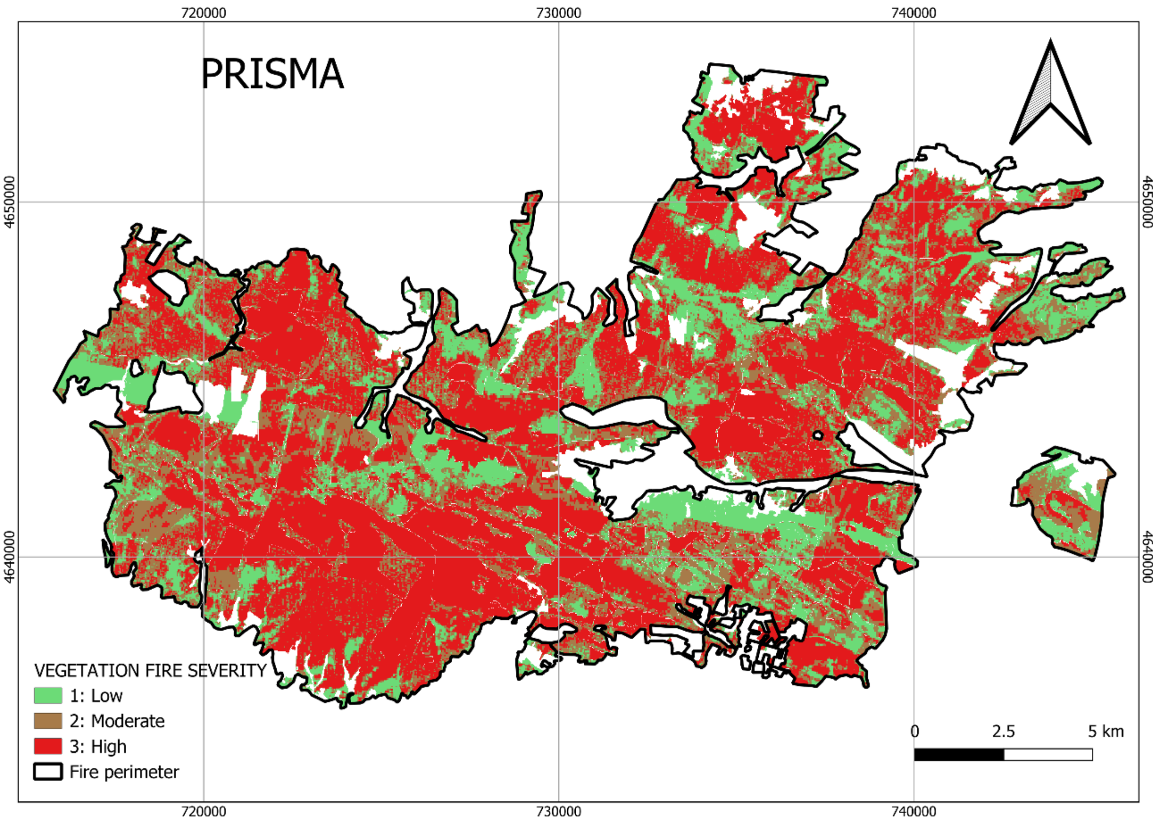

Figure 5. *Map of vegetation fire severity in the Sierra de la Culebra wildfire area using hyperspectral indices across ecosystem types.*

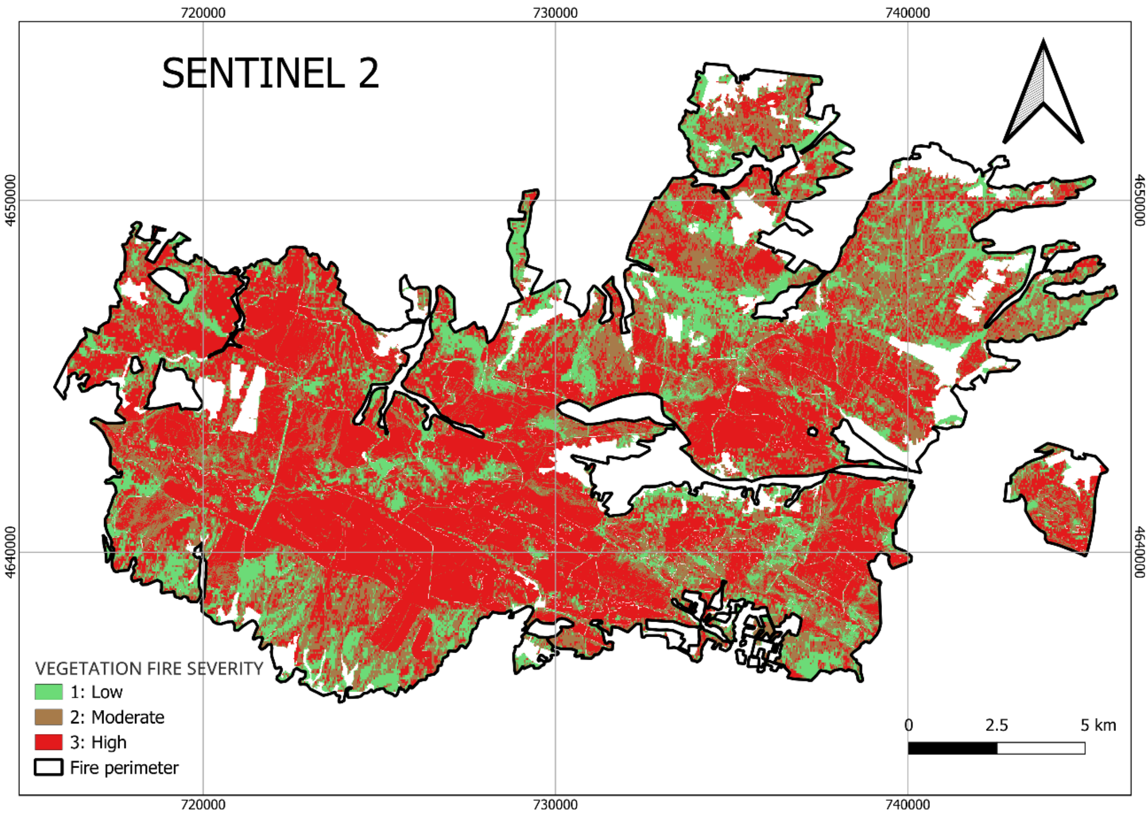

Figure 6. *Map of vegetation fire severity in the Sierra de la Culebra wildfire area using multispectral indices across ecosystem types*

Soil fire severity analysis using hyperspectral (PRISMA) and multispectral (Sentinel-2) indices is shown in Table 3. For coniferous forests, PRISMA's EVI index indicated moderate severity as the dominant category (7326 ha, 29.3%), with low (708 ha, 2.8%) and high (1021 ha, 4.1%) severity areas being less extensive, while Sentinel-2's CIREDGE index showed a significant moderate severity area (8577 ha, 34.2%) and minimal high severity (143 ha, 0.6%). In broadleaf forests, PRISMA's CAI index identified moderate severity as prevalent (2667 ha, 10.7%), with low (2129 ha, 8.5%) and high (520 ha, 2.1%) severity areas, whereas Sentinel-2's ENDVI index showed a higher moderate severity area (3663 ha, 14.6%) and low severity (1634 ha, 6.5%). For shrubland, PRISMA's CAI index revealed a substantial low severity area (3669 ha, 14.7%), with moderate (4648 ha, 18.6%) and high (2347 ha, 9.4%) severity regions, while Sentinel-2's GNDVI index indicated a dominant moderate severity area (5621 ha, 22.4%) and a notable low severity area (3647 ha, 14.6%). The spatial maps (Figures 7 & 8) depict a widespread distribution of moderate severity (brown) across all ecosystems, with high severity (red) concentrated in central regions and low severity (green) patches scattered throughout, suggesting that both spectral indices effectively capture soil fire severity variations, with PRISMA providing finer detail and Sentinel-2 offering a robust broad-scale perspective.

Table 3. *Soil fire severity areas by ecosystem type using hyperspectral (PRISMA) and multispectral (Sentinel-2) indices*

Ecosystem	Soil fire severity	PRISMA (hyperspectral)			SENTINEL-2 (multispectral)		
		VI	Area (ha)	%	VI	Area (ha)	%
Coniferous forest	Low	$\mathrm{EVI}_{[\rho_{485(VIS)}, \rho_{614(VIS)}, \rho_{877(NIR)}]}$	708	2.8	$\mathrm{CIREDGE}_{[B5_{(Red\ edge)}, B8_{(NIR)}]}$	334	1.3
	Moderate		7326	29.3		8577	34.2
	High		1021	4.1		143	0.6
Broadleaf forest	Low	$\mathrm{CAI}_{[\rho_{2036(SWIR)}, \rho_{2199(SWIR)}, \rho_{2103(SWIR)}]}$	2129	8.5	$\mathrm{ENDVI}_{[B5_{(Red\ edge)}, B3_{(Green)}, B2_{(Blue)}]}$	1634	6.5
	Moderate		2667	10.7		3663	14.6
	High		520	2.1		88	0.4
Shrubland	Low	$\mathrm{CAI}_{[\rho_{1993(SWIR)}, \rho_{2199(SWIR)}, \rho_{2086(SWIR)}]}$	3669	14.7	GNDVI $[B3_{(Green)}, B5_{(Red\ edge)}, B8A_{(NIR\ narrow)}]$	3647	14.6
	Moderate		4648	18.6		5621	22.4
	High		2347	9.4		1353	5.4

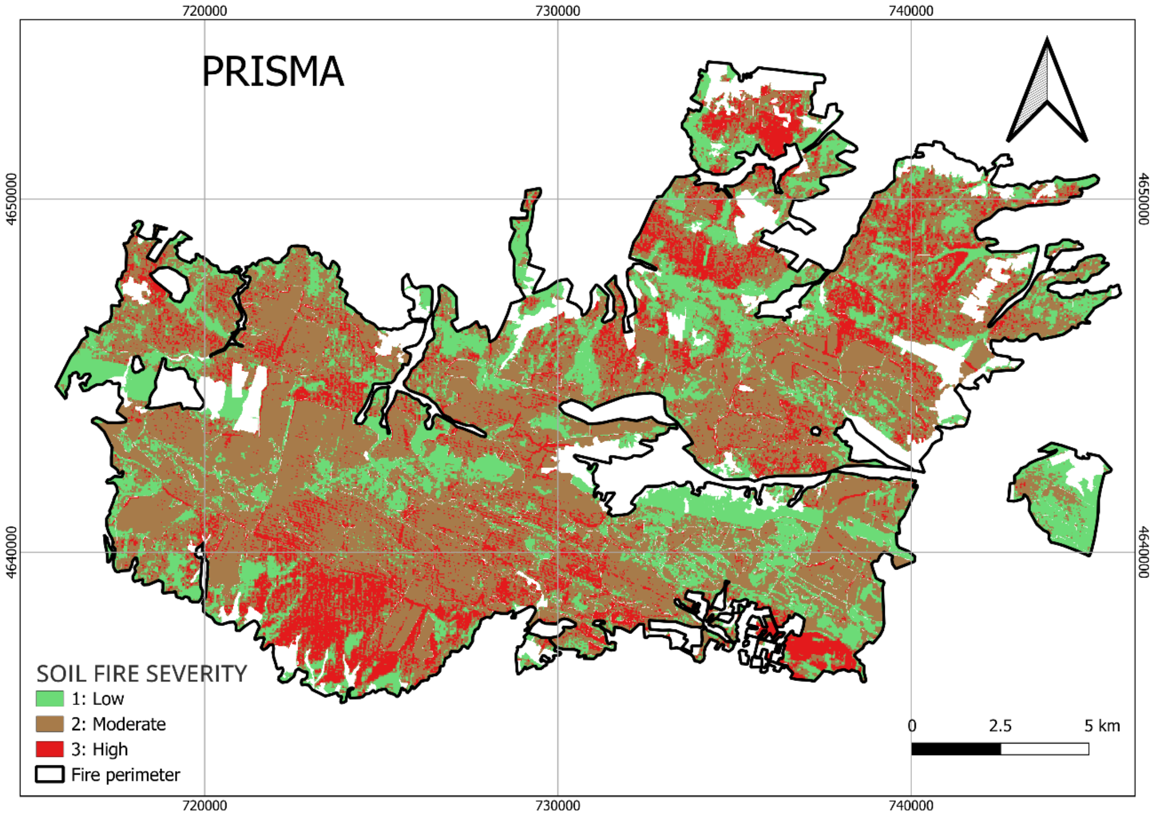

Figure 7. *Map of soil fire severity in the Sierra de la Culebra wildfire area using hyperspectral indices across ecosystem types.*

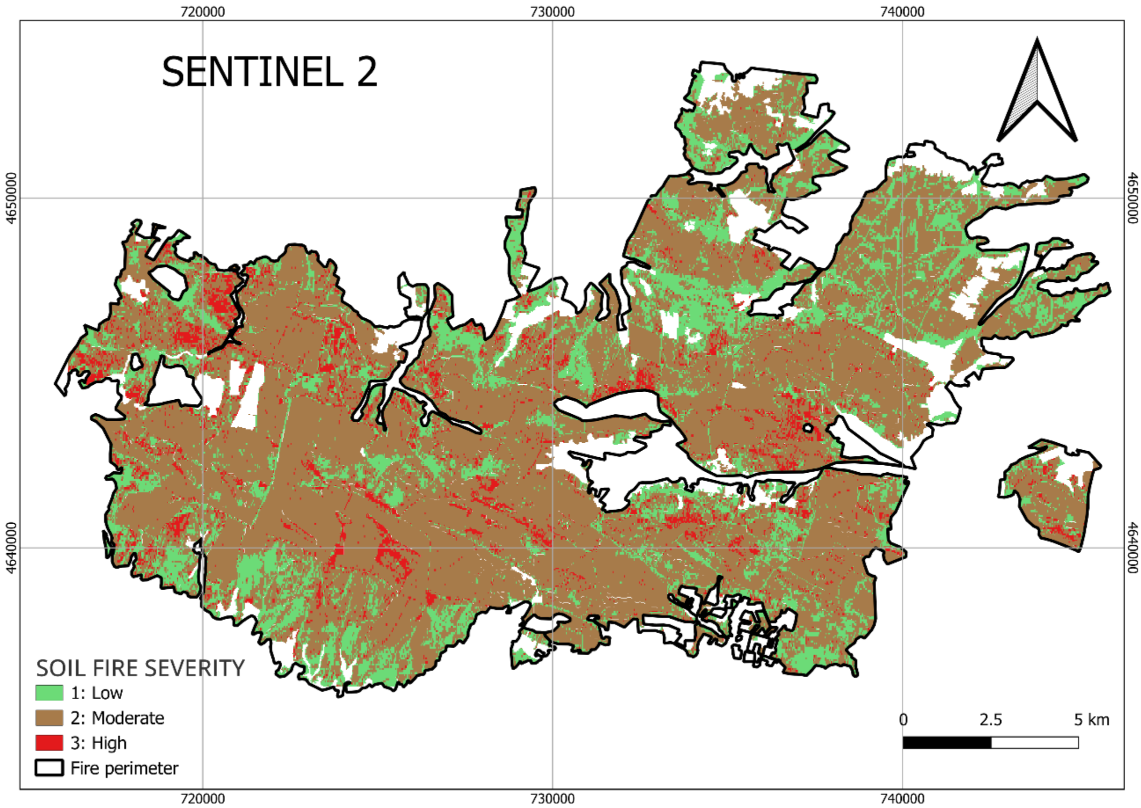

Figure 8. *Map of soil fire severity in the Sierra de la Culebra wildfire area using multispectral indices across ecosystem types.*

Site fire severity analysis across coniferous forest, broadleaf forest, and shrubland ecosystems in the Sierra de la Culebra wildfire area, as assessed using hyperspectral (PRISMA) and multispectral (Sentinel-2) indices is shown in Table 4. For coniferous forests, PRISMA's EVI index identified moderate severity as the most extensive category (3607 ha, 14.4%), with high severity (4920 ha, 19.6%) and low severity (528 ha, 2.1%) areas also significant, while Sentinel-2's CIREDE index showed a dominant high severity area (5649 ha, 22.5%) and moderate severity (3047 ha, 12.2%). In broadleaf forests, PRISMA's CAI index highlighted moderate severity (2506 ha, 10.0%) as prevalent, with low (1883 ha, 7.5%) and high (991 ha, 3.9%) severity areas, whereas Sentinel-2's ENDVI index indicated a substantial moderate severity area (3319 ha, 13.2%) and low severity (1394 ha, 5.6%). For shrublands, PRISMA's CAI index revealed a notable low severity area (3251 ha, 13.0%), with moderate (3922 ha, 15.6%) and high (3392 ha, 13.9%) severity regions, while Sentinel-2's GNDVI index showed a significant moderate severity area (4608 ha, 18.4%) and low severity (3300 ha, 13.2%). The spatial maps (Figures 9 & 10) describe a widespread presence of high severity (red) across all ecosystems, particularly in central regions, with moderate (brown) and low (green) severity patches distributed throughout, indicating that both hyperspectral and multispectral indices effectively map site fire severity.

Table 4. *Site fire severity areas by ecosystem type using hyperspectral (PRISMA) and multispectral (Sentinel-2) indices*

Ecosystem	Site fire severity	PRISMA (hyperspectral)			SENTINEL-2 (multispectral)		
		VI	Area (ha)	%	VI	Area (ha)	%
Coniferous forest	Low	$\mathrm{EVI}_{[\rho_{485(VIS)}, \rho_{699(VIS)}, \rho_{877(NIR)}]}$	528	2.1	$\mathrm{CIREDGE}_{[B5_{(Red\ edge)}, B8_{(NIR)}]}$	359	1.4
	Moderate		3607	14.4		3047	12.2
	High		4920	19.6		5649	22.5
Broadleaf forest	Low	$\mathrm{CAI}_{[\rho_{2036(SWIR)}, \rho_{2199(SWIR)}, \rho_{2103(SWIR)}]}$	1883	7.5	$\mathrm{ENDVI}_{[B5_{(Red\ edge)}, B3_{(Green)}, B2_{(Blue)}]}$	1394	5.6
	Moderate		2506	10.0		3319	13.2
	High		991	3.9		662	2.6
Shrubland	Low	$\mathrm{CAI}_{[\rho_{1993(SWIR)}, \rho_{2199(SWIR)}, \rho_{2086(SWIR)}]}$	3251	13.0	$\mathrm{GNDVI}\ [B3_{(Green)}, B5_{(Red\ edge)}, B8A_{(NIR\ narrow)}]$	3300	13.2
	Moderate		3922	15.6		4608	18.4
	High		3492	13.9		2712	10.8

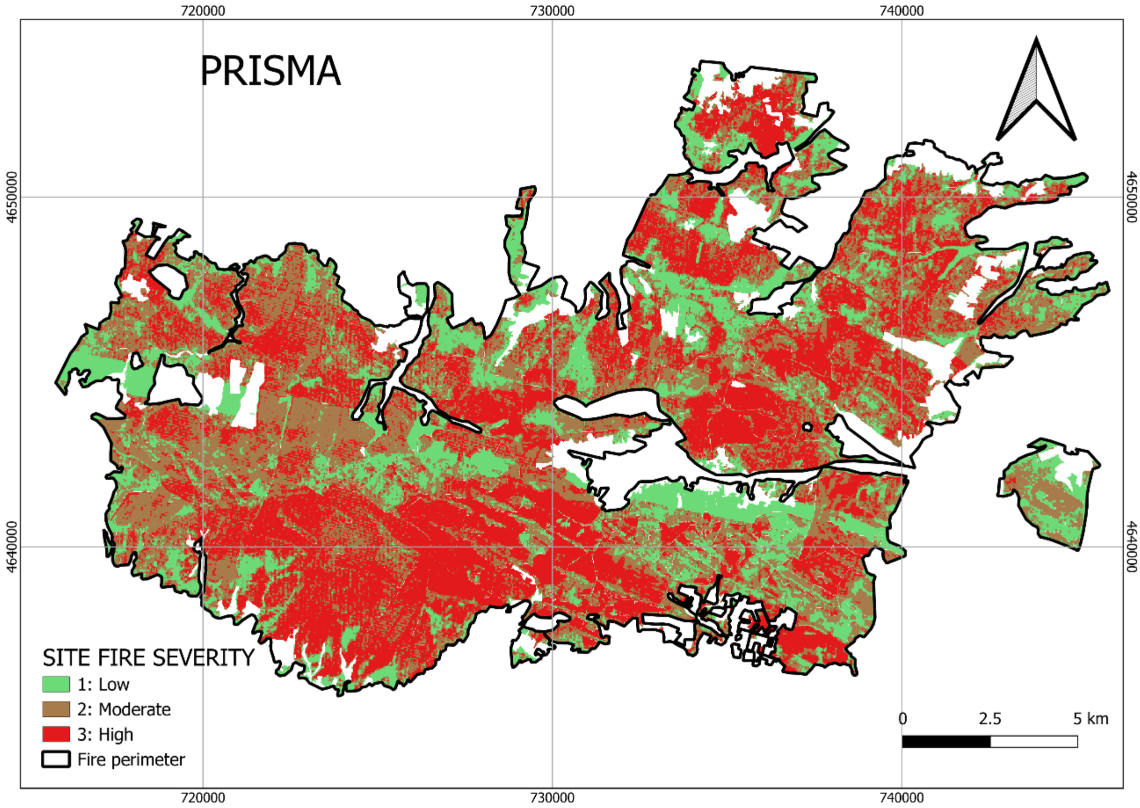

Figure 9. *Map of site fire severity in the Sierra de la Culebra wildfire area using hyperspectral indices across ecosystem types.*

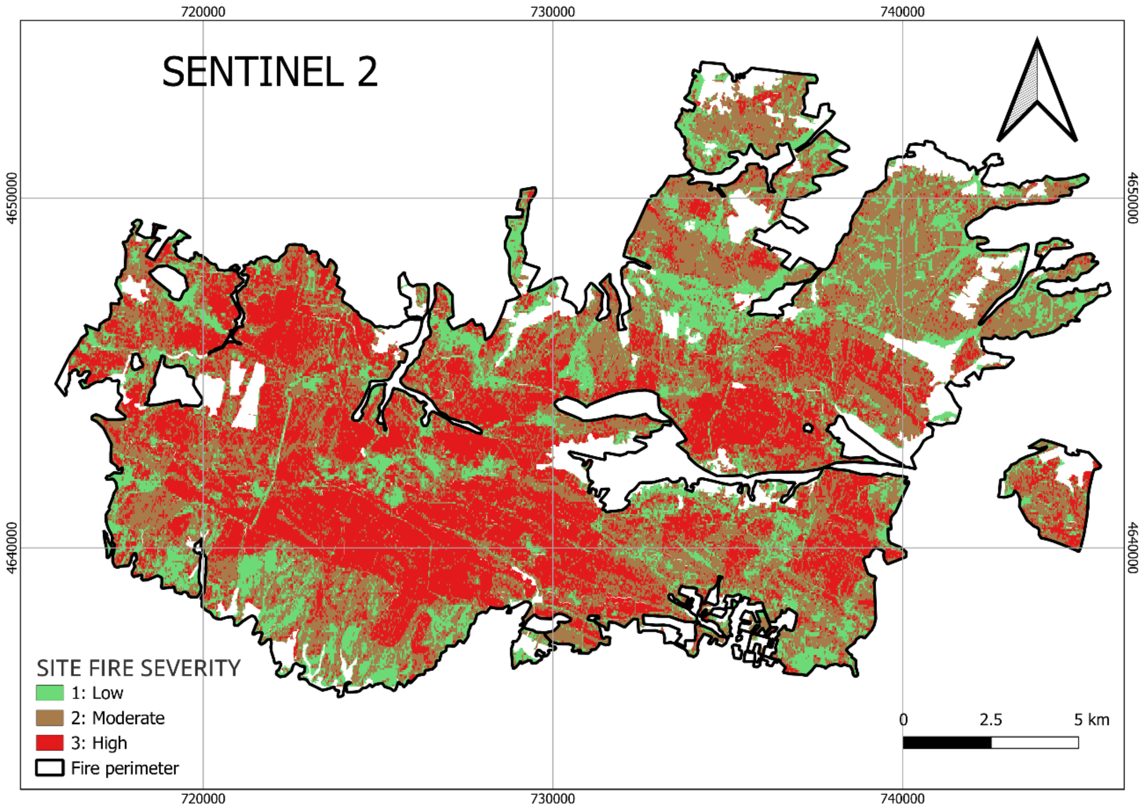

Figure 10. *Map of site fire severity in the Sierra de la Culebra wildfire area using multispectral indices across ecosystem types.*

5. DISCUSSION

The hyperspectral data obtained from the PRISMA satellite provided a more thorough and continuous characterization of the spectral properties associated with fire severity levels across various ecosystem types compared to multispectral data. This finding aligns with a previous study conducted in a hilly and mountainous landscape dominated by Mediterranean oak and pine species (Vangi et al., 2021). The spectral signatures of vegetation display distinct variations across fire severity levels, particularly in the red, near-infrared (NIR), and short-wave infrared (SWIR) regions of the electromagnetic spectrum. Areas affected by low-severity fires exhibit high reflectance in the NIR band, attributed to intact internal leaf structures, and reduced reflectance in the red band due to chlorophyll absorption. Conversely, high-severity fires result in significantly decreased NIR reflectance, caused by the degradation of canopy structure and loss of pigment content, alongside elevated SWIR reflectance due to reduced water content and the presence of char and ash (Key & Benson, 2006).

Hyperspectral indices showed a stronger correlation with CBI values compared to those derived from multispectral data. For example, the hyperspectral indices in relation to the site CBI presented a mean correlation of -0.852 (R^2 = 0.728), while the corresponding multispectral index reached a correlation of -0.788 (R^2 = 0. 624). These results confirm the greater capacity of hyperspectral images to capture greater details in fire severity, in agreement with previous studies that also highlight the superiority of PRISMA images over Sentinel-2 images (Vangi et al., 2021; Quintano et al., 2023). The higher sensitivity of the narrow bands of hyperspectral images allows a more precise detection of physical and chemical changes in vegetation, making them suitable for assessing fire severity (Adam et al., 2010). Furthermore, it was determined that the coarser spatial resolution of PRISMA does not inherently underperform compared to the finer spatial resolution of Sentinel-2 (M. Liu et al., 2020; Vangi et al., 2021).

The vegetation CBI showed the best correlations with spectral indices across all ecosystem types (coniferous forest, broadleaf forest, and shrubland), using both PRISMA hyperspectral and Sentinel-2 multispectral data. This may be because vegetation indices (VIs) are specifically designed to detect vegetation cover-related characteristics, such as chlorophyll content, vegetation density, and plant vigor (Meng & Zhao, 2017). Besides, outperforming correlations of vegetation CBI over soil is likely due to the planimetry of the images, which better captures the upper vegetation strata rather than the soil (Peña & Martínez, 2021).

On the other hand, the strongest negative correlations between spectral indices and soil and site CBIs were observed primarily in broadleaf forest and shrubland ecosystems, but not in coniferous forests. One possible explanation is the distinct spectral responses emitted depending on the vegetation type assessed (Aldana et al., 2020; Flores Rodríguez et al., 2021; Peña & Martínez, 2021). Furthermore, factors such as forest density and stem structure can influence sensor detection of soil conditions, as these characteristics affect the amount of remaining biomass and soil exposure after a fire (Robichaud et al., 2007; García-Llamas et al., 2019).

The calculated hyperspectral indices showed strong negative correlations, greater than -0.850 (R^2 = 0.722), with the vegetation CBI and all ecosystems. Broadleaf forest and shrubland ecosystems stood out for presenting the best correlations between hyperspectral indices and all CBI types. This behavior can be attributed to the different dynamics of ecosystems and the adaptive characteristics of plant species in response to fire, such as tolerance or resistance to burning, which result chemical compositions that are detected more accurately by the narrow bands of hyperspectral sensors through specific band combinations (Rodríguez-Trejo & Fulé, 2003; Adam et al., 2010).

Soil composition varies across ecosystems due to differences in the biomass input provided by plant species. This input includes differences in mass, volume, and chemical compounds, such as leaves, needles, and other organic debris (Calvo et al., 2003). These differences explain why certain spectral indices performed better depending on the ecosystem type.

The hyperspectral and multispectral image bands that more frequently came up in the best correlated indices with the CBI were the red edge, NIR, and SWIR bands which have proved their usefulness in forest fire analysis (Chuvieco et al., 2006; Carvajal-Ramírez et al., 2019; Fernández-Manso & Quintano, 2020). In contrast to commonly utilized VIs, such as the Normalized Difference Vegetation Index (NDVI) and the Normalized Burn Ratio (NBR), these indices showed limited effectiveness in correlating with the Composite Burn Index (CBI) due to their reliance on the red spectral band, which exhibited weak correlations with field-based burn severity measurements. This reduced correlation is likely attributable to their heightened sensitivity to denser canopy structures (Fernández-Manso et al., 2016). The selection of the most appropriate index for fire severity analysis is context-dependent, and the optimal index should be chosen based on the specific conditions of each case (Flores Rodríguez et al., 2021).

Hyperspectral indices such as DVIRED, EVI, and CAI are particularly valuable for assessing vegetation health due to their sensitivity to variations in leaf reflectance and biomass (Qiao et al., 2022). DVIRED can be used to assess vegetation-covered areas, particularly under heterogeneous conditions, though its value for shadowed soil is typically low and less responsive to vegetation cover on such soil (Y. Liu et al., 2021). EVI is designed for high-biomass forests to account for the combined effects of canopy background and atmospheric influences (H. Q. Liu & Huete, 1995). CAI measures the relative depth of reflectance spectra at 2100 nm to distinguish plant litter from soils based on spectral reflectance differences driven by physical and chemical properties, with coniferous litter exhibiting a higher response value than deciduous litter, both surpassing soil, due to the cellulose-lignin absorption feature in the SWIR wavelengths (Nagler et al., 2000).

The most effective Sentinel-2 spectral indices for assessing fire severity are those derived from band B5, located in the red-edge region near red wavelengths and primarily associated with variations in chlorophyll content, and bands B8 or B8A, situated in the narrow NIR region and predominantly linked to changes in leaf structure. These findings are consistent with previous studies (Fernández-Manso et al., 2016). In this study, multispectral indices such as NDRE, CIREDGE, ENDVI, and GNDVI were effective for detecting variations in chlorophyll, biomass, and fire severity, providing insights into vegetation health and density (Imran et al., 2020). NDRE, derived from the NDVI formula but utilizing the red edge band, serves as a reliable indicator of chlorophyll or nitrogen status (Fitzgerald et al., 2006). CIREDGE enables estimation of chlorophyll content in canopies, facilitating the monitoring of physiological status, mainly in crops such as maize and soybean (Gitelson et al., 2005). ENDVI, which leverages green and blue wavelengths to enhance chlorophyll absorption values, particularly chlorophyll-b, is applied in agricultural monitoring and assessing peatland disturbance (Strong et al., 2017). GNDVI was originally developed to evaluate plant chlorophyll status in wheat, closely associated with nitrogen status and other stress factors (Hunt et al., 2010). Unlike multispectral indices, the identification of specific hyperspectral VIs enhances the remote assessment of vegetation and soil fire severity, offering greater precision (Hudak et al., 2007; Carvajal-Ramírez et al., 2019). This detailed understanding of vegetation and soil fire severity supports the planning of ecological restoration strategies and post-fire monitoring, concentrating efforts on priority areas (García-Llamas et al., 2019).

The findings of this study highlight several key directions for future research to refine fire severity assessment methodologies. Developing adaptive algorithms that incorporate vegetation type, meteorological conditions during image acquisition, and topographic slope could enhance the accuracy of fire severity detection (Chuvieco et al., 2019). However, the timing of image acquisition requires careful consideration; extended intervals, such as 1-year post-fire, could compromise precision due to seasonal precipitation and high r

ate regrowth of shrubs and grasses, which can mask fire severity signals (Key & Benson, 2006; Fornacca et al., 2018). Furthermore, defining forest fire boundaries as the study area is critical to reduce variability in spectral index values, thereby improving result reliability (Flores Rodríguez et al., 2021). SWIR-based VIs have been shown in other research studies to exhibit greater accuracy when applied to wildfire areas larger than 25 ha, indicating that larger fire extents may yield better detection outcomes (Bastarrika et al., 2011). To ensure robust validation, maximizing the number of field reference sites (plots) is essential for achieving a representative distribution across the study area (Flores Rodríguez et al., 2021). Additionally, adopting a bitemporal image analysis approach—comparing pre- and post-fire conditions—could better isolate vegetation changes caused by fire, distinguishing them from changes due to pre-existing stressors such as plagues, drought, hurricanes, or prior fires (Flores Rodríguez et al., 2021). Additionally, other hyperspectral imagery source is necessary to study. Fire severity analyses should be designed to support wildfire management agencies responsible for forest monitoring, enhancing their ability to make timely and informed decisions.

6. CONCLUSION

This study demonstrates that hyperspectral indices derived from PRISMA imagery provided superior estimates of fire severity in the Sierra de La Culebra following the 2022 wildfire compared to multispectral indices from Sentinel-2 imagery. Specifically, stronger correlations were observed with the Composite Burn Index (CBI) at the vegetation level, likely due to the enhanced detectability of vegetation strata in satellite imagery planimetry compared to soil and site levels. Among the vegetation types assessed, broadleaf forest and shrubland ecosystems exhibited higher correlations with CBI than coniferous forests, suggesting that plant species' adaptations to fire significantly influence spectral responses captured by satellite imagery. The Cellulose Absorption Index (CAI) emerged as the most effective hyperspectral index, achieving the highest correlation in the study (R^2 = 0.808, r = -0.899, RMSE = 0.359). Meanwhile, Green Normalized Difference Vegetation Index (GNDVI) became the best-performing multispectral index (R^2 = 0.738, r = -0.859, RMSE = 0.466). These findings highlight the efficacy of hyperspectral imagery for precise fire severity assessment and its potential for mapping fire impacts across diverse ecosystems.

7. ACKNOWLEDGMENTS

I would like to express my sincere gratitude to my advisors, Camen Quintano and José Manuel Fernández-Guisuraga, for their invaluable guidance and support in accomplishing this study. I also extend my thanks to Felipe Bravo, whose initial contact set me on the path to successfully completing this master's program. My appreciation also goes out to my friends and colleagues from the University of Valladolid, who made my stay in Palencia truly enjoyable.

Last but certainly not least, I wish to thank my parents, Inés and José, my unwavering source of strength and perseverance. To my siblings, Marco and Maricielo, my dear beloved accomplices in life, thank you. Luna.

8. REFERENCES

Adam, E., Mutanga, O., & Rugege, D. (2010). Multispectral and hyperspectral remote sensing for identification and mapping of wetland vegetation: A review. *Wetlands Ecology and Management*, *18*(3), 281-296. https://doi.org/10.1007/s11273-009-9169-z

Aldana, C., Revilla, M., Gonzales, J., Saavedra, Y., Moncada, W., & Maicelo, J. (2020). Relación de firmas espectrales para la identificación de bosque seco en imágenes de satélite Sentinel 2, cuenca baja del río Chira, Región Piura. *Revista de Teledetección*, *56*, 147. https://doi.org/10.4995/raet.2020.14110

Amici, S., & Piscini, A. (2021). Exploring PRISMA Scene for Fire Detection: Case Study of 2019 Bushfires in Ben Halls Gap National Park, NSW, Australia. *Remote Sensing*, *13*(8), 1410. https://doi.org/10.3390/rs13081410

Atun, R., Kalkan, K., & Gürsoy, Ö. (2020). *Determining The Forest Fire Risk with Sentinel 2 Images*. *1*(1), 22-26.

Bastarrika, A., Chuvieco, E., & Martín, M. P. (2011). Mapping burned areas from Landsat TM/ETM+ data with a two-phase algorithm: Balancing omission and commission errors. *Remote Sensing of Environment*, *115*(4), 1003-1012. https://doi.org/10.1016/j.rse.2010.12.005

Boer, M. M., Nolan, R. H., Resco De Dios, V., Clarke, H., Price, O. F., & Bradstock, R. A. (2017). Changing Weather Extremes Call for Early Warning of Potential for Catastrophic Fire. *Earth's Future*, *5*(12), 1196-1202. https://doi.org/10.1002/2017EF000657

Boer, M., Macfarlane, C., Norris, J., Sadler, R., Wallace, J., & Grierson, P. (2008). Mapping burned areas and burn severity patterns in SW Australian eucalypt forest using remotely-sensed changes in leaf area index. *Remote Sensing of Environment*, *112*(12), 4358-4369. https://doi.org/10.1016/j.rse.2008.08.005

Calvo, L., Santalla, S., Marcos, E., Valbuena, L., Tárrega, R., & Luis, E. (2003). Regeneration after wildfire in communities dominated by Pinus pinaster, an obligate seeder, and in others dominated by Quercus pyrenaica, a typical resprouter. *Forest Ecology and Management*, *184*(1-3), 209-223. https://doi.org/10.1016/S0378-1127(03)00207-X

Carvajal-Ramírez, F., Marques Da Silva, J. R., Agüera-Vega, F., Martínez-Carricondo, P., Serrano, J., & Moral, F. J. (2019). Evaluation of Fire Severity Indices Based on Pre- and Post-Fire Multispectral Imagery Sensed from UAV. *Remote Sensing*, *11*(9), 993. https://doi.org/10.3390/rs11090993

Chen, C., Yuan, X., Gan, S., Luo, W., Bi, R., Li, R., & Gao, S. (2024). A new vegetation index based on UAV for extracting plateau vegetation information. *International Journal of Applied Earth Observation and Geoinformation*, *128*, 103668. https://doi.org/10.1016/j.jag.2024.103668

Chrysafis, I., Mallinis, G., Tsakiri, M., & Patias, P. (2019). Evaluation of single-date and multi-seasonal spatial and spectral information of Sentinel-2 imagery to assess growing stock volume of a Mediterranean forest. *International Journal of Applied Earth Observation and Geoinformation*, *77*, 1-14. https://doi.org/10.1016/j.jag.2018.12.004

Chuvieco, E., Mouillot, F., Van Der Werf, G. R., San Miguel, J., Tanase, M., Koutsias, N., García, M., Yebra, M., Padilla, M., Gitas, I., Heil, A., Hawbaker, T. J., & Giglio, L. (2019). Historical background and current developments for mapping burned area from satellite Earth observation. *Remote Sensing of Environment*, *225*, 45-64. https://doi.org/10.1016/j.rse.2019.02.013

Chuvieco, E., Riaño, D., Danson, F. M., & Martin, P. (2006). Use of a radiative transfer model to simulate the postfire spectral response to burn severity. *Journal of Geophysical Research: Biogeosciences*, *111*(G4). https://doi.org/10.1029/2005jg000143

Clark, M. L., Roberts, D. A., & Clark, D. B. (2005). Hyperspectral discrimination of tropical rain forest tree species at leaf to crown scales. *Remote Sensing of Environment*, *96*(3-4), 375-398. https://doi.org/10.1016/j.rse.2005.03.009

De Bonis, R., & Laneve, G. (2013). *Development of a vegetation damage severity index for the Italian hyperspectral sensor PRISMA*. *EARSeL*, 711-724.

De Santis, A., & Chuvieco, E. (2007). Burn severity estimation from remotely sensed data: Performance of simulation versus empirical models. *Remote Sensing of Environment*, *108*(4), 422-435. https://doi.org/10.1016/j.rse.2006.11.022

Evangelides, C., & Nobajas, A. (2020). Red-Edge Normalised Difference Vegetation Index (NDVI705) from Sentinel-2 imagery to assess post-fire regeneration. *Remote Sensing Applications: Society and Environment*, *17*, 100283. https://doi.org/10.1016/j.rsase.2019.100283

Fernández-García, V., Santamarta, M., Fernández-Manso, A., Quintano, C., Marcos, E., & Calvo, L. (2018). Burn severity metrics in fire-prone pine ecosystems along a climatic gradient using Landsat imagery. *Remote Sensing of Environment*, *206*, 205-217. https://doi.org/10.1016/j.rse.2017.12.029

Fernández-Guisuraga, J. M., Calvo, L., Quintano, C., Fernández-Manso, A., & Fernandes, P. M. (2023). Fractional vegetation cover ratio estimated from radiative transfer modeling outperforms spectral indices to assess fire severity in several Mediterranean plant communities. *Remote Sensing of Environment*, *290*, 113542. https://doi.org/10.1016/j.rse.2023.113542

Fernández-Guisuraga, J. M., Suárez-Seoane, S., & Calvo, L. (2019). Modeling Pinus pinaster forest structure after a large wildfire using remote sensing data at high spatial resolution. *Forest Ecology and Management*, *446*, 257-271. https://doi.org/10.1016/j.foreco.2019.05.028

Fernández-Manso, A., Fernández-Manso, O., & Quintano, C. (2016). SENTINEL-2A red-edge spectral indices suitability for discriminating burn severity. *International Journal of*

Applied Earth Observation and Geoinformation, *50*, 170-175. https://doi.org/10.1016/j.jag.2016.03.005

Fernández-Manso, A., & Quintano, C. (2020). A Synergetic Approach to Burned Area Mapping Using Maximum Entropy Modeling Trained with Hyperspectral Data and VIIRS Hotspots. *Remote Sensing*, *12*(5), 858. https://doi.org/10.3390/rs12050858

Fitzgerald, G. J., Rodriguez, D., Christensen, L. K., Belford, R., Sadras, V. O., & Clarke, T. R. (2006). Spectral and thermal sensing for nitrogen and water status in rainfed and irrigated wheat environments. *Precision Agriculture*, *7*(4), 233-248. https://doi.org/10.1007/s11119-006-9011-z

Flores Rodríguez, A. G., Flores-Garnica, J. G., Gonz´alez-Eguiarte, D. R., Gallegos-Rodríguez, A., Zarazúa-Villaseñor, P., & Mena-Munguía, S. (2021). Análisis comparativo de índices espectrales para ubicar y dimensionar niveles de severidad de incendios forestales. *Investigaciones Geográficas*, *106*. https://doi.org/10.14350/rig.60396

Fornacca, D., Ren, G., & Xiao, W. (2018). Evaluating the Best Spectral Indices for the Detection of Burn Scars at Several Post-Fire Dates in a Mountainous Region of Northwest Yunnan, China. *Remote Sensing*, *10*(8), 1196. https://doi.org/10.3390/rs10081196

García-Llamas, P., Suárez-Seoane, S., Taboada, A., Fernández-Manso, A., Quintano, C., Fernández-García, V., Fernández-Guisuraga, J. M., Marcos, E., & Calvo, L. (2019). Environmental drivers of fire severity in extreme fire events that affect Mediterranean pine forest ecosystems. *Forest Ecology and Management*, *433*, 24-32. https://doi.org/10.1016/j.foreco.2018.10.051

Gitelson, A. A., Viña, A., Ciganda, V., Rundquist, D. C., & Arkebauer, T. J. (2005). Remote estimation of canopy chlorophyll content in crops. *Geophysical Research Letters*, *32*(8), 2005GL022688. https://doi.org/10.1029/2005GL022688

Goetz, A. F. H. (2009). Three decades of hyperspectral remote sensing of the Earth: A personal view. *Remote Sensing of Environment*, *113*, S5-S16. https://doi.org/10.1016/j.rse.2007.12.014

Gonçalves, A. C., & Sousa, A. M. O. (2017). The Fire in the Mediterranean Region: A Case Study of Forest Fires in Portugal. En B. Fuerst-Bjelis (Ed.), *Mediterranean Identities—Environment, Society, Culture*. InTech. https://doi.org/10.5772/intechopen.69410

Gorelick, N., Hancher, M., Dixon, M., Ilyushchenko, S., Thau, D., & Moore, R. (2017). Google Earth Engine: Planetary-scale geospatial analysis for everyone. *Remote Sensing of Environment*, *202*, 18-27. https://doi.org/10.1016/j.rse.2017.06.031

Holden, Z. A., Morgan, P., & Evans, J. S. (2009). A predictive model of burn severity based on 20-year satellite-inferred burn severity data in a large southwestern US wilderness area. *Forest Ecology and Management*, *258*(11), 2399-2406. https://doi.org/10.1016/j.foreco.2009.08.017

Hudak, A. T., Morgan, P., Bobbitt, M. J., Smith, A. M. S., Lewis, S. A., Lentile, L. B., Robichaud, P. R., Clark, J. T., & McKinley, R. A. (2007). The Relationship of Multispectral Satellite Imagery to Immediate Fire Effects. *Fire Ecology*, *3*(1), 64-90. https://doi.org/10.4996/fireecology.0301064

Hunt, E. R., Hively, W. D., Fujikawa, S. J., Linden, D. S., Daughtry, C. S. T., & McCarty, G. W. (2010). Acquisition of NIR-Green-Blue Digital Photographs from Unmanned Aircraft for Crop Monitoring. *Remote Sensing*, *2*(1), 290-305. https://doi.org/10.3390/rs2010290

Imran, H. A., Gianelle, D., Rocchini, D., Dalponte, M., Martín, M. P., Sakowska, K., Wohlfahrt, G., & Vescovo, L. (2020). VIS-NIR, Red-Edge and NIR-Shoulder Based Normalized Vegetation Indices Response to Co-Varying Leaf and Canopy Structural Traits in Heterogeneous Grasslands. *Remote Sensing*, *12*(14), 2254. https://doi.org/10.3390/rs12142254

Keeley, J. E. (2009). Fire intensity, fire severity and burn severity: A brief review and suggested usage. *International Journal of Wildland Fire*, *18*(1), 116. https://doi.org/10.1071/WF07049

Key, C. H., & Benson, N. C. (2006). Landscape assessment (LA): Sampling and analysis methods. En *FIREMON: Fire effects monitoring and inventory system*. USDA Forest Service.

Lentile, L. B., Holden, Z. A., Smith, A. M. S., Falkowski, M. J., Hudak, A. T., Morgan, P., Lewis, S. A., Gessler, P. E., & Benson, N. C. (2006). Remote sensing techniques to assess active fire characteristics and post-fire effects. *International Journal of Wildland Fire*, *15*(3), 319. https://doi.org/10.1071/WF05097

Lentile, L. B., Smith, A. M. S., Hudak, A. T., Morgan, P., Bobbitt, M. J., Lewis, S. A., & Robichaud, P. R. (2009). Remote sensing for prediction of 1-year post-fire ecosystem condition. *International Journal of Wildland Fire*, *18*(5), 594. https://doi.org/10.1071/WF07091

Lewis, S. A., Hudak, A. T., Robichaud, P. R., Morgan, P., Satterberg, K. L., Strand, E. K., Smith, A. M. S., Zamudio, J. A., & Lentile, L. B. (2017). Indicators of burn severity at extended temporal scales: A decade of ecosystem response in mixed-conifer forests of western Montana. *International Journal of Wildland Fire*, *26*(9), 755. https://doi.org/10.1071/WF17019

Liu, H. Q., & Huete, A. (1995). A feedback based modification of the NDVI to minimize canopy background and atmospheric noise. *IEEE Transactions on Geoscience and Remote Sensing*, *33*(2), 457-465. https://doi.org/10.1109/36.377946

Liu, M., Yu, T., Gu, X., Sun, Z., Yang, J., Zhang, Z., Mi, X., Cao, W., & Li, J. (2020). The Impact of Spatial Resolution on the Classification of Vegetation Types in Highly Fragmented Planting Areas Based on Unmanned Aerial Vehicle Hyperspectral Images. *Remote Sensing*, *12*(1), 146. https://doi.org/10.3390/rs12010146

Liu, Y., Qian, J., & Yue, H. (2021). Comprehensive Evaluation of Sentinel-2 Red Edge and Shortwave-Infrared Bands to Estimate Soil Moisture. *IEEE Journal of Selected Topics in Applied Earth Observations and Remote Sensing*, *14*, 7448-7465. https://doi.org/10.1109/JSTARS.2021.3098513

Meng, R., & Zhao, F. (2017). Remote sensing of fire effects: A review for recent advances in burned area and burn severity mapping. En *Remote sensing of hydrometeoroloical hazards* (1st edition, pp. 261-283). CRC Press. https://www.taylorfrancis.com/chapters/edit/10.1201/9781315154947-12/remote-sensing-fire-effects-ran-meng-feng-zhao

Miller, J. D., & Thode, A. E. (2007). Quantifying burn severity in a heterogeneous landscape with a relative version of the delta Normalized Burn Ratio (dNBR). *Remote Sensing of Environment*, *109*(1), 66-80. https://doi.org/10.1016/j.rse.2006.12.006

Ministerio para la Transición Ecológica y el Reto Demográfico. (2025). *Mapa Forestal de España (MFE50)* [Dataset]. Banco de Datos de la Naturaleza (BDN). https://www.miteco.gob.es/es/biodiversidad/servicios/banco-datos-naturaleza/informacion-disponible/mfe50_descargas_ccaa.html

Morgan, P., Keane, R. E., Dillon, G. K., Jain, T. B., Hudak, A. T., Karau, E. C., Sikkink, P. G., Holden, Z. A., & Strand, E. K. (2014). Challenges of assessing fire and burn severity using field measures, remote sensing and modelling. *International Journal of Wildland Fire*, *23*(8), 1045. https://doi.org/10.1071/WF13058

Nagler, P. L., Daughtry, C. S. T., & Goward, S. N. (2000). Plant litter and soil reflectance. *Remote Sensing of Environment*, *71*, 207-215.

Ninyerola, M., Pons, X., & Roure, J. M. (2005). *Atlas climático digital de la Península Ibérica. Metodología y aplicaciones en bioclimatología y geobotánica*. Universitat Autónoma de

Barcelona. https://pascal-francis.inist.fr/vibad/index.php?action=getRecordDetail&idt=18200972

Oliveira, S., Oehler, F., San-Miguel-Ayanz, J., Camia, A., & Pereira, J. M. C. (2012). Modeling spatial patterns of fire occurrence in Mediterranean Europe using Multiple Regression and Random Forest. *Forest Ecology and Management*, *275*, 117-129. https://doi.org/10.1016/j.foreco.2012.03.003

Parsons, A., Robichaud, P. R., Lewis, S. A., Napper, C., & Clark, J. T. (2010). *Field guide for mapping post-fire soil burn severity* (RMRS-GTR-243; p. RMRS-GTR-243). U.S. Department of Agriculture, Forest Service, Rocky Mountain Research Station. https://doi.org/10.2737/RMRS-GTR-243

Peña, M. A., & Martínez, G. (2021). Mapeo del daño en bosques incendiados de Chile central, mediante el modelado de índices espectrales ex-ante y ex-post. *Bosque (Valdivia)*, *42*(2), 205-215. https://doi.org/10.4067/S0717-92002021000200205

Pour, A. B., Ranjbar, H., Sekandari, M., Abd El-Wahed, M., Hossain, M. S., Hashim, M., Yousefi, M., Zoheir, B., Wambo, J. D. T., & Muslim, A. M. (2023). Remote sensing for mineral exploration. En *Geospatial Analysis Applied to Mineral Exploration* (pp. 17-149). Elsevier. https://doi.org/10.1016/B978-0-323-95608-6.00002-0

Qiao, L., Tang, W., Gao, D., Zhao, R., An, L., Li, M., Sun, H., & Song, D. (2022). UAV-based chlorophyll content estimation by evaluating vegetation index responses under different crop coverages. *Computers and Electronics in Agriculture*, *196*, 106775. https://doi.org/10.1016/j.compag.2022.106775

Quintano, C., Calvo, L., Fernández-Manso, A., Suárez-Seoane, S., Fernandes, P. M., & Fernández-Guisuraga, J. M. (2023). First evaluation of fire severity retrieval from PRISMA hyperspectral data. *Remote Sensing of Environment*, *295*, 113670. https://doi.org/10.1016/j.rse.2023.113670

R Development Core Team. (2019). *R: A Language and Environmenta for Statistical Computing* [Software]. R Foundation for Statistical Computing. http://www.r-project.org/

Robichaud, P. R., Lewis, S. A., Laes, D. Y. M., Hudak, A. T., Kokaly, R. F., & Zamudio, J. A. (2007). Postfire soil burn severity mapping with hyperspectral image unmixing. *Remote Sensing of Environment*, *108*(4), 467-480. https://doi.org/10.1016/j.rse.2006.11.027

Rodríguez-Trejo, D. A., & Fulé, P. Z. (2003). Fire ecology of Mexican pines and a fire management proposal. *International Journal of Wildland Fire*, *12*(1), 23. https://doi.org/10.1071/WF02040

Strong, C. J., Burnside, N. G., & Llewellyn, D. (2017). The potential of small-Unmanned Aircraft Systems for the rapid detection of threatened unimproved grassland communities using an Enhanced Normalized Difference Vegetation Index. *PLOS ONE*, *12*(10), e0186193. https://doi.org/10.1371/journal.pone.0186193

Tane, Z., Roberts, D., Veraverbeke, S., Casas, Á., Ramirez, C., & Ustin, S. (2018). Evaluating Endmember and Band Selection Techniques for Multiple Endmember Spectral Mixture Analysis using Post-Fire Imaging Spectroscopy. *Remote Sensing*, *10*(3), 389. https://doi.org/10.3390/rs10030389

Tessler, N., Sapir, Y., Wittenberg, L., & Greenbaum, N. (2016). Recovery of Mediterranean Vegetation after Recurrent Forest Fires: Insight from the 2010 Forest Fire on Mount Carmel, Israel. *Land Degradation & Development*, *27*(5), 1424-1431. https://doi.org/10.1002/ldr.2419

Transon, J., D'Andrimont, R., Maugnard, A., & Defourny, P. (2018). Survey of Hyperspectral Earth Observation Applications from Space in the Sentinel-2 Context. *Remote Sensing*, *10*(2), 157. https://doi.org/10.3390/rs10020157

Vangi, E., D'Amico, G., Francini, S., Giannetti, F., Lasserre, B., Marchetti, M., & Chirici, G. (2021). The New Hyperspectral Satellite PRISMA: Imagery for Forest Types Discrimination. *Sensors*, *21*(4), 1182. https://doi.org/10.3390/s21041182

Veraverbeke, S., Lhermitte, S., Verstraeten, W. W., & Goossens, R. (2010). The temporal dimension of differenced Normalized Burn Ratio (dNBR) fire/burn severity studies: The case of the large 2007 Peloponnese wildfires in Greece. *Remote Sensing of Environment*, *114*(11), 2548-2563. https://doi.org/10.1016/j.rse.2010.05.029

Veraverbeke, S., Stavros, E. N., & Hook, S. J. (2014). Assessing fire severity using imaging spectroscopy data from the Airborne Visible/Infrared Imaging Spectrometer (AVIRIS) and comparison with multispectral capabilities. *Remote Sensing of Environment*, *154*, 153-163. https://doi.org/10.1016/j.rse.2014.08.019

Wang, B., Dai, D., Yu, D., Gao, W., Feng, J., Zhou, S., Liu, Y., Tu, L., Cao, D., Huang, C., He, X., & Cui, X. (2024). The variation in climate conditions and fire-related traits across Pinus (Pinaceae) species. *Global Ecology and Conservation*, *54*, e03152. https://doi.org/10.1016/j.gecco.2024.e03152

Yin, C., He, B., Yebra, M., Quan, X., Edwards, A. C., Liu, X., & Liao, Z. (2020). Improving burn severity retrieval by integrating tree canopy cover into radiative transfer model simulation. *Remote Sensing of Environment*, *236*, 111454. https://doi.org/10.1016/j.rse.2019.111454

ANNEX 1 – Field data

A1.1. Composite Burn Index (CBI) mean values for study plots in the Sierra de la Culebra Wildfire.

Ecosystem type	Number of plots	CBI mean values		
		Vegetation	Soil	Site
Coniferous forest	34	2.25	1.82	2.03
Broadleaf forest	20	1.82	1.52	1.67
Shrubland	16	2.07	1.68	1.88
Total	**70**	**2.09**	**1.70**	**1.89**

ANNEX 2 – Wavelengths of PRISMA hyperspectral imagery

A2.1. Spectral band alignment of PRISMA based on Sentinel-2 wavelengths

Hyperspectral band name	Multispectral band name	Wavelength (nm)
1	Blue	434.31
2	Blue	441.66
3	Blue	449.03
4	Blue	456.38
5	Blue	463.73
6	Blue	470.95
7	Blue	478.18
8	Blue	485.41
9	Blue	492.70
10	Green	500.14
11	Green	507.66
12	Green	515.18
13	Green	522.92
14	Green	530.67
15	Green	538.49
16	Green	546.48
17	Green	554.56
18	Green	562.74
19	Green	571.00
20	Green	579.35
21	Green	587.82
22	Green	596.48
23	Red	605.39
24	Red	614.17
25	Red	623.20
26	Red	632.13
27	Red	641.33
28	Red	650.79
29	Red	660.26
30	Red	669.82
31	Red	679.47
32	Red	689.42
33	Red	699.10
34	Red Edge	709.00
35	Red Edge	719.17
36	Red Edge	729.24
37	Red Edge	739.42
38	Red Edge	749.73
39	NIR	760.10
40	NIR	770.53

41	NIR	780.91
42	NIR	791.36
43	NIR	801.94
44	NIR	812.54
45	NIR	823.15
46	NIR	833.75
47	NIR	844.43
48	NIR	855.18
49	NIR	865.95
50	NIR	876.64
51	NIR	887.27
52	NIR	897.99
53	NIR	908.64
54	NIR	919.18
55	NIR	929.39
56	NIR	939.86
57	NIR	951.36
58	NIR	962.26
59	NIR	972.63
60	NIR	951.01
61	NIR	959.52
62	NIR	969.39
63	NIR	978.74
64	NIR	988.41
65	NIR	998.37
66	NIR	1008.17
67	NIR	1017.98
68	NIR	1028.81
69	NIR	1037.76
70	NIR	1047.43
71	SWIR 1	1057.38
72	SWIR 1	1067.61
73	SWIR 1	1078.04
74	SWIR 1	1088.59
75	SWIR 1	1099.11
76	SWIR 1	1109.74
77	SWIR 1	1120.49
78	SWIR 1	1131.14
79	SWIR 1	1141.87
80	SWIR 1	1152.47
81	SWIR 1	1163.48
82	SWIR 1	1174.53
83	SWIR 1	1185.40
84	SWIR 1	1196.17
85	SWIR 1	1207.11

86	SWIR 1	1217.70
87	SWIR 1	1229.00
88	SWIR 1	1240.06
89	SWIR 1	1250.80
90	SWIR 1	1262.33
91	SWIR 1	1273.31
92	SWIR 1	1284.28
93	SWIR 1	1295.20
94	SWIR 1	1306.05
95	SWIR 1	1317.02
96	SWIR 1	1328.09
97	SWIR 1	1338.95
98	SWIR 1	1349.60
99	SWIR 1	1459.07
100	SWIR 1	1469.70
101	SWIR 1	1480.62
102	SWIR 1	1491.20
103	SWIR 1	1501.78
104	SWIR 1	1512.41
105	SWIR 1	1523.01
106	SWIR 1	1533.56
107	SWIR 1	1544.03
108	SWIR 1	1554.58
109	SWIR 1	1565.12
110	SWIR 1	1575.39
111	SWIR 1	1585.63
112	SWIR 1	1595.98
113	SWIR 1	1606.24
114	SWIR 1	1616.58
115	SWIR 1	1626.78
116	SWIR 1	1636.85
117	SWIR 1	1646.97
118	SWIR 1	1656.77
119	SWIR 1	1666.97
120	SWIR 1	1677.12
121	SWIR 1	1687.17
122	SWIR 1	1697.01
123	SWIR 1	1706.81
124	SWIR 1	1716.60
125	SWIR 1	1726.44
126	SWIR 1	1736.26
127	SWIR 1	1745.93
128	SWIR 1	1755.55
129	SWIR 1	1765.25
130	SWIR 1	1774.91

131	SWIR 2	1975.78
132	SWIR 2	1984.55
133	SWIR 2	1993.29
134	SWIR 2	2036.00
135	SWIR 2	2044.42
136	SWIR 2	2052.76
137	SWIR 2	2061.14
138	SWIR 2	2069.54
139	SWIR 2	2077.75
140	SWIR 2	2086.10
141	SWIR 2	2094.41
142	SWIR 2	2102.55
143	SWIR 2	2110.82
144	SWIR 2	2118.96
145	SWIR 2	2127.09
146	SWIR 2	2135.24
147	SWIR 2	2143.23
148	SWIR 2	2151.13
149	SWIR 2	2159.29
150	SWIR 2	2167.25
151	SWIR 2	2175.07
152	SWIR 2	2183.18
153	SWIR 2	2190.84
154	SWIR 2	2198.89
155	SWIR 2	2206.60
156	SWIR 2	2214.34
157	SWIR 2	2222.19
158	SWIR 2	2229.75
159	SWIR 2	2237.65
160	SWIR 2	2245.21
161	SWIR 2	2252.85
162	SWIR 2	2260.63
163	SWIR 2	2268.04
164	SWIR 2	2275.77
165	SWIR 2	2283.28
166	SWIR 2	2290.57
167	SWIR 2	2298.33
168	SWIR 2	2305.50
169	SWIR 2	2312.91
170	SWIR 2	2320.64
171	SWIR 2	2327.61
172	SWIR 2	2335.24
173	SWIR 2	2342.59
174	SWIR 2	2349.58
175	SWIR 2	2357.02

176	SWIR 2	2364.37
177	SWIR 2	2371.34
178	SWIR 2	2378.51
179	SWIR 2	2385.81
180	SWIR 2	2392.84
181	SWIR 2	2399.80
182	SWIR 2	2407.34
183	SWIR 2	2414.16
184	SWIR 2	2420.99
185	SWIR 2	2428.40
186	SWIR 2	2435.33
187	SWIR 2	2442.19
188	SWIR 2	2448.92
189	SWIR 2	2456.33
190	SWIR 2	2462.81
191	SWIR 2	2469.42

A2.2. Spectral characteristics of Sentinel-2 bands

Band	Multispectral band name	Band range (nm)	Spatial resolution (m)
B2	Blue	458-523	10
B3	Green	543-578	10
B4	Red	650-680	10
B5	Red edge	698-713	20
B6	Red edge	734-748	20
B7	Red edge	765-785	20
B8	NIR	785-900	10
B8A	NIR	855-875	20
B11	SWIR 1	1565-1655	20
B12	SWIR 2	2100-2280	20

Source: (Pour et al., 2023)

ANNEX 3 – Vegetation indices formulas

A3.1. Summary of Vegetation Indices with Formulas, Applications, and References (H: Hyperspectral; M: Multispectral)

R, G, and B represent the proportions of red, green, and blue light reflected by vegetation, each normalized by the sum of all three bands (R = red / (red + green + blue), and similarly for G and B).

Vegetation index	Formula	Applied in	Reference
Normalized Difference Vegetation Index: NDVI	$ndvi = \frac{(nir - red)}{(nir + red)}$	H & M	(Rouse et al., 1974)
Normalized Burn Ratio: NBR	$nbr = \frac{(nir - swir2)}{(nir + swir2)}$	H & M	(García & Caselles, 1991)
Normalized Difference Moisture Index: NDMI	$ndmi = \frac{(nir - swir1)}{(nir + swir1)}$	H & M	(Shi et al., 2016)
Difference Vegetation Index: DVI	$dvi = nir - red$	H & M	(Jordan, 1969)
Green Difference Vegetation Index: GDVI	$dvigre = nir - green$	H & M	(Jordan, 1969)
Red Edge Difference Vegetation Index: DVIRED	$dvired = nir - redge$	H & M	(Jordan, 1969)
Chlorophyll Index With Red Edge: CIREDGE	$ciredge = \frac{nir}{redge} - 1$	H & M	(A. A. Gitelson et al., 2005)
Chlorophyll Index With Green: CIGREEN	$cigreen = \frac{nir}{green} - 1$	H & M	(A. A. Gitelson et al., 2003)
Infrared Percentage Vegetation Index: IPVI	$ipvi = \frac{nir}{(nir + red)}$	H & M	(Jabbar & Chen, 2006)
Near-Infrared Reflectance of Vegetation: NIRV	$nirv = nir * \frac{(nir - red)}{(nir + red)}$	H & M	(Zeng et al., 2021)
Modified Non-Linear Index: MNLI	$mnli = 1.5 * \frac{(nir^2 - red)}{(nir^2 + red + 0.5)}$	H & M	(Z. Yang et al., 2008)
Non-Linear Index: NLI	$nli = \frac{(nir^2 - red)}{(nir^2 + red)}$	H & M	(Goel & Qin, 1994)
Wide Dynamic Range Vegetation Index: WDRVI	$wdrvi = \frac{(0.2 * nir - red)}{(0.2 * nir + red)}$	H & M	(A. A. Gitelson, 2004)

Normalized Difference Red Edge Index: NDRE	$ndre = \frac{(nir - redge)}{(nir + redge)}$	H & M	(F. Li et al., 2014)
Burn Area Index: BAI	$bai = \frac{1}{((redge - 0.1)^2 + (nir - 0.06)^2)}$	H & M	(Fornacca et al., 2018)
Structural Vegetation Index: SVI	$svi = \frac{(redge - red)}{(redge + red)}$	H & M	(R. Li et al., 2024)
Modified Red-Edge Simple Ratio: MRESR	$mresr = \frac{nir}{redge}$	H & M	(Hallik et al., 2019)
Three-Band Difference Vegetation Index: TBDVI	$tbdvi = nir - \frac{(red + swir1)}{2}$	H & M	(Zhao et al., 2024)
Enhanced Vegetation Index: EVI	$evi = 2.5 * \frac{(nir - red)}{(nir + 6 * red - 7.5 * blue + 1)}$	H & M	(Liu & Huete, 1995)
Excess Green Index: EXG2	$exg2 = 2 * green - red - blue$	H & M	(Woebbecke et al., 1995)
Red Light Normalized Value: NRI	$nri = \frac{red}{(red + green + blue)}$	H & M	(Silleos et al., 2006)
Green Light Normalized Value: NGI	$ngi = \frac{green}{(red + green + blue)}$	H & M	(Silleos et al., 2006)
Green Normalized Difference Vegetation Index: GNDVI	$gndvi = \frac{(nir - green)}{(nir + redge)}$	H & M	(A. A. Gitelson & Merzlyak, 1998)
Enhances Normalized Difference Vegetation Index: ENDVI	$endvi = \frac{(redge + green - 2 * blue)}{(redge + green + 2 * blue)}$	H & M	(Traba et al., 2022)
Modified Red Green- Blue Vegetation Index: MRGBVI	$mrgbvi = \frac{(redge + 2 * green - 2 * blue)}{(redge + 2 * green + 2 * blue)}$	H & M	(Guo et al., 2022)
Nitrogen Reflectance Index: NREI	$nrei = \frac{redge}{(redge + nir + green)}$	H & M	(Diker & Bausch, 2003)
Red Edge Position Index: REP	$rep = 700 + 40 * \frac{(red + nir)}{(2 - redge)}$	H & M	(Clevers et al., 2001)
Excess Green Index: EXG	$exg = 2 * G - R - B$	H & M	(Qiao et al., 2022)
Excess Blue Index: EXB	$exb = 1.4 * R - G$	H & M	(Meyer & Neto, 2008)
Excess Red Index: EXR	$exr = 1.4 * B - G$	H & M	(Guijarro et al., 2011)
Red / Green Ratio: RGR	$rgr = \frac{R}{G}$	H & M	(Gamon & Surfus, 1999)

Blue / Green Ratio: BGR	$bgr = \frac{B}{G}$	H & M	(Sellaro et al., 2010)
Normalized Green-Red Difference Index: NGRDI	$ngrdi = \frac{(G-R)}{(G+R)}$	H & M	(Tucker, 1979)
Normalized Green-Blue Difference Index: NGBDI	$ngbdi = \frac{(G-B)}{(G+B)}$	H & M	(Hunt et al., 2005)
Modified Green-Red Vegetation Index: MGRVI	$mgrvi = \frac{(G^2-R^2)}{(G^2+R^2)}$	H & M	(Bendig et al., 2015)
Red Green- Blue Vegetation Index: RGBVI	$rgbvi = \frac{(G^2-R*B)}{(G^2+R*B)}$	H & M	(Bendig et al., 2015)
Green Leaf Index: GLI	$gli = \frac{(2*G-R-B)}{(2*G+R+B)}$	H & M	(Louhaichi et al., 2001)
Color Index of Vegetation Extraction: CIVE	$cive = 0.441*R - 0.881*G + 0.385*R + 1878745$	H & M	(Kataoka et al., 2003)
Excess Green Minus Excess Red Index: ExGR	$exgr = exg - exr$	H & M	(Meyer & Neto, 2008)
Improved Red Green- Blue Vegetation Index: IRGBVI	$irgbvi = \frac{(5*G^2-2*R^2-5*B^2)}{(5*G^2+2*R^2+5*B^2)}$	H & M	(C. Chen et al., 2024)
Greenness Index: G	$g = \frac{\rho_{554}}{\rho_{677}}$	H	(Xue & Su, 2017)
Simple R. Pigment Ind.: SRPI	$srpi = \frac{\rho_{430}}{\rho_{680}}$	H	(Xue & Su, 2017)
Lichtenthaler Index 2: Lic2	$lic2 = \frac{\rho_{440}}{\rho_{690}}$	H	(Xue & Su, 2017)
Carter Index 1: Ctr1	$ctr1 = \frac{\rho_{695}}{\rho_{420}}$	H	(Xue & Su, 2017)
Carter Index 2: Ctr2	$ctr2 = \frac{\rho_{695}}{\rho_{760}}$	H	(Xue & Su, 2017)
Vogelmann Index 1: Vog1	$vog1 = \frac{\rho_{740}}{\rho_{720}}$	H	(Vogelmann et al., 1993)
Gitelson and Merzlyak Index 1: GM1	$gm1 = \frac{\rho_{750}}{\rho_{550}}$	H	(Xue & Su, 2017)
Gitelson and Merzlyak Index 2: GM2	$gm2 = \frac{\rho_{750}}{\rho_{700}}$	H	(Xue & Su, 2017)
Zarco-Tejada & Miller: ZM	$zm = \frac{\rho_{750}}{\rho_{710}}$	H	(Xue & Su, 2017)
Fluorescence Ratio Index 1: FRI1	$fri1 = \frac{\rho_{740}}{\rho_{800}}$	H	(Dobrowski et al., 2005)
Fluorescence Ratio Index 2: FRI2	$fri2 = \frac{\rho_{690}}{\rho_{600}}$	H	(Dobrowski et al., 2005)

Simple Ratio Index: SR	$sr = \frac{\rho_{800}}{\rho_{670}}$	H	(Birth & McVey, 1968)
Water Index: WI1	$wi1 = \frac{\rho_{900}}{\rho_{970}}$	H	(Xue & Su, 2017)
Water Index: WI2	$wi2 = \frac{\rho_{1600}}{\rho_{820}}$	H	(Xue & Su, 2017)
Moisture Stress Index: MSI	$msi = \frac{\rho_{1599}}{\rho_{819}}$	H	(Hunt Jr & Rock, 1989)
Ratio Vegetation Index: RVI	$rvi = \frac{\rho_{887}}{\rho_{678}}$	H	(X. L. Gao & Wang, 2008)
Green Ratio Vegetation Index: GRVI	$grvi = \frac{\rho_{865}}{\rho_{550}}$	H	(Xue & Su, 2017)
Green Red Ratio Vegetation Index: GR	$gr = \frac{\rho_{550}}{\rho_{650}}$	H	(Xue & Su, 2017)
Green Blue Ratio Vegetation Index: GB	$gb = \frac{\rho_{550}}{\rho_{485}}$	H	(Xue & Su, 2017)
Vegetation Index 8 :VI8	$vi8 = \frac{\rho_{998}}{\rho_{713}}$	H	(Jiang et al., 2022)
Water Band Index: WBI	$wbi = \frac{\rho_{970}}{\rho_{900}}$	H	(Peñuelas et al., 1994)
Normalized Phaeophytinization Index: NPQI	$npqi = \frac{(\rho_{415} - \rho_{435})}{(\rho_{415} + \rho_{435})}$	H	(Peñuelas et al., 1995)
Photochemical Reflectance Index 1: PRI1	$pri1 = \frac{(\rho_{528} - \rho_{567})}{(\rho_{528} + \rho_{567})}$	H	(Xue & Su, 2017)
Normalized Pigment Chlorophyll Index: NPCI	$npci = \frac{(\rho_{680} - \rho_{430})}{(\rho_{680} + \rho_{430})}$	H	(Xue & Su, 2017)
Lichtenthaler Index 1: Lic1	$lic1 = \frac{(\rho_{800} - \rho_{680})}{(\rho_{800} + \rho_{680})}$	H	(Xue & Su, 2017)
Visible Atmospherically Resistant Index: VARI	$vari = \frac{(\rho_{550} - \rho_{670})}{(\rho_{550} + \rho_{670})}$	H	(Xue & Su, 2017)
Normalized Difference Water Index: NDWI	$ndwi = \frac{(\rho_{800} - \rho_{1600})}{(\rho_{800} + \rho_{1600})}$	H	(Xue & Su, 2017)
Normalized Difference Water Index 2: NDWI2	$ndwi2 = \frac{(\rho_{857} - \rho_{1241})}{(\rho_{857} + \rho_{1241})}$	H	(B. Gao, 1996)
Depth Water Index: DWI	$dwi = \frac{(\rho_{816} - \rho_{2218})}{(\rho_{816} + \rho_{2218})}$	H	(Pasqualotto et al., 2018)
Hyperspectral Fire Detection Index: HFDI	$hfdi = \frac{(\rho_{2430} - \rho_{2060})}{(\rho_{2430} + \rho_{2060})}$	H	(Dennison & Roberts, 2009)

Vegetation Index 7 :VI7	$vi7 = \frac{(\rho_{998} - \rho_{713})}{(\rho_{998} + \rho_{713})}$	H	(Jiang et al., 2022)
Normalized Difference Vegetation Index red-edge 1: NDVIre1	$ndvire1 = \frac{(\rho_{833} - \rho_{699})}{(\rho_{833} + \rho_{699})}$	H	(A. Gitelson & Merzlyak, 1994)
Normalized Difference Vegetation Index red-edge 1: NDVIre1n	$ndvire1n = \frac{(\rho_{865} - \rho_{699})}{(\rho_{865} + \rho_{699})}$	H	(A. Gitelson & Merzlyak, 1994)
Normalized Difference Vegetation Index red-edge 2: NDVIre2	$ndvire2 = \frac{(\rho_{833} - \rho_{729})}{(\rho_{833} + \rho_{729})}$	H	(A. Gitelson & Merzlyak, 1994)
Normalized Difference Vegetation Index red-edge 2: NDVIre2n	$ndvire2n = \frac{(\rho_{865} - \rho_{729})}{(\rho_{865} + \rho_{729})}$	H	(A. Gitelson & Merzlyak, 1994)
Normalized Difference Vegetation Index red-edge 3: NDVIre3	$ndvire3 = \frac{(\rho_{833} - \rho_{780})}{(\rho_{833} + \rho_{780})}$	H	(A. Gitelson & Merzlyak, 1994)
Normalized Difference Vegetation Index red-edge 3: NDVIre3n	$ndvire3n = \frac{(\rho_{865} - \rho_{780})}{(\rho_{865} + \rho_{780})}$	H	(A. Gitelson & Merzlyak, 1994)
Normalized Difference red-edge 1: NDre1	$ndre1 = \frac{(\rho_{729} - \rho_{699})}{(\rho_{729} + \rho_{699})}$	H	(A. Gitelson & Merzlyak, 1994)
Normalized Difference red-edge 2: NDre2	$ndre2 = \frac{(\rho_{780} - \rho_{699})}{(\rho_{780} + \rho_{699})}$	H	(Barnes et al., 2000)
Leaf Water Vegetation Index 1: LWVI1	$lwvi1 = \frac{(\rho_{1099} - \rho_{988})}{(\rho_{1099} + \rho_{988})}$	H	(Galvão et al., 2005)
Leaf Water Vegetation Index 2: LWVI2	$lwvi2 = \frac{(\rho_{1099} - \rho_{1207})}{(\rho_{1099} + \rho_{1207})}$	H	(Galvão et al., 2005)
Normalized Difference Infrared Index: NDII	$ndii = \frac{(\rho_{823} - \rho_{1646})}{(\rho_{823} + \rho_{1646})}$	H	(Hardisky et al., 1983)
Structure Intensive Pigment Index: SIPI	$sipi = \frac{(\rho_{800} - \rho_{450})}{(\rho_{800} + \rho_{650})}$	H	(Fiodortsev et al., 2019)
Meris Terrestrial Chlorophyll Index: MTCI	$mtci = \frac{(\rho_{865} - \rho_{717})}{(\rho_{865} - \rho_{650})}$	H	(Zhang & Liu, 2014)

Leaf Chlorophyll Index: LCI	$lci = \frac{(\rho_{855} - \rho_{708})}{(\rho_{855} + \rho_{679})}$	H	(Datt, 1999)
Mangrove Vegetation Index: MVI	$mvi = \frac{(\rho_{842} - \rho_{561})}{(\rho_{1610} - \rho_{561})}$	H	(G. Yang et al., 2022)
Vogelmann Index 2: Vog2	$vog2 = \frac{(\rho_{734} - \rho_{747})}{(\rho_{715} + \rho_{726})}$	H	(Xue & Su, 2017)
Vogelmann Index 3: Vog3	$vog3 = \frac{(\rho_{734} - \rho_{747})}{(\rho_{715} + \rho_{720})}$	H	(Xue & Su, 2017)
Disease Water Stress Index: DWSI	$dwsi = \frac{(\rho_{801} - \rho_{546})}{(\rho_{1656} + \rho_{879})}$	H	(Galvão et al., 2005)
Vegetation Index 5: VI5	$vi5 = \frac{((\rho_{513})^2 - (\rho_{504})^2)}{((\rho_{513})^2 + (\rho_{504})^2)}$	H	(Jiang et al., 2022)
Simple Ratio red-edge 1: SRre1	$srre1 = \frac{(\rho_{729} - \rho_{441})}{(\rho_{699} - \rho_{441})}$	H	(Sims & Gamon, 2002)
Simple Ratio red-edge 2: SRre2	$srre2 = \frac{(\rho_{780} - \rho_{441})}{(\rho_{699} - \rho_{441})}$	H	(Sims & Gamon, 2002)
Structure Independent Pigment Index: SIPI1	$sipi1 = \frac{(\rho_{445} - \rho_{800})}{(\rho_{670} + \rho_{800})}$	H	(Peñuelas et al., 1994)
Renormalized Difference Vegetation Index: RDVI	$rdvi = \frac{({}^{\rho_{800}}/_{\rho_{670}})}{\sqrt{({}^{\rho_{800}}/_{\rho_{670}})}}$	H	(Roujean & Breon, 1995)
Renormalized Difference Vegetation Index: RDVI2	$rdvi2 = \frac{({}^{\rho_{865}}/_{\rho_{670}})}{\sqrt{({}^{\rho_{865}}/_{\rho_{670}})}}$	H	(Roujean & Breon, 1995)
Red Difference Vegetation Index With Red Edge: RDVIREG	$rdvireg = \frac{(\rho_{865} - \rho_{717})}{\sqrt{(\rho_{865} + \rho_{717})}}$	H	(Qiao et al., 2022)
Modified Simple Ratio: MSR	$msr = \frac{(\rho_{865} - (\rho_{660} - 1))}{\sqrt{(\rho_{865} + (\rho_{660} + 1))}}$	H	(J. M. Chen, 1996)
Modified Simple Ratio With Red Edge: MSRREG	$msrreg = \frac{({}^{\rho_{865}}/_{(\rho_{717} - 1)})}{\sqrt{({}^{\rho_{865}}/_{(\rho_{717} + 1)})}}$	H	(C. Wu et al., 2008)
Modified Simple Ratio Index: MSR2	$msr2 = \frac{(({}^{\rho_{800}}/_{\rho_{670}}) - 1)}{\sqrt{(({}^{\rho_{800}}/_{\rho_{670}}) + 1)}}$	H	(Xue & Su, 2017)
Optimized Soil-Adjusted Vegetation Index: OSAVI	$osavi = \frac{(1 + 0.16) * (\rho_{800} - \rho_{670})}{(\rho_{800} + \rho_{670} + 0.16)}$	H	(Rondeaux et al., 1996)
Soil-Adjusted Vegetation Index: SAVI	$savi = \frac{(1 + 0.16) * (\rho_{887} - \rho_{678})}{(\rho_{887} + \rho_{678} + 0.16)}$	H	(Huete, 1988)

Optimized Soil-adjusted Vegetation Index With Red Edge: OSAVIREG	$osavireg = \frac{(1+0.16)*(\rho_{865}-\rho_{717})}{(\rho_{865}+\rho_{717}+0.16)}$	H	(Qiao et al., 2022)
Green Soil Adjusted Vegetation Index: GSAVI	$gsavi = \frac{1.5*(\rho_{800}-\rho_{560})}{(\rho_{800}+\rho_{560}+0.5)}$	H	(Sripada, 2005)
Modified Chlorophyll Absorption in Reflectance Index 1: MCARI1	$mcari1 = \left((\rho_{700}-\rho_{670})-0.2*(\rho_{700}-\rho_{550})\right)*(\frac{\rho_{700}}{\rho_{670}})$	H	(Xue & Su, 2017)
Modified Chlorophyll Absorption in Reflectance Index 2: MCARI2	$mcari2 = 1.2*[2.5*(\rho_{800}-\rho_{670})-1.3*(\rho_{800}-\rho_{550})]$	H	(Xue & Su, 2017)
Modified Chlorophyll Absorption in Reflectance Index 3: MCARI3	$mcari3 = \frac{1.5*[2.5*(\rho_{800}-\rho_{670})-1.3*(\rho_{800}-\rho_{550})]}{(2*\rho_{800}+1)^2-\sqrt{(6*\rho_{800}-5*\sqrt{\rho_{670}}-0.5)}}$	H	(Xue & Su, 2017)
Transformed CARI: TCARI	$tcari = 3*[(\rho_{700}-\rho_{670})-0.2*(\rho_{700}-\rho_{550})*\left(\frac{\rho_{700}}{\rho_{670}}\right)]$	H	(Xue & Su, 2017)
Triangular Vegetation Index: TVI	$tvi = 0.5*[120*(\rho_{750}-\rho_{550})-200*(\rho_{670}-\rho_{550})]$	H	(Xue & Su, 2017)
Modified Triangular Vegetation Index 1: MTVI1	$mtvi1 = 1.2*[1.2*(\rho_{800}-\rho_{550})-2.5*(\rho_{670}-\rho_{550})]$	H	(Xue & Su, 2017)
Modified Triangular Vegetation Index 2: MTVI2	$mtvi2 = \frac{1.5*[1.2*(\rho_{800}-\rho_{550})-2.5*(\rho_{670}-\rho_{550})]}{\sqrt{(2*\rho_{800}+1)^2-\left(6*\rho_{800}-\left(5*\sqrt{\rho_{670}}\right)\right)-0.5}}$	H	(Xue & Su, 2017)
Improved SAVI with self-adjustment factor L: MSAVI	$msavi = 0.5*[2*\rho_{800}+1-\sqrt{((2*\rho_{800}+1)^2-8*(\rho_{800}-\rho_{670}))}]$	H	(Wan et al., 2019)
Enhanced Vegetation Index 2: EVI2	$evi2 = 2.5*\frac{\rho_{800}-\rho_{670}}{\rho_{800}+2.4*\rho_{670}+1}$	H	(Xue & Su, 2017)
Combine Mangrove Recognition Index (CMRI)	$cmri = \frac{(\rho_{865}-\rho_{660})}{(\rho_{865}+\rho_{660})}+\frac{(\rho_{857}-\rho_{1241})}{(\rho_{857}+\rho_{1241})}$	H	(Xue & Su, 2017)
Temperature Condition Index: TCI	$tci = \frac{\rho_{887}+1.5*\rho_{524}-\rho_{678}}{\rho_{887}+\rho_{701}}$	H	(Zhou et al., 2018)

Normalized Red Green Difference Vegetation Index: NDIG	$ndig = \frac{\rho_{650} - \rho_{560}}{\rho_{650} + \rho_{560} + 0.01}$	H	(W. Wu, 2016)
Normalized Red Blue Difference Vegetation Index: NDIB	$ndib = \frac{\rho_{650} - \rho_{485}}{\rho_{650} + \rho_{485} + 0.01}$	H	(W. Wu, 2016)
Soil-adjusted Vegetation Index with Green: SAVIGRE	$savigre = 1.5 * \frac{\rho_{865} - \rho_{560}}{\rho_{865} + \rho_{560} + 0.5}$	H	(Huete, 1988)
Visible Atmospherically Resistant Index: VARI2	$vari2 = \frac{\rho_{560} - \rho_{650}}{\rho_{560} + \rho_{650} - \rho_{485}}$	H	(A. A. Gitelson, Kaufman, et al., 2002)
Green Atmospherically Resistant Index: GARI	$gari = \frac{\rho_{865} - \rho_{560} + 1.7 * (\rho_{485} - \rho_{650})}{\rho_{865} + \rho_{560} - 1.7 * (\rho_{485} - \rho_{650})}$	H	(A. A. Gitelson et al., 1996)
Carbon Dioxide Continuum Interpolated Band Ratio: CO2-CIBR	$co2 - cibr = \frac{\rho_{2010}}{0.666 * \rho_{1990} + 0.334 * \rho_{2040}}$	H	(Dennison, 2006)
Vegetation Index 1: VI1	$vi1 = \frac{\rho_{712}}{\rho_{998} + \rho_{693}}$	H	(Jiang et al., 2022)
Vegetation Index 3: VI3	$vi3 = \frac{\rho_{708} - \rho_{693}}{\rho_{758}}$	H	(Jiang et al., 2022)
Plant Senescence Reflectance Index: PSRI	$psri = \frac{\rho_{660} - \rho_{554}}{\rho_{729}}$	H	(Merzlyak et al., 1999)
Vegetation Index 6: VI6	$vi6 = \frac{1}{\rho_{1000}} - \frac{1}{\rho_{713}}$	H	(Jiang et al., 2022)
Anthocyanin Reflectance Index 1: ARI1	$ari1 = \frac{1}{\rho_{554}} - \frac{1}{\rho_{699}}$	H	(A. A. Gitelson et al., 2001)
Carotenoid Reflectance Index 1: CRI1	$cri1 = \frac{1}{\rho_{507}} - \frac{1}{\rho_{546}}$	H	(A. A. Gitelson, Stark, et al., 2002)
Carotenoid Reflectance Index 2: CRI2	$cri2 = \frac{1}{\rho_{507}} - \frac{1}{\rho_{699}}$	H	(A. A. Gitelson, Stark, et al., 2002)
Chlorophyll Index red-edge: Clre	$clre = \frac{\rho_{780}}{\rho_{699}} - 1$	H	(A. A. Gitelson et al., 2003)
Normalized Difference red-edge 1 modified: NDre1m	$ndre1m = \frac{\rho_{729} - \rho_{699}}{\rho_{729} + \rho_{699} - 2 * \rho_{441}}$	H	(Sims & Gamon, 2002)

Normalized Difference red-edge 2 modified: NDre2m	$ndre2m = \frac{\rho_{780} - \rho_{699}}{\rho_{780} + \rho_{699} - 2 * \rho_{441}}$	H	(Sims & Gamon, 2002)
Modified Simple Ratio red-edge: MSRre	$msrre = \frac{\rho_{833}/\rho_{699} - 1}{\sqrt{\rho_{833}/\rho_{699} + 1}}$	H	(J. M. Chen, 1996)
Modified Simple Ratio red-edge narrow: MSRren	$msrren = \frac{\rho_{865}/\rho_{699} - 1}{\sqrt{\rho_{865}/\rho_{699} + 1}}$	H	(Fernández-Manso et al., 2016)
Atmospherically Resistant Vegetation Index: ARVI	$arvi = \frac{\rho_{801} - (\rho_{679} - (\rho_{449} - \rho_{679}))}{\rho_{801} + (\rho_{679} - (\rho_{449} - \rho_{679}))}$	H	(A. A. Gitelson, Stark, et al., 2002)
Modified Red Edge Normalized Difference Vegetation Index: MRENDVI	$mrendvi = \frac{\rho_{749} - \rho_{708}}{\rho_{749} + \rho_{708} - 2 * \rho_{441}}$	H	(Sims & Gamon, 2002)
Normalized Difference Nitrogen Index: NDNI	$ndni = \frac{\log\frac{1}{\rho_{1512}} - \log\frac{1}{\rho_{1677}}}{\log\frac{1}{\rho_{1512}} + \log\frac{1}{\rho_{1677}}}$	H	(Serrano et al., 2002)
Normalized Difference Lignin Index: NDLI	$ndli = \frac{\log\frac{1}{\rho_{1755}} - \log\frac{1}{\rho_{1677}}}{\log\frac{1}{\rho_{1755}} + \log\frac{1}{\rho_{1677}}}$	H	(Serrano et al., 2002)
Cellulose Absorption Index: CAI	$cai = 0.5 * (\rho_{1993} + \rho_{2206}) - \rho_{2102}$	H	(Nagler et al., 2000)
Lignin Cellulose Absorption Index: LCAI	$lcai = 100 * ((\rho_{2206} - \rho_{2159}) + (\rho_{2206} - \rho_{2335}))$	H	(Daughtry et al., 2005)
Anthocyanin Reflectance Index 2: ARI2	$ari2 = \rho_{801} * (\left(\frac{1}{\rho_{554}}\right) - \left(\frac{1}{\rho_{699}}\right))$	H	(A. A. Gitelson et al., 2001)
Normalized Multi-band Drought Index: NMDI	$nmdi = \frac{\rho_{855} - (\rho_{1636} - \rho_{2127})}{\rho_{855} + (\rho_{1636} - \rho_{2127})}$	H	(Wang & Qu, 2007)

REFERENCE

Barnes, E. M., Clarke, T. R., Richards, S. E., Colaizzi, P. D., Haberland, J., Kostrzewski, M., Waller, P., Choi, C., & Riley, E. (2000). *Coincident Detection of Crop Water Stress, Nitrogen Status, and Canopy Density Using Ground-Based Multispectral Data*. 1-15.

Bendig, J., Yu, K., Aasen, H., Bolten, A., Bennertz, S., Broscheit, J., Gnyp, M. L., & Bareth, G. (2015). Combining UAV-based plant height from crop surface models, visible, and near infrared vegetation indices for biomass monitoring in barley. *International Journal of Applied Earth Observation and Geoinformation*, *39*, 79-87. https://doi.org/10.1016/j.jag.2015.02.012

Birth, G. S., & McVey, G. R. (1968). Measuring the Color of Growing Turf with a Reflectance Spectrophotometer. *Agronomy Journal*, *60*(6), 640-643. https://doi.org/10.2134/agronj1968.00021962006000060016x

Chen, C., Yuan, X., Gan, S., Luo, W., Bi, R., Li, R., & Gao, S. (2024). A new vegetation index based on UAV for extracting plateau vegetation information. *International Journal of Applied Earth Observation and Geoinformation*, *128*, 103668. https://doi.org/10.1016/j.jag.2024.103668

Chen, J. M. (1996). Evaluation of Vegetation Indices and a Modified Simple Ratio for Boreal Applications. *Canadian Journal of Remote Sensing*, *22*(3), 229-242. https://doi.org/10.1080/07038992.1996.10855178

Clevers, J. G. P. W., De Jong, S. M., Epema, G. F., Van Der Meer, F., Bakker, W. H., Skidmore, A. K., & Addink, E. A. (2001). MERIS and the red-edge position. *International Journal of Applied Earth Observation and Geoinformation*, *3*(4), 313-320. https://doi.org/10.1016/S0303-2434(01)85038-8

Datt, B. (1999). Remote Sensing of Water Content in Eucalyptus Leaves. *Australian Journal of Botany*, *47*(6), 909. https://doi.org/10.1071/BT98042

Daughtry, C. S. T., Hunt Jr., E. R., Doraiswamy, P. C., & Mcmurtrey, I. (2005). Remote sensing the spatial distribution of crop residues. *Agronomy Journal*, *97*, 864-871.

Dennison, P. E. (2006). Fire detection in imaging spectrometer data using atmospheric carbon dioxide absorption. *International Journal of Remote Sensing*, *27*(14), 3049-3055. https://doi.org/10.1080/01431160600660871

Dennison, P. E., & Roberts, D. A. (2009). Daytime fire detection using airborne hyperspectral data. *Remote Sensing of Environment*, *113*(8), 1646-1657. https://doi.org/10.1016/j.rse.2009.03.010

Diker, K., & Bausch, W. C. (2003). Potential Use of Nitrogen Reflectance Index to estimate Plant Parameters and Yield of Maize. *Biosystems Engineering*, *85*(4), 437-447. https://doi.org/10.1016/S1537-5110(03)00097-7

Dobrowski, S., Pushnik, J., Zarcotejada, P., & Ustin, S. (2005). Simple reflectance indices track heat and water stress-induced changes in steady-state chlorophyll fluorescence at the canopy scale. *Remote Sensing of Environment*, *97*(3), 403-414. https://doi.org/10.1016/j.rse.2005.05.006

Fernández-Manso, A., Fernández-Manso, O., & Quintano, C. (2016). SENTINEL-2A red-edge spectral indices suitability for discriminating burn severity. *International Journal of Applied Earth Observation and Geoinformation*, *50*, 170-175. https://doi.org/10.1016/j.jag.2016.03.005

Fiodortsev, R. V., Silie Cuenca, A. R., Kozhevnikov, D. A., Medina, V. M., & Delgado, R. (2019). Application of Satellite Image Processing Methods for Hydrocarbon Field Search. *Devices and Methods of Measurements*, *10*(4), 373-381. https://doi.org/10.21122/2220-9506-2019-10-4-373-381

Fornacca, D., Ren, G., & Xiao, W. (2018). Evaluating the Best Spectral Indices for the Detection of Burn Scars at Several Post-Fire Dates in a Mountainous Region of Northwest Yunnan, China. *Remote Sensing*, *10*(8), 1196. https://doi.org/10.3390/rs10081196

Galvão, L. S., Formaggio, A. R., & Tisot, D. (2005). Discrimination of sugarcane varieties with hyperspectral data from the Hyperion/EO-1 sensor. *Revista Brasileira de Cartografía*, *57*(1).

Gamon, J. A., & Surfus, J. S. (1999). Assessing leaf pigment content and activity with a reflectometer. *New Phytologist*, *143*(1), 105-117. https://doi.org/10.1046/j.1469-8137.1999.00424.x

Gao, B. (1996). NDWI—A normalized difference water index for remote sensing of vegetation liquid water from space. *Remote Sensing of Environment*, *58*(3), 257-266. https://doi.org/10.1016/S0034-4257(96)00067-3

Gao, X. L., & Wang, X. Q. (2008). An application of multi-source remote sensing data in vegetation identification and extraction of vegetation information. *Resources Science*, *30*(1), 153-158.

García, M. L., & Caselles, V. (1991). Mapping burns and natural reforestation using thematic mapper data. *Geocarto International*, *6*(1), 31-37.

Gitelson, A. A. (2004). Wide Dynamic Range Vegetation Index for Remote Quantification of Biophysical Characteristics of Vegetation. *Journal of Plant Physiology*, *161*(2), 165-173. https://doi.org/10.1078/0176-1617-01176

Gitelson, A. A., Gritz †, Y., & Merzlyak, M. N. (2003). Relationships between leaf chlorophyll content and spectral reflectance and algorithms for non-destructive chlorophyll assessment in higher plant leaves. *Journal of Plant Physiology*, *160*(3), 271-282. https://doi.org/10.1078/0176-1617-00887

Gitelson, A. A., Kaufman, Y. J., & Merzlyak, M. N. (1996). Use of a green channel in remote sensing of global vegetation from EOS-MODIS. *Remote Sensing of Environment*, *58*(3), 289-298. https://doi.org/10.1016/S0034-4257(96)00072-7

Gitelson, A. A., Kaufman, Y. J., Stark, R., & Rundquist, D. (2002). Novel algorithms for remote estimation of vegetation fraction. *Remote Sensing of Environment*, *80*(1), 76-87. https://doi.org/10.1016/S0034-4257(01)00289-9

Gitelson, A. A., & Merzlyak, M. N. (1998). Remote sensing of chlorophyll concentration in higher plant leaves. *Advances in Space Research*, *22*(5), 689-692. https://doi.org/10.1016/S0273-1177(97)01133-2

Gitelson, A. A., Merzlyak, M. N., & Chivkunova, O. B. (2001). Optical Properties and Nondestructive Estimation of Anthocyanin Content in Plant Leaves¶. *Photochemistry and Photobiology*, *74*(1), 38. https://doi.org/10.1562/0031-8655(2001)074<0038:OPANEO>2.0.CO;2

Gitelson, A. A., Stark, R., Grits, U., Rundquist, D., Kaufman, Y., & Derry, D. (2002). Vegetation and soil lines in visible spectral space: A concept and technique for remote estimation of vegetation fraction. *International Journal of Remote Sensing*, *23*(13), 2537-2562. https://doi.org/10.1080/01431160110107806

Gitelson, A. A., Viña, A., Ciganda, V., Rundquist, D. C., & Arkebauer, T. J. (2005). Remote estimation of canopy chlorophyll content in crops. *Geophysical Research Letters*, *32*(8), 2005GL022688. https://doi.org/10.1029/2005GL022688

Gitelson, A., & Merzlyak, M. N. (1994). Spectral Reflectance Changes Associated with Autumn Senescence of Aesculus hippocastanum L. and Acer platanoides L. Leaves. Spectral Features and Relation to Chlorophyll Estimation. *Journal of Plant Physiology*, *143*(3), 286-292. https://doi.org/10.1016/S0176-1617(11)81633-0

Goel, N. S., & Qin, W. (1994). Influences of canopy architecture on relationships between various vegetation indices and LAI and Fpar: A computer simulation. *Remote Sensing Reviews*, *10*(4), 309-347. https://doi.org/10.1080/02757259409532252

Guijarro, M., Pajares, G., Riomoros, I., Herrera, P. J., Burgos-Artizzu, X. P., & Ribeiro, A. (2011). Automatic segmentation of relevant textures in agricultural images. *Computers and Electronics in Agriculture*, *75*(1), 75-83. https://doi.org/10.1016/j.compag.2010.09.013

Guo, Y., Chen, S., Li, X., Cunha, M., Jayavelu, S., Cammarano, D., & Fu, Y. (2022). Machine Learning-Based Approaches for Predicting SPAD Values of Maize Using Multi-Spectral Images. *Remote Sensing*, *14*(6), 1337. https://doi.org/10.3390/rs14061337

Hallik, L., Kuusk, A., Lang, M., & Kuusk, J. (2019). Reflectance Properties of Hemiboreal Mixed Forest Canopies with Focus on Red Edge and Near Infrared Spectral Regions. *Remote Sensing*, *11*(14), 1717. https://doi.org/10.3390/rs11141717

Hardisky, M. A., Klemas, V., & Smart, R. M. (1983). The Influence of Soil Salinity Growth Form and Leaf Moisture on the Spectral Radiance of Spartina alterniflora Canopies. *Photogrammetric Engineering & Remote Sensing*, *49*, 77-83.

Huete, A. R. (1988). A soil-adjusted vegetation index (SAVI). *Remote Sensing of Environment*, *25*(3), 295-309. https://doi.org/10.1016/0034-4257(88)90106-X

Hunt, E. R., Cavigelli, M., Daughtry, C. S. T., Mcmurtrey, J. E., & Walthall, C. L. (2005). Evaluation of Digital Photography from Model Aircraft for Remote Sensing of Crop Biomass and Nitrogen Status. *Precision Agriculture*, *6*(4), 359-378. https://doi.org/10.1007/s11119-005-2324-5

Hunt Jr, E., & Rock, B. (1989). Detection of changes in leaf water content using Near- and Middle-Infrared reflectances☆. *Remote Sensing of Environment*, *30*(1), 43-54. https://doi.org/10.1016/0034-4257(89)90046-1

Jabbar, M. T., & Chen, X. (2006). Land degradation assessment with the aid of geo-information techniques. *Earth Surface Processes and Landforms*, *31*(6), 777-784. https://doi.org/10.1002/esp.1298

Jiang, X., Zhen, J., Miao, J., Zhao, D., Shen, Z., Jiang, J., Gao, C., Wu, G., & Wang, J. (2022). Newly-developed three-band hyperspectral vegetation index for estimating leaf relative chlorophyll content of mangrove under different severities of pest and disease. *Ecological Indicators*, *140*, 108978. https://doi.org/10.1016/j.ecolind.2022.108978

Jordan, C. F. (1969). Derivation of Leaf-Area Index from Quality of Light on the Forest Floor. *Ecology*, *50*(4), 663-666. https://doi.org/10.2307/1936256

Kataoka, T., Kaneko, T., Okamoto, H., & Hata, S. (2003). Crop growth estimation system using machine vision. *Proceedings 2003 IEEE/ASME International Conference on Advanced Intelligent Mechatronics (AIM 2003)*, *2*, b1079-b1083. https://doi.org/10.1109/AIM.2003.1225492

Li, F., Miao, Y., Feng, G., Yuan, F., Yue, S., Gao, X., Liu, Y., Liu, B., Ustin, S. L., & Chen, X. (2014). Improving estimation of summer maize nitrogen status with red edge-based spectral vegetation indices. *Field Crops Research*, *157*, 111-123. https://doi.org/10.1016/j.fcr.2013.12.018

Li, R., Ye, S., Bai, Z., Nedzved, A., & Tuzikov, A. (2024). Moderate Red-Edge vegetation index for High-Resolution multispectral remote sensing images in urban areas. *Ecological Indicators*, *167*, 112645. https://doi.org/10.1016/j.ecolind.2024.112645

Liu, H. Q., & Huete, A. (1995). A feedback based modification of the NDVI to minimize canopy background and atmospheric noise. *IEEE Transactions on Geoscience and Remote Sensing*, *33*(2), 457-465. https://doi.org/10.1109/36.377946

Louhaichi, M., Borman, M. M., & Johnson, D. E. (2001). Spatially Located Platform and Aerial Photography for Documentation of Grazing Impacts on Wheat. *Geocarto International*, *16*(1), 65-70. https://doi.org/10.1080/10106040108542184

Merzlyak, M. N., Gitelson, A. A., Chivkunova, O. B., & Rakitin, V. Yu. (1999). Non-destructive optical detection of pigment changes during leaf senescence and fruit ripening. *Physiologia Plantarum*, *106*(1), 135-141. https://doi.org/10.1034/j.1399-3054.1999.106119.x

Meyer, G. E., & Neto, J. C. (2008). Verification of color vegetation indices for automated crop imaging applications. *Computers and Electronics in Agriculture*, *63*(2), 282-293. https://doi.org/10.1016/j.compag.2008.03.009

Nagler, P. L., Daughtry, C. S. T., & Goward, S. N. (2000). Plant litter and soil reflectance. *Remote Sensing of Environment*, *71*, 207-215.

Pasqualotto, N., Delegido, J., Van Wittenberghe, S., Verrelst, J., Rivera, J. P., & Moreno, J. (2018). Retrieval of canopy water content of different crop types with two new hyperspectral indices: Water Absorption Area Index and Depth Water Index. *International Journal of Applied Earth Observation and Geoinformation*, *67*, 69-78. https://doi.org/10.1016/j.jag.2018.01.002

Peñuelas, J., Filella, I., Lloret, P., Muñóz, F., & Vilajeliu, M. (1995). Reflectance assessment of mite effects on apple trees. *International Journal of Remote Sensing*, *16*(14), 2727-2733. https://doi.org/10.1080/01431169508954588

Peñuelas, J., Gamon, J. A., Fredeen, A. L., Merino, J., & Field, C. B. (1994). Reflectance indices associated with physiological changes in nitrogen- and water-limited sunflower leaves. *Remote Sensing of Environment*, *48*(2), 135-146. https://doi.org/10.1016/0034-4257(94)90136-8

Qiao, L., Tang, W., Gao, D., Zhao, R., An, L., Li, M., Sun, H., & Song, D. (2022). UAV-based chlorophyll content estimation by evaluating vegetation index responses under different crop coverages. *Computers and Electronics in Agriculture*, *196*, 106775. https://doi.org/10.1016/j.compag.2022.106775

Rondeaux, G., Steven, M., & Baret, F. (1996). Optimization of soil-adjusted vegetation indices. *Remote Sensing of Environment*, *55*(2), 95-107. https://doi.org/10.1016/0034-4257(95)00186-7

Roujean, J.-L., & Breon, F.-M. (1995). Estimating PAR absorbed by vegetation from bidirectional reflectance measurements. *Remote Sensing of Environment*, *51*(3), 375-384. https://doi.org/10.1016/0034-4257(94)00114-3

Rouse, J. W. Jr., Haas, R. H., Schell, J. A., & Deering, D. W. (1974). Monitoring vegetation systems in the Great Plains with ERTS. *NASA. Goddard Space Flight Center 3d ERTS-1 Symp. Paper-A20*, *1*(Sect. A), 309-317.

Sellaro, R., Crepy, M., Trupkin, S. A., Karayekov, E., Buchovsky, A. S., Rossi, C., & Casal, J. J. (2010). Cryptochrome as a Sensor of the Blue/Green Ratio of Natural Radiation in Arabidopsis. *Plant Physiology*, *154*(1), 401-409. https://doi.org/10.1104/pp.110.160820

Serrano, L., Peñuelas, J., & Ustin, S. L. (2002). Remote sensing of nitrogen and lignin in Mediterranean vegetation from AVIRIS data. *Remote Sensing of Environment*, *81*(2-3), 355-364. https://doi.org/10.1016/S0034-4257(02)00011-1

Shi, T., Liu, J., Hu, Z., Liu, H., Wang, J., & Wu, G. (2016). New spectral metrics for mangrove forest identification. *Remote Sensing Letters*, *7*(9), 885-894. https://doi.org/10.1080/2150704X.2016.1195935

Silleos, N. G., Alexandridis, T. K., Gitas, I. Z., & Perakis, K. (2006). Vegetation Indices: Advances Made in Biomass Estimation and Vegetation Monitoring in the Last 30 Years. *Geocarto International*, *21*(4), 21-28. https://doi.org/10.1080/10106040608542399

Sims, D. A., & Gamon, J. A. (2002). Relationships between leaf pigment content and spectral reflectance across a wide range of species, leaf structures and developmental stages. *Remote Sensing of Environment*, *81*(2-3), 337-354. https://doi.org/10.1016/S0034-4257(02)00010-X

Sripada, R. P. (2005). *Determining in-season nitrogen requirements for corn using aerial color-infrared photography* [North Carolina State University]. https://repository.lib.ncsu.edu/items/69abed43-4eb9-44c5-86a1-08b8692147aa

Traba, J., Gómez-Catasús, J., Barrero, A., Bustillo-de La Rosa, D., Zurdo, J., Hervás, I., Pérez-Granados, C., García De La Morena, E. L., Santamaría, A., & Reverter, M. (2022). Comparative assessment of satellite- and drone-based vegetation indices to predict arthropod biomass in shrub-steppes. *Ecological Applications*, *32*(8), e2707. https://doi.org/10.1002/eap.2707

Tucker, C. J. (1979). Red and photographic infrared linear combinations for monitoring vegetation. *Remote Sensing of Environment*, *8*(2), 127-150. https://doi.org/10.1016/0034-4257(79)90013-0

Vogelmann, J. E., Rock, B. N., & Moss, D. M. (1993). Red edge spectral measurements from sugar maple leaves. *International Journal of Remote Sensing*, *14*(8), 1563-1575. https://doi.org/10.1080/01431169308953986

Wan, L., Cen, H., Zhu, J., Li, Y., Zhu, Y., Sun, D., Weng, H., & He, Y. (2019). Combining UAV-based vegetation indices, canopy height and canopy coverage to improve rice yield prediction under different nitrogen levels. *2019 Boston, Massachusetts July 7- July 10, 2019*. 2019 Boston, Massachusetts July 7- July 10, 2019. https://doi.org/10.13031/aim.201900626

Wang, L., & Qu, J. J. (2007). NMDI: A normalized multi-band drought index for monitoring soil and vegetation moisture with satellite remote sensing. *Geophysical Research Letters*, *34*(20), 2007GL031021. https://doi.org/10.1029/2007GL031021

Woebbecke, D. M., Meyer, G. E., Von Bargen, K., & Mortensen, D. A. (1995). Color indices for weed identification under various soil, residue, and lighting conditions. *Transactions of the ASAE*, *38*(1), 259-269. https://doi.org/10.13031/2013.27838

Wu, C., Niu, Z., Tang, Q., & Huang, W. (2008). Estimating chlorophyll content from hyperspectral vegetation indices: Modeling and validation. *Agricultural and Forest Meteorology*, *148*(8-9), 1230-1241. https://doi.org/10.1016/j.agrformet.2008.03.005

Wu, W. (2016). *Intelligent monitoring and system development of diagnostic index of the wheat seedling growth*. YangZhou University.

Xue, J., & Su, B. (2017). Significant Remote Sensing Vegetation Indices: A Review of Developments and Applications. *Journal of Sensors*, *2017*, 1-17. https://doi.org/10.1155/2017/1353691

Yang, G., Huang, K., Sun, W., Meng, X., Mao, D., & Ge, Y. (2022). Enhanced mangrove vegetation index based on hyperspectral images for mapping mangrove. *ISPRS Journal of Photogrammetry and Remote Sensing*, *189*, 236-254. https://doi.org/10.1016/j.isprsjprs.2022.05.003

Yang, Z., Willis, P., & Mueller, R. (2008). *Impact of band-ratio enhanced AWIFS image to crop classification accuracy*. https://www.asprs.org/a/publications/proceedings/pecora17/0041.pdf

Zeng, Y., Hao, D., Badgley, G., Damm, A., Rascher, U., Ryu, Y., Johnson, J., Krieger, V., Wu, S., Qiu, H., Liu, Y., Berry, J. A., & Chen, M. (2021). Estimating near-infrared reflectance of vegetation from hyperspectral data. *Remote Sensing of Environment*, *267*, 112723. https://doi.org/10.1016/j.rse.2021.112723

Zhang, S. U., & Liu, L. (2014). The potential of the MERIS Terrestrial Chlorophyll Index for crop yield prediction. *Remote Sensing Letters*, *5*(8), 733-742.

Zhao, C., Pan, Y., Ren, S., Gao, Y., Wu, H., & Ma, G. (2024). Accurate vegetation destruction detection using remote sensing imagery based on the three-band difference vegetation index (TBDVI) and dual-temporal detection method. *International Journal of Applied Earth Observation and Geoinformation*, *127*, 103669. https://doi.org/10.1016/j.jag.2024.103669

Zhou, X. M., Zheng, N. S., Qi, Y., & Chen, S. (2018). Using GPS-R remote sensing technology to invert vegetation biomass. *Surveying Mapp Bull*, *1*, 129-132.

ANNEX 4 – Pearson and R^2 metrics

A4.1. Pearson correlation and Coefficient of determination for vegetation indices derived from hyperspectral imagery across ecosystem and CBI type.

Vegetation Indices	Coniferous forest						Broadleaf forest						Shrubland					
	vegetation CBI		soil CBI		site CBI		vegetation CBI		soil CBI		site CBI		vegetation CBI		soil CBI		site CBI	
	r	R^2	r	R^2	r	R^2	r	R^2	r	R^2	r	R^2	r	R^2	r	R^2	r	R^2
ARI1	0.288	0.083	0.192	0.037	0.266	0.071	0.357	0.127	0.407	0.166	0.401	0.161	0.270	0.073	0.405	0.164	0.336	0.113
ARI2	-0.660	0.435	-0.355	0.126	-0.566	0.320	-0.340	0.116	-0.452	0.204	-0.412	0.170	-0.490	0.240	-0.421	0.178	-0.465	0.217
ARVI	-0.789	0.622	-0.593	0.352	-0.749	0.560	-0.403	0.163	-0.611	0.374	-0.526	0.277	-0.461	0.212	-0.473	0.224	-0.472	0.223
BAI	0.728	0.531	0.383	0.147	0.619	0.384	0.676	0.457	0.602	0.362	0.672	0.451	0.724	0.524	0.768	0.589	0.751	0.564
BGR	0.630	0.397	0.321	0.103	0.458	0.210	0.488	0.238	0.485	0.236	0.419	0.175	0.642	0.412	0.693	0.480	0.674	0.454
Blue	0.252	0.064	0.142	0.020	0.219	0.048	-0.322	0.104	-0.221	0.049	-0.291	0.084	-0.213	0.045	-0.346	0.120	-0.276	0.076
CAI	-0.666	0.444	-0.413	0.170	-0.599	0.358	-0.867	0.752	-0.840	0.705	-0.875	0.766	-0.894	0.798	-0.878	0.770	-0.899	0.808
CIGREEN	-0.744	0.554	-0.453	0.205	-0.659	0.434	-0.438	0.192	-0.543	0.295	-0.513	0.264	-0.646	0.417	-0.547	0.299	-0.605	0.366
CIREDGE	-0.820	0.672	-0.547	0.299	-0.748	0.559	-0.764	0.584	-0.659	0.435	-0.718	0.516	-0.571	0.326	-0.531	0.282	-0.542	0.294
CIVE	-0.525	0.276	0.428	0.183	-0.430	0.185	0.459	0.210	0.581	0.337	0.543	0.295	-0.428	0.183	-0.283	0.080	-0.363	0.132
Clre	-0.812	0.660	-0.547	0.299	-0.739	0.545	-0.385	0.148	-0.552	0.304	-0.485	0.235	-0.537	0.288	-0.571	0.326	-0.560	0.313
CMRI	-0.199	0.040	-0.149	0.022	-0.191	0.037	-0.243	0.059	-0.492	0.242	-0.372	0.139	-0.232	0.054	-0.079	0.006	-0.164	0.027
CO2-CIBR	0.711	0.506	0.407	0.165	0.622	0.387	0.242	0.058	0.363	0.131	0.314	0.099	0.385	0.148	0.281	0.079	0.343	0.117
CRI1	-0.396	0.157	-0.080	0.006	-0.259	0.067	-0.200	0.040	-0.268	0.072	-0.224	0.050	-0.331	0.110	-0.334	0.112	-0.337	0.114
CRI2	-0.152	0.023	0.088	0.008	-0.098	0.010	0.220	0.048	0.230	0.053	0.237	0.056	0.216	0.047	0.353	0.125	0.280	0.079
Ctr1	-0.624	0.390	-0.301	0.091	-0.486	0.236	-0.362	0.131	-0.339	0.115	-0.370	0.137	-0.530	0.281	-0.461	0.213	-0.506	0.256
Ctr2	0.780	0.608	0.537	0.289	0.720	0.519	0.455	0.207	0.599	0.358	0.544	0.296	0.547	0.299	0.580	0.337	0.570	0.325
DVI	-0.853	0.728	-0.511	0.261	-0.755	0.570	-0.615	0.378	-0.657	0.432	-0.666	0.443	-0.763	0.581	-0.787	0.620	-0.781	0.609
DVIGRE	-0.839	0.704	-0.488	0.238	-0.738	0.544	-0.651	0.424	-0.659	0.434	-0.680	0.463	-0.775	0.601	-0.806	0.649	-0.800	0.640
DVIRED	-0.860	0.739	-0.522	0.272	-0.765	0.585	-0.823	0.677	-0.751	0.564	-0.780	0.608	-0.711	0.506	-0.746	0.556	-0.727	0.528

DWI	-0.742	0.551	-0.424	0.179	-0.643	0.414	-0.584	0.341	-0.647	0.419	-0.643	0.413	-0.652	0.425	-0.736	0.542	-0.700	0.489
DWSI	-0.767	0.588	-0.442	0.195	-0.670	0.449	-0.506	0.256	-0.576	0.331	-0.563	0.317	-0.713	0.508	-0.751	0.564	-0.740	0.548
ENDVI	-0.638	0.407	-0.346	0.120	-0.517	0.267	-0.404	0.163	-0.432	0.187	-0.407	0.166	-0.550	0.302	-0.484	0.235	-0.525	0.275
EVI	-0.831	0.691	-0.666	0.443	-0.782	0.611	-0.494	0.244	-0.643	0.414	-0.574	0.330	-0.632	0.400	-0.595	0.355	-0.624	0.390
EVI2	-0.786	0.618	-0.498	0.248	-0.710	0.504	-0.401	0.161	-0.567	0.321	-0.504	0.254	-0.574	0.329	-0.537	0.289	-0.560	0.313
EXB	-0.531	0.282	0.304	0.092	-0.430	0.185	0.326	0.106	0.517	0.267	0.438	0.192	-0.429	0.184	-0.302	0.091	-0.374	0.140
EXG	-0.687	0.471	-0.510	0.260	-0.640	0.410	-0.521	0.271	-0.617	0.380	-0.568	0.323	-0.595	0.354	-0.599	0.359	-0.583	0.340
EXG2	-0.732	0.535	-0.524	0.275	-0.674	0.454	0.662	0.439	0.669	0.447	0.664	0.441	0.634	0.402	-0.728	0.530	-0.672	0.452
EXGR	-0.731	0.535	-0.460	0.212	-0.643	0.414	-0.565	0.319	-0.640	0.409	-0.594	0.352	-0.702	0.493	-0.729	0.531	-0.724	0.524
EXR	0.638	0.407	0.334	0.112	0.495	0.245	0.438	0.192	0.463	0.214	0.400	0.160	0.637	0.406	0.646	0.418	0.637	0.406
FRI1	0.771	0.595	0.538	0.290	0.723	0.523	0.558	0.311	0.638	0.407	0.614	0.378	0.540	0.292	0.534	0.285	0.545	0.297
FRI2	-0.651	0.424	-0.410	0.168	-0.588	0.346	-0.376	0.142	-0.474	0.225	-0.439	0.192	-0.563	0.317	-0.508	0.258	-0.545	0.297
G	0.438	0.192	0.206	0.042	0.361	0.130	-0.263	0.069	-0.473	0.223	-0.380	0.145	0.280	0.079	0.168	0.028	0.233	0.054
GARI	-0.799	0.638	-0.611	0.373	-0.756	0.571	-0.407	0.165	-0.627	0.393	-0.533	0.284	-0.455	0.207	-0.437	0.191	-0.448	0.201
GB	-0.570	0.324	-0.216	0.047	-0.433	0.188	-0.329	0.108	-0.362	0.131	-0.336	0.113	-0.621	0.386	-0.624	0.389	-0.622	0.387
GLI	-0.687	0.471	-0.505	0.255	-0.638	0.407	-0.520	0.271	-0.619	0.383	-0.572	0.327	-0.594	0.353	-0.599	0.359	-0.583	0.340
GM1	-0.700	0.490	-0.410	0.168	-0.617	0.381	-0.355	0.126	-0.481	0.231	-0.432	0.186	-0.562	0.316	-0.497	0.247	-0.540	0.292
GM2	-0.791	0.626	-0.547	0.299	-0.733	0.537	-0.385	0.148	-0.548	0.300	-0.485	0.235	-0.537	0.288	-0.571	0.326	-0.560	0.313
GNDVI	-0.757	0.573	-0.498	0.248	-0.679	0.461	-0.571	0.326	-0.592	0.351	-0.597	0.357	-0.653	0.426	-0.597	0.356	-0.636	0.405
GR	0.155	0.024	-0.138	0.019	-0.101	0.010	-0.263	0.069	-0.502	0.252	-0.385	0.149	0.121	0.015	-0.151	0.023	-0.073	0.005
Green	-0.438	0.192	-0.188	0.035	-0.347	0.120	-0.490	0.240	-0.311	0.097	-0.429	0.184	-0.450	0.203	-0.580	0.336	-0.516	0.266
GRVI	-0.657	0.432	-0.369	0.136	-0.567	0.321	-0.334	0.112	-0.496	0.246	-0.431	0.186	-0.437	0.191	-0.328	0.108	-0.387	0.150
GSAVI	-0.694	0.482	-0.441	0.194	-0.629	0.395	-0.430	0.185	-0.546	0.299	-0.506	0.256	-0.519	0.269	-0.427	0.183	-0.484	0.234
HFDI	0.206	0.043	0.138	0.019	0.167	0.028	0.631	0.398	0.676	0.457	0.671	0.450	0.797	0.635	0.695	0.484	0.762	0.580
IPVI	-0.810	0.657	-0.529	0.280	-0.735	0.540	-0.483	0.233	-0.598	0.357	-0.562	0.316	-0.657	0.432	-0.598	0.357	-0.626	0.392
IRGBVI	-0.688	0.474	-0.505	0.255	-0.636	0.404	-0.502	0.252	0.632	0.400	-0.550	0.302	-0.611	0.374	-0.627	0.393	-0.622	0.386
LCAI	-0.643	0.413	-0.438	0.192	-0.582	0.339	0.820	0.673	-0.758	0.575	-0.786	0.618	-0.871	0.758	-0.833	0.694	-0.866	0.749
LCI	-0.808	0.652	-0.554	0.307	-0.743	0.552	-0.410	0.168	-0.643	0.413	-0.547	0.299	-0.483	0.233	-0.404	0.163	-0.452	0.204

Lic1	-0.802	0.644	-0.510	0.260	-0.724	0.524	-0.415	0.172	-0.577	0.333	-0.517	0.267	-0.576	0.332	-0.540	0.291	-0.562	0.315
Lic2	0.535	0.286	0.272	0.074	0.441	0.195	0.313	0.098	0.195	0.038	0.248	0.062	0.428	0.183	0.358	0.128	0.402	0.162
LWVI1	-0.186	0.034	-0.125	0.016	-0.170	0.029	0.463	0.215	-0.423	0.179	0.405	0.164	0.226	0.051	0.468	0.219	0.339	0.115
LWVI2	-0.469	0.220	-0.261	0.068	-0.407	0.165	-0.487	0.238	-0.659	0.434	-0.590	0.348	-0.278	0.077	-0.302	0.091	-0.291	0.085
MCARI1	-0.727	0.528	-0.459	0.211	-0.657	0.432	-0.506	0.256	-0.611	0.374	-0.585	0.343	-0.655	0.429	-0.708	0.501	-0.688	0.474
MCARI2	-0.835	0.698	-0.541	0.293	-0.756	0.571	-0.421	0.177	-0.587	0.345	-0.521	0.271	-0.613	0.375	-0.644	0.415	-0.636	0.404
MCARI3	-0.797	0.634	-0.566	0.320	-0.731	0.535	-0.418	0.174	-0.629	0.396	-0.532	0.283	-0.459	0.211	-0.495	0.245	-0.476	0.227
MGRVI	0.513	0.263	-0.398	0.159	0.433	0.188	-0.463	0.215	-0.579	0.335	-0.545	0.297	0.400	0.160	0.243	0.059	0.323	0.105
MNLI	0.376	0.141	-0.319	0.102	0.361	0.131	0.505	0.255	-0.451	0.203	-0.485	0.235	0.518	0.268	0.509	0.259	0.520	0.270
MRENDVI	-0.773	0.598	-0.590	0.348	-0.719	0.517	-0.617	0.381	-0.623	0.388	-0.630	0.397	0.425	0.180	0.512	0.262	0.470	0.221
MRESR	-0.820	0.672	-0.547	0.299	-0.748	0.559	-0.764	0.584	-0.659	0.435	-0.718	0.516	-0.571	0.326	-0.531	0.282	-0.542	0.294
MRGBVI	-0.647	0.419	-0.348	0.121	-0.520	0.271	-0.411	0.169	-0.441	0.195	-0.414	0.172	-0.577	0.333	-0.519	0.269	-0.551	0.304
MSAVI	-0.778	0.605	-0.499	0.249	-0.704	0.495	-0.423	0.179	-0.594	0.353	-0.527	0.277	-0.552	0.305	-0.516	0.266	-0.541	0.293
MSI	0.753	0.567	0.465	0.216	0.672	0.451	0.612	0.375	0.635	0.404	0.650	0.423	0.459	0.211	0.593	0.352	0.526	0.276
MSR	-0.780	0.608	-0.496	0.246	-0.704	0.496	-0.373	0.139	-0.573	0.328	-0.490	0.240	-0.519	0.269	-0.448	0.201	-0.490	0.240
MSR2	-0.787	0.619	-0.498	0.248	-0.710	0.505	-0.392	0.153	-0.559	0.312	-0.495	0.245	-0.572	0.328	-0.536	0.287	-0.559	0.312
MSRre	-0.801	0.642	-0.535	0.286	-0.736	0.542	-0.392	0.153	-0.583	0.340	-0.495	0.245	-0.551	0.304	-0.536	0.287	-0.552	0.305
MSRREG	-0.815	0.664	-0.543	0.295	-0.745	0.554	-0.430	0.185	-0.659	0.434	-0.553	0.306	-0.470	0.221	-0.394	0.155	-0.441	0.194
MSRren	-0.816	0.666	-0.544	0.296	-0.746	0.556	-0.377	0.142	-0.592	0.350	-0.494	0.244	-0.507	0.257	-0.452	0.205	-0.488	0.238
MTCI	-0.805	0.648	-0.548	0.300	-0.734	0.539	-0.466	0.217	-0.647	0.419	-0.546	0.299	-0.483	0.233	-0.404	0.163	-0.452	0.204
MTVI1	-0.835	0.698	-0.541	0.293	-0.756	0.571	-0.421	0.177	-0.587	0.345	-0.521	0.271	-0.613	0.375	-0.644	0.415	-0.636	0.404
MTVI2	-0.791	0.626	-0.555	0.308	-0.732	0.536	-0.415	0.172	-0.628	0.394	-0.534	0.285	-0.496	0.246	-0.492	0.242	-0.487	0.237
MVI	-0.773	0.598	-0.444	0.197	-0.676	0.457	-0.464	0.215	-0.583	0.340	-0.545	0.298	-0.542	0.294	-0.621	0.385	-0.586	0.343
NBR	-0.743	0.552	-0.443	0.196	-0.653	0.427	-0.725	0.526	-0.736	0.541	-0.731	0.534	-0.814	0.663	-0.878	0.771	-0.847	0.717
NDIB	-0.399	0.159	-0.118	0.014	-0.288	0.083	-0.142	0.020	0.178	0.032	0.108	0.012	-0.364	0.133	-0.288	0.083	-0.331	0.109
NDIG	-0.180	0.033	-0.140	0.020	-0.149	0.022	0.247	0.061	0.492	0.242	0.373	0.139	-0.202	0.041	-0.116	0.013	-0.149	0.022
NDII	-0.770	0.592	-0.454	0.206	-0.676	0.457	-0.544	0.296	-0.612	0.375	-0.603	0.364	-0.475	0.225	-0.610	0.372	-0.541	0.293
NDLI	0.731	0.534	0.412	0.169	0.631	0.398	0.715	0.511	0.790	0.625	0.764	0.584	0.794	0.631	0.835	0.696	0.824	0.678

NDMI	-0.780	0.608	-0.499	0.249	-0.696	0.485	-0.689	0.474	-0.720	0.519	-0.667	0.444	-0.636	0.404	-0.760	0.578	-0.701	0.492
NDNI	0.402	0.162	0.395	0.156	0.407	0.166	0.289	0.083	0.565	0.319	0.440	0.194	-0.243	0.059	-0.210	0.044	-0.231	0.053
NDRE	-0.812	0.659	-0.545	0.297	-0.743	0.551	-0.768	0.589	-0.666	0.443	-0.721	0.519	-0.563	0.317	-0.533	0.284	-0.543	0.295
NDre1	-0.783	0.613	-0.509	0.259	-0.711	0.506	-0.445	0.198	-0.571	0.326	-0.523	0.274	-0.534	0.286	-0.613	0.376	-0.571	0.326
NDre1m	-0.773	0.598	-0.555	0.308	-0.719	0.517	-0.488	0.238	-0.618	0.382	-0.559	0.312	-0.552	0.305	-0.624	0.390	-0.592	0.350
NDre2	-0.806	0.649	-0.541	0.293	-0.734	0.539	-0.426	0.181	-0.580	0.337	-0.520	0.270	-0.543	0.295	-0.577	0.333	-0.566	0.321
NDre2m	-0.804	0.646	-0.614	0.377	-0.757	0.573	-0.445	0.198	-0.630	0.397	-0.553	0.306	-0.414	0.171	-0.495	0.245	-0.457	0.209
NDVI	-0.810	0.657	-0.529	0.280	-0.735	0.540	-0.483	0.233	-0.598	0.357	-0.562	0.316	-0.657	0.432	-0.598	0.357	-0.626	0.392
NDVIre1	-0.797	0.635	-0.534	0.285	-0.732	0.536	-0.415	0.172	-0.599	0.359	-0.517	0.267	-0.557	0.310	-0.540	0.291	-0.557	0.310
NDVIre1n	-0.812	0.659	-0.545	0.297	-0.743	0.551	-0.399	0.160	-0.607	0.368	-0.515	0.265	-0.510	0.260	-0.450	0.203	-0.489	0.239
NDVIre2	-0.791	0.626	-0.534	0.285	-0.732	0.536	-0.560	0.314	-0.666	0.443	-0.608	0.370	-0.506	0.256	-0.470	0.221	-0.497	0.247
NDVIre2n	-0.812	0.659	-0.545	0.297	-0.743	0.551	-0.446	0.199	-0.666	0.443	-0.561	0.315	-0.449	0.202	-0.322	0.104	-0.397	0.158
NDVIre3	-0.568	0.322	-0.381	0.145	-0.485	0.235	0.261	0.068	-0.336	0.113	0.296	0.088	-0.296	0.087	-0.266	0.071	-0.286	0.082
NDVIre3n	-0.568	0.322	-0.381	0.145	-0.485	0.235	-0.260	0.068	-0.336	0.113	0.162	0.026	-0.327	0.107	-0.287	0.082	-0.313	0.098
NDWI	-0.769	0.592	-0.456	0.207	-0.678	0.460	-0.541	0.293	-0.602	0.362	-0.595	0.355	-0.457	0.208	-0.596	0.355	-0.527	0.277
NDWI2	-0.474	0.225	-0.282	0.079	-0.413	0.171	-0.540	0.291	-0.592	0.351	-0.575	0.330	-0.313	0.098	-0.480	0.230	-0.393	0.154
NGBDI	-0.651	0.424	-0.345	0.119	-0.470	0.221	-0.494	0.244	-0.492	0.242	-0.428	0.183	-0.641	0.411	-0.691	0.478	-0.673	0.453
NGI	-0.687	0.471	-0.510	0.260	-0.640	0.410	-0.521	0.271	-0.617	0.380	-0.568	0.323	-0.595	0.354	-0.599	0.359	-0.583	0.340
NGRDI	0.512	0.263	-0.398	0.159	0.431	0.185	-0.463	0.215	-0.579	0.335	-0.545	0.297	0.406	0.165	0.250	0.062	0.330	0.109
NIR	-0.829	0.688	-0.453	0.205	-0.714	0.509	-0.686	0.471	-0.658	0.432	-0.700	0.490	-0.718	0.515	-0.762	0.580	-0.738	0.545
NIRV	-0.854	0.729	-0.519	0.269	-0.759	0.577	-0.572	0.327	-0.641	0.411	-0.635	0.404	-0.753	0.567	-0.772	0.596	-0.769	0.591
NLI	0.376	0.141	-0.319	0.102	0.361	0.131	0.505	0.255	-0.451	0.203	-0.485	0.235	0.518	0.268	0.509	0.259	0.520	0.270
NMDI	0.206	0.043	0.119	0.014	0.181	0.033	0.800	0.641	0.752	0.566	0.818	0.669	0.784	0.615	0.815	0.665	0.808	0.652
NPCI	-0.527	0.277	-0.250	0.062	-0.411	0.169	-0.264	0.070	-0.161	0.026	-0.205	0.042	-0.403	0.162	-0.325	0.105	-0.367	0.135
NPQI	0.769	0.592	0.456	0.207	0.678	0.460	0.541	0.293	0.611	0.373	0.599	0.359	0.459	0.211	0.596	0.355	0.527	0.277
NREI	0.808	0.653	0.581	0.337	0.762	0.581	-0.517	0.267	0.654	0.428	0.602	0.362	-0.642	0.412	-0.656	0.430	-0.656	0.430
NRI	-0.534	0.285	-0.261	0.068	-0.425	0.181	-0.294	0.087	0.370	0.137	-0.288	0.083	-0.424	0.180	-0.355	0.126	-0.396	0.157
OSAVI	-0.784	0.615	-0.498	0.248	-0.708	0.502	-0.415	0.172	-0.577	0.333	-0.517	0.267	-0.576	0.332	-0.540	0.291	-0.562	0.315

OSAVIREG	-0.812	0.659	-0.545	0.297	-0.743	0.551	-0.446	0.199	-0.666	0.443	-0.562	0.315	-0.474	0.224	-0.394	0.155	-0.443	0.196
PRI1	0.375	0.141	0.204	0.041	0.297	0.088	-0.241	0.058	-0.477	0.228	-0.370	0.137	-0.153	0.023	-0.270	0.073	-0.205	0.042
PSRI	0.658	0.434	0.504	0.254	0.624	0.390	0.401	0.161	0.616	0.379	0.514	0.265	0.221	0.049	0.327	0.107	0.263	0.069
RDVI	-0.787	0.619	-0.498	0.248	-0.710	0.505	-0.389	0.151	-0.557	0.310	-0.493	0.243	-0.572	0.327	-0.536	0.287	-0.558	0.312
RDVI2	-0.793	0.630	-0.506	0.256	-0.719	0.517	-0.374	0.140	-0.574	0.329	-0.491	0.241	-0.523	0.274	-0.452	0.205	-0.494	0.244
RDVIREG	-0.817	0.667	-0.544	0.296	-0.746	0.557	-0.446	0.199	-0.662	0.438	-0.558	0.311	-0.475	0.226	-0.399	0.159	-0.446	0.198
Red	-0.643	0.413	-0.285	0.081	-0.521	0.271	-0.565	0.319	-0.322	0.104	-0.477	0.228	-0.581	0.338	-0.656	0.430	-0.623	0.389
Red Edge	-0.820	0.672	-0.442	0.196	-0.704	0.495	-0.663	0.439	-0.608	0.370	-0.641	0.411	-0.666	0.444	-0.735	0.540	-0.704	0.496
REP	0.834	0.696	0.577	0.333	0.773	0.598	0.531	0.282	0.647	0.419	0.607	0.369	-0.644	0.415	-0.659	0.434	-0.647	0.418
RGBVI	-0.709	0.503	-0.467	0.218	-0.623	0.389	-0.594	0.353	-0.660	0.435	-0.624	0.389	-0.692	0.479	-0.731	0.534	-0.702	0.493
RGR	-0.510	0.260	0.395	0.156	-0.425	0.180	0.464	0.215	0.578	0.335	0.545	0.297	-0.420	0.176	-0.264	0.070	-0.346	0.119
RVI	-0.816	0.666	-0.522	0.272	-0.740	0.547	-0.368	0.135	-0.561	0.315	-0.480	0.230	-0.531	0.282	-0.455	0.207	-0.500	0.250
SAVI	-0.810	0.657	-0.521	0.271	-0.735	0.540	-0.400	0.160	-0.597	0.357	-0.515	0.265	-0.532	0.283	-0.450	0.203	-0.497	0.247
SAVIGRE	-0.697	0.486	-0.450	0.202	-0.634	0.402	-0.413	0.171	-0.563	0.317	-0.506	0.256	-0.478	0.228	-0.359	0.129	-0.430	0.185
SIPI	-0.695	0.483	-0.408	0.167	-0.606	0.368	-0.430	0.185	-0.508	0.258	-0.470	0.221	-0.548	0.300	-0.470	0.221	-0.517	0.267
SIPI1	0.743	0.553	0.609	0.371	0.721	0.520	0.513	0.263	0.710	0.504	0.632	0.399	0.418	0.175	0.445	0.198	0.436	0.190
SR	-0.787	0.619	-0.498	0.248	-0.710	0.504	-0.375	0.140	-0.547	0.299	-0.480	0.230	-0.568	0.323	-0.532	0.283	-0.556	0.309
SRPI	0.508	0.258	0.244	0.059	0.411	0.169	0.262	0.068	-0.164	0.027	0.194	0.038	0.389	0.151	0.307	0.094	0.352	0.124
SRre1	-0.776	0.603	-0.563	0.317	-0.727	0.529	0.499	0.249	-0.581	0.338	0.554	0.307	-0.548	0.301	-0.620	0.384	-0.588	0.345
SRre2	-0.776	0.603	-0.563	0.317	-0.727	0.529	0.499	0.249	-0.581	0.338	0.554	0.307	-0.548	0.301	-0.620	0.384	-0.588	0.345
SVI	-0.783	0.613	-0.495	0.245	-0.708	0.502	-0.438	0.192	-0.571	0.326	-0.523	0.274	-0.641	0.411	-0.637	0.406	-0.627	0.393
SWIR 1	-0.676	0.457	-0.361	0.131	-0.578	0.334	-0.728	0.530	-0.666	0.443	-0.723	0.522	-0.700	0.490	-0.737	0.544	-0.724	0.524
SWIR 2	0.446	0.199	0.310	0.096	0.416	0.173	0.661	0.437	0.697	0.485	0.666	0.443	0.635	0.403	0.702	0.492	0.674	0.454
TCARI	-0.725	0.526	-0.452	0.204	-0.653	0.426	-0.535	0.286	-0.631	0.398	-0.611	0.374	-0.660	0.436	-0.706	0.498	-0.690	0.476
TCI	0.687	0.473	0.451	0.204	0.624	0.389	0.490	0.240	0.624	0.389	0.548	0.301	0.478	0.228	0.385	0.148	0.442	0.195
TVI	0.613	0.375	0.426	0.181	0.541	0.293	0.654	0.428	0.790	0.624	0.710	0.505	-0.591	0.350	-0.613	0.376	-0.608	0.370
VARI	0.198	0.039	-0.137	0.019	0.134	0.018	-0.247	0.061	-0.462	0.213	-0.366	0.134	0.186	0.035	-0.138	0.019	0.128	0.016
VARI2	-0.295	0.087	-0.294	0.086	-0.320	0.103	-0.373	0.139	-0.582	0.339	-0.488	0.238	0.159	0.025	-0.190	0.036	-0.144	0.021

VI1	-0.266	0.071	-0.163	0.027	-0.236	0.056	-0.403	0.163	0.544	0.295	0.461	0.213	0.435	0.189	-0.383	0.146	0.395	0.156
VI3	-0.304	0.092	-0.077	0.006	-0.217	0.047	0.026	0.001	0.076	0.006	0.052	0.003	-0.220	0.049	-0.352	0.124	-0.284	0.081
VI6	-0.675	0.456	-0.338	0.114	-0.549	0.302	-0.545	0.297	-0.434	0.189	-0.521	0.271	-0.463	0.215	-0.608	0.369	-0.536	0.287
VI7	0.124	0.015	0.077	0.006	0.109	0.012	-0.350	0.123	-0.541	0.292	-0.456	0.208	-0.408	0.166	-0.284	0.081	-0.357	0.127
VI8	-0.467	0.218	-0.290	0.084	-0.420	0.176	-0.338	0.114	-0.536	0.287	-0.444	0.197	-0.410	0.168	-0.294	0.086	-0.363	0.132
Vog1	-0.578	0.334	-0.464	0.215	-0.572	0.327	-0.230	0.053	-0.531	0.282	-0.390	0.152	-0.097	0.009	0.029	0.001	-0.041	0.002
Vog2	0.486	0.237	0.275	0.076	0.424	0.180	0.350	0.123	0.247	0.061	0.319	0.102	0.186	0.035	0.348	0.121	0.263	0.069
Vog3	0.473	0.224	0.264	0.070	0.411	0.169	0.356	0.126	0.248	0.061	0.322	0.104	0.186	0.034	0.348	0.121	0.262	0.069
WBI	0.570	0.325	0.421	0.177	0.530	0.281	0.447	0.199	0.580	0.336	0.513	0.263	0.305	0.093	0.407	0.165	0.325	0.106
WDRVI	-0.814	0.663	-0.532	0.283	-0.738	0.545	-0.460	0.211	-0.581	0.337	-0.540	0.291	-0.658	0.433	-0.600	0.361	-0.628	0.395
WI1	-0.572	0.328	-0.415	0.172	-0.539	0.291	-0.444	0.197	-0.581	0.338	-0.514	0.264	-0.307	0.094	-0.408	0.167	-0.327	0.107
WI2	0.753	0.567	0.465	0.216	0.672	0.451	0.612	0.375	0.635	0.404	0.650	0.423	0.459	0.211	0.593	0.352	0.526	0.276
ZM	-0.781	0.610	-0.514	0.264	-0.717	0.514	-0.334	0.112	-0.544	0.296	-0.456	0.208	-0.367	0.135	-0.311	0.096	-0.347	0.120

A4.2. Pearson correlation and Coefficient of determination for vegetation indices derived from multispectral imagery across ecosystem and CBI type.

Vegetation Indices	Coniferous forest						Broadleaf forest						Shrubland					
	vegetation CBI		soil CBI		site CBI		vegetation CBI		soil CBI		site CBI		vegetation CBI		soil CBI		site CBI	
	r	R^2	r	R^2	r	R^2	r	R^2	r	R^2	r	R^2	r	R^2	r	R^2	r	R^2
BAI	0.787	0.619	0.454	0.207	0.690	0.476	0.625	0.390	0.544	0.296	0.620	0.384	0.565	0.319	0.447	0.200	0.519	0.269
BGR	0.836	0.699	0.521	0.271	0.752	0.566	0.660	0.436	0.623	0.388	0.678	0.460	0.483	0.234	0.388	0.150	0.446	0.199
Blue	-0.193	0.037	0.059	0.003	-0.084	0.007	0.060	0.004	0.220	0.048	0.142	0.020	0.283	0.080	0.377	0.142	0.330	0.109
CIGREEN	-0.855	0.731	-0.541	0.293	-0.774	0.599	-0.577	0.333	-0.633	0.401	-0.636	0.405	-0.851	0.724	-0.785	0.616	-0.832	0.693
CIREDGE	-0.881	0.776	-0.556	0.309	-0.796	0.634	-0.669	0.447	-0.653	0.426	-0.698	0.487	-0.787	0.619	-0.691	0.478	-0.754	0.569
CIVE	0.348	0.121	0.176	0.031	0.293	0.086	0.006	0.000	0.284	0.081	0.143	0.020	-0.763	0.583	-0.703	0.494	-0.746	0.557
DVI	-0.849	0.720	-0.526	0.277	-0.763	0.582	-0.524	0.274	-0.604	0.365	-0.592	0.350	-0.816	0.666	-0.737	0.543	-0.791	0.626
DVIGRE	-0.850	0.723	-0.530	0.280	-0.765	0.586	-0.577	0.333	-0.622	0.387	-0.631	0.398	-0.820	0.672	-0.738	0.544	-0.794	0.630
DVIRED	-0.869	0.755	-0.542	0.294	-0.783	0.612	-0.616	0.380	-0.646	0.417	-0.665	0.442	-0.783	0.613	-0.719	0.517	-0.752	0.566
ENDVI	-0.840	0.706	-0.532	0.283	-0.761	0.579	-0.714	0.509	-0.665	0.442	-0.729	0.532	-0.730	0.534	-0.658	0.432	-0.707	0.500
EVI	-0.461	0.213	-0.343	0.118	-0.443	0.196	-0.099	0.010	-0.317	0.101	-0.211	0.045	0.191	0.036	0.127	0.016	0.164	0.027
EXB	0.219	0.048	0.094	0.009	0.176	0.031	-0.053	0.003	0.240	0.058	0.088	0.008	-0.753	0.567	-0.685	0.469	-0.732	0.536
EXG	-0.762	0.580	-0.453	0.205	-0.675	0.455	-0.299	0.090	-0.478	0.228	-0.403	0.163	0.197	0.039	0.259	0.067	0.228	0.052
EXG2	0.737	0.543	0.368	0.135	0.618	0.381	0.215	0.046	0.381	0.145	0.308	0.095	0.171	0.029	0.225	0.050	0.198	0.039
EXGR	-0.833	0.693	-0.508	0.258	-0.744	0.554	-0.470	0.221	-0.567	0.321	-0.543	0.295	-0.299	0.089	-0.205	0.042	-0.260	0.068
EXR	0.830	0.688	0.520	0.271	0.749	0.560	0.696	0.484	0.626	0.391	0.700	0.490	0.514	0.264	0.419	0.176	0.478	0.228
GLI	-0.762	0.581	-0.452	0.204	-0.675	0.455	-0.297	0.088	-0.477	0.227	-0.401	0.161	0.197	0.039	0.259	0.067	0.228	0.052
GNDVI	-0.858	0.737	-0.539	0.290	-0.775	0.600	-0.675	0.456	-0.661	0.437	-0.706	0.498	-0.859	0.738	-0.790	0.624	-0.840	0.705
Green	-0.618	0.382	-0.278	0.077	-0.503	0.253	-0.302	0.091	-0.164	0.027	-0.251	0.063	-0.039	0.002	0.071	0.005	0.011	0.000
IPVI	-0.854	0.729	-0.529	0.280	-0.767	0.589	-0.549	0.301	-0.624	0.389	-0.616	0.379	-0.847	0.718	-0.774	0.599	-0.826	0.682
IRGBVI	-0.828	0.685	-0.503	0.253	-0.739	0.546	-0.439	0.193	-0.551	0.303	-0.518	0.268	-0.246	0.061	-0.154	0.024	-0.207	0.043

MGRVI	-0.340	0.115	-0.171	0.029	-0.286	0.082	-0.010	0.000	-0.288	0.083	-0.147	0.022	0.760	0.578	0.700	0.490	0.743	0.552
MNLI	-0.366	0.134	-0.079	0.006	-0.255	0.065	0.310	0.096	0.178	0.032	0.218	0.047	-0.322	0.103	-0.339	0.115	-0.334	0.112
MRESR	-0.881	0.776	-0.556	0.309	-0.796	0.634	-0.669	0.447	-0.653	0.426	-0.698	0.487	-0.787	0.619	-0.691	0.478	-0.754	0.569
MRGBVI	-0.844	0.712	-0.534	0.285	-0.763	0.583	-0.709	0.503	-0.662	0.439	-0.725	0.526	-0.697	0.485	-0.619	0.383	-0.671	0.450
NBR	0.683	0.466	0.414	0.171	0.609	0.371	0.391	0.153	0.449	0.201	0.428	0.183	0.196	0.038	0.070	0.005	0.141	0.020
NDMI	0.731	0.534	0.312	0.097	0.586	0.344	0.514	0.264	0.517	0.267	0.544	0.295	0.586	0.343	0.466	0.217	0.539	0.291
NDRE	-0.882	0.778	-0.549	0.301	-0.794	0.630	-0.670	0.449	-0.649	0.421	-0.697	0.485	-0.785	0.616	-0.689	0.475	-0.752	0.566
NDVI	-0.854	0.729	-0.529	0.280	-0.767	0.589	-0.549	0.301	-0.624	0.389	-0.616	0.379	-0.847	0.718	-0.774	0.599	-0.826	0.682
NGBDI	-0.837	0.700	-0.521	0.272	-0.753	0.567	-0.660	0.435	-0.626	0.392	-0.680	0.462	-0.489	0.239	-0.395	0.156	-0.453	0.205
NGI	-0.762	0.580	-0.453	0.205	-0.675	0.455	-0.299	0.090	-0.478	0.228	-0.403	0.163	0.197	0.039	0.259	0.067	0.228	0.052
NGRDI	-0.339	0.115	-0.171	0.029	-0.285	0.081	-0.008	0.000	-0.286	0.082	-0.145	0.021	0.760	0.578	0.700	0.490	0.743	0.553
NIR	-0.833	0.695	-0.499	0.249	-0.740	0.548	-0.577	0.333	-0.595	0.354	-0.618	0.382	-0.624	0.390	-0.515	0.265	-0.583	0.340
NIRV	-0.843	0.711	-0.527	0.277	-0.760	0.577	-0.496	0.246	-0.591	0.349	-0.570	0.325	-0.814	0.663	-0.737	0.543	-0.790	0.624
NLI	-0.366	0.134	-0.079	0.006	-0.255	0.065	0.310	0.096	0.178	0.032	0.218	0.047	-0.322	0.103	-0.339	0.115	-0.334	0.112
NREI	0.871	0.758	0.538	0.290	0.782	0.611	-0.531	0.282	-0.600	0.360	-0.585	0.342	-0.682	0.466	-0.672	0.452	-0.687	0.472
NRI	-0.214	0.046	-0.174	0.030	-0.213	0.045	-0.261	0.068	0.070	0.005	-0.113	0.013	-0.706	0.499	-0.626	0.392	-0.679	0.462
Red	-0.419	0.175	-0.179	0.032	-0.336	0.113	-0.260	0.068	0.039	0.002	-0.128	0.016	-0.255	0.065	-0.142	0.020	-0.207	0.043
Red Edge	-0.816	0.666	-0.493	0.243	-0.727	0.528	-0.571	0.326	-0.572	0.327	-0.587	0.345	-0.573	0.329	-0.475	0.226	-0.537	0.288
REP	-0.803	0.645	-0.468	0.219	-0.707	0.500	-0.605	0.366	-0.565	0.319	-0.617	0.380	-0.512	0.262	-0.398	0.158	-0.467	0.218
RGBVI	-0.775	0.601	-0.462	0.213	-0.687	0.472	-0.327	0.107	-0.495	0.245	-0.427	0.182	0.070	0.005	0.141	0.020	0.103	0.011
RGR	0.332	0.110	0.161	0.026	0.276	0.076	-0.015	0.000	0.269	0.073	0.124	0.015	-0.762	0.581	-0.702	0.493	-0.745	0.556
SVI	0.095	0.009	0.157	0.025	0.134	0.018	-0.508	0.258	-0.598	0.358	-0.580	0.337	-0.774	0.599	-0.737	0.544	-0.768	0.590
SWIR 1	-0.352	0.124	-0.039	0.001	-0.227	0.051	-0.459	0.211	-0.092	0.009	-0.305	0.093	-0.555	0.308	-0.444	0.197	-0.512	0.262
SWIR 2	0.566	0.321	0.448	0.200	0.557	0.310	0.397	0.158	0.598	0.358	0.518	0.268	0.012	0.000	0.121	0.015	0.062	0.004
WDRVI	-0.850	0.723	-0.530	0.281	-0.766	0.586	-0.514	0.265	-0.607	0.368	-0.588	0.346	-0.846	0.715	-0.773	0.598	-0.824	0.680

ANNEX 5 – Scripts in Python and R

A5.1. Python script for calculating vegetation indices from PRISMA hyperspectral imagery aligned with CBI plots

```
# Calculate indices from HYPERSPECTRAL image
#### Install libraries
# !pip install rasterio matplotlib pyproj
#### Import libraries and read hyperspectral image (.tiff)
from math import log
import numpy as np
import pandas as pd
import rasterio
from rasterio.plot import show
from rasterio.transform import rowcol
import matplotlib.pyplot as plt
from pyproj import Proj, transform
import openpyxl
import shutil
# Path to the .tiff file
working_dir = "C:/Users/User/OneDrive - UVa/1_ASIGNATURAS/TFM/1_DataProcessing/"
tiff_file_orig = working_dir + "2_SatellitalImages/2_HYP/inicial_2_mtotal.tiff"
tiff_file = working_dir +
"2_SatellitalImages/2_HYP/z_CoRegisteredImage/imagen_coregistered_global_191band.ti
f"
#### Open hyperspectral image and classify wavelengths by landsat approach
def open_tiff(tiff_file):
  # Open the GeoTIFF file
  with rasterio.open(tiff_file) as src:
    # Read the custom metadata (wavelengths)
    wavelengths = src.tags().get('Wavelengths', 'No wavelengths information found')
    if wavelengths != 'No wavelengths information found':
      wavelengths = eval(wavelengths)  # Convert string representation back to list

    # Convert a list of strings to a list of numbers
    wavelength = []
    for wv in wavelengths:
      wavelength.append(float(wv))
  return wavelength

def classify_wavelength(wl):
  if 1900 <= wl < 2500:
    return 'SWIR 2'
  elif 1050 <= wl < 1900:
    return 'SWIR 1'
  elif 750 <= wl < 1050:
    return 'NIR'
```

```
    elif 700 <= wl < 750:
        return 'Red Edge'
    elif 600 <= wl < 700:
        return 'Red'
    elif 500 <= wl < 600:
        return 'Green'
    elif 400 <= wl < 500:
        return 'Blue'
    else:
        return '***'

def create_band_list(wavelength):
    band_lst = []
    count = 1
    for wl in wavelength:
        bandL9 = classify_wavelength(wl)
        band_classL9_tuples = (count, bandL9, wl)
        band_lst.append(band_classL9_tuples)
        count += 1
    return band_lst

# Run the classification
wavelength = open_tiff(tiff_file_orig)
band_lst = create_band_list(wavelength)
for m in band_lst:
    print(m)
#### Vegetation Indices Formulas
# Normalized Difference Vegetation Index: NDVI
def calculate_ndvi(red, nir):
    ndvi = (nir - red) / (nir + red)
    return ndvi
# Normalized Burn Ratio: NBR
def calculate_nbr(nir, swir2):
    nbr = (nir - swir2) / (nir + swir2)
    return nbr
# Normalized Difference Moisture Index: NDMI
def calculate_ndmi(nir, swir1):
    ndmi = (nir - swir1) / (nir + swir1)
    return ndmi
# Difference Vegetation Index: DVI
def calculate_dvi(red, nir):
    dvi = nir - red
    return dvi
# Green Difference Vegetation Index: DVIGRE o GDVI
def calculate_dvigre(green, nir):
    dvigre = nir - green
    return dvigre
```

```
# Red Difference Vegetation Index: DVIRED
def calculate_dvired(redge, nir):
    dvired = nir - redge
    return dvired
# Chlorophyll Index With Red Edge: CIREDGE
def calculate_ciredge(redge, nir):
    ciredge = (nir / redge) - 1
    return ciredge
# Chlorophyll Index With Green: CIGREEN
def calculate_cigreen(green, nir):
    cigreen = (nir / green) - 1
    return cigreen
# Infrared Percentage Vegetation Index: IPVI
def calculate_ipvi(red, nir):
    ipvi = nir / (nir + red)
    return ipvi
# Near-Infrared Reflectance of Vegetation: NIRV
def calculate_nirv(red, nir):
    nirv = nir * ((nir - red) / (nir + red))
    return nirv
# Modified Non-Linear Index: MNLI
def calculate_mnli(nir, red):
    mnli = 1.5 * (nir ** 2 - red) / (nir ** 2 + red + 0.5)
    return mnli
# Non-Linear Index: NLI
def calculate_nli(nir, red):
    nli = (nir ** 2 - red) / (nir ** 2 + red)
    return nli
# Wide Dynamic Range Vegetation Index: WDRVI
def calculate_wdrvi(nir, red):
    wdrvi = (0.2 * nir - red) / (0.2 * nir + red)
    return wdrvi
# Normalized Difference Red Edge Index: NDRE
def calculate_ndre(redge, nir):
    ndre = (nir - redge) / (nir + redge)
    return ndre
# Burn Area Index: BAI
def calculate_bai(redge, nir):
    bai = 1 / (((redge - 0.1) ** 2) + ((nir - 0.06) ** 2))
    return bai
# Structural Vegetation Index: SVI
def calculate_svi(redge, red):
    svi = (redge - red) / (redge + red)
    return svi
# Modified Red-Edge Simple Ratio: MRESR
def calculate_mresr(redge, nir):
    mresr = nir / redge
```

```
    return mresr
# Three-Band Difference Vegetation Index: TBDVI
def calculate_tbdvi(red, nir, swir1):
    tbdvi = nir - (red - swir1) / 2
    return tbdvi
# Enhanced Vegetation Index: EVI
def calculate_evi(blue, red, nir):
    evi = 2.5 * ((nir - red)/(nir + 6 * red - 7.5 * blue + 1))
    return evi
# Excess Green Index: EXG2
def calculate_exg2(blue, green, red):
    exg2 = 2 * green - red - blue
    return exg2
# Red Light Normalized Value: NRI
def calculate_nri(blue, green, red):
    nri = red / (red + green + blue)
    return nri
# Green Light Normalized Value: NGI
def calculate_ngi(blue, green, red):
    ngi = green / (red + green + blue)
    return ngi
# Green Normalized Difference Vegetation Index: GNDVI
def calculate_gndvi(green, redge, nir):
    gndvi = (nir - green) / (nir + redge)
    return gndvi
# Enhances Normalized Difference Vegetation Index: ENDVI
def calculate_endvi(redge, green, blue):
    endvi = (redge + green - 2 * blue) / (redge + green + 2 * blue)
    return endvi
# Modified Red Green- Blue Vegetation Index: MRGBVI
def calculate_mrgbvi(redge, green, blue):
    mrgbvi = (redge + 2 * green - 2 * blue) / (redge + 2 * green + 2 * blue)
    return mrgbvi
# Nitrogen Reflectance Index: NREI
def calculate_nrei(green, redge, nir):
    nrei = redge / (redge + nir + green)
    return nrei
# Red Edge Position Index: REP
def calculate_rep(red, redge, nir):
    rep = 700 + 40 * ((red + nir)/(2 - redge))
    return rep
##############################################
def normalized_band (red, green, blue):
    R = red / (red + green + blue)
    G = green / (red + green + blue)
    B = blue / (red + green + blue)
    return R, G, B
```

```
##########################################
# Excess Green Index: EXG
def calculate_exg(red, green, blue):
    R,G,B = normalized_band(red, green, blue)
    exg = 2 * G - R - B
    return exg
# Excess Blue Index: EXB
def calculate_exb(red, green, blue):
    R,G,B = normalized_band(red, green, blue)
    exb = 1.4 * R - G
    return exb
# Excess Red Index: EXR
def calculate_exr(red, green, blue):
    R,G,B = normalized_band(red, green, blue)
    exr = 1.4 * B - G
    return exr
# Red / Green Ratio: RGR
def calculate_rgr(red, green, blue):
    R,G,B = normalized_band(red, green, blue)
    rgr = R / G
    return rgr
# Blue / Green Ratio: BGR
def calculate_bgr(red, green, blue):
    R,G,B = normalized_band(red, green, blue)
    bgr = B / G
    return bgr
# Normalized Green-Red Difference Index: NGRDI
def calculate_ngrdi(red, green, blue):
    R,G,B = normalized_band(red, green, blue)
    ngrdi = (G - R) / (G + R)
    return ngrdi
# Normalized Green-Blue Difference Index: NGBDI
def calculate_ngbdi(red, green, blue):
    R,G,B = normalized_band(red, green, blue)
    ngbdi = (G - B) / (G + B)
    return ngbdi
# Modified Green-Red Vegetation Index: MGRVI
def calculate_mgrvi(red, green, blue):
    R,G,B = normalized_band(red, green, blue)
    mgrvi = (G**2 - R**2) / (G**2 + R**2)
    return mgrvi
# Red Green- Blue Vegetation Index: RGBVI
def calculate_rgbvi(red, green, blue):
    R,G,B = normalized_band(red, green, blue)
    rgbvi = (G**2 - R * B) / (G**2 + R * B)
    return rgbvi
# Green Leaf Index: GLI
```

```
def calculate_gli(red, green, blue):
    R,G,B = normalized_band(red, green, blue)
    gli = (2*G - R - B) / (2*G + R + B)
    return gli
# Color Index of Vegetation Extraction: CIVE
def calculate_cive(red, green, blue):
    R,G,B = normalized_band(red, green, blue)
    cive = 0.441*R - 0.881*G + 0.385*R + 18.78745
    return cive
# Excess Green Minus Excess Red Index: ExGR
def calculate_exgr(red, green, blue):
    exg = calculate_exg(red, green, blue)
    exr = calculate_exr(red, green, blue)
    exgr = exg - exr
    return exgr
# Improved Red Green- Blue Vegetation Index: IRGBVI
def calculate_irgbvi(red, green, blue):
    R,G,B = normalized_band(red, green, blue)
    irgbvi = (5*G**2 - 2*R**2 - 5*B**2) / (5*G**2 + 2*R**2 + 5*B**2)
    return irgbvi
# Model 1 in Vegetation Index
def calculate_vi_model1(band_a, band_b, band_c, band_d):
    vi_model1 = band_a / band_b
    return vi_model1
    # Greenness Index: G = r554/r677
    # Simple R. Pigment Ind.: SRPI = r430/r680
    # Lichtenthaler Index 2: Lic2 = r440 / r690
    # Carter Index 1: Ctr1 = r695 / r420
    # Carter Index 2: Ctr2 = r695 / r760
    # Vogelmann Index 1: Vog1 = r740 / r720
    # Gitelson and Merzlyak Index 1: GM1 = r750 / r550
    # Gitelson and Merzlyak Index 2: GM2 = r750 / r700
    # Zarco-Tejada & Miller: ZM = r750 / r710
    # Fluorescence Ratio Index 1: FRI1 = r740 / r800
    # Fluorescence Ratio Index 2: FRI2 = r690 / r600
    # Simple Ratio Index: SR = r800 / r670
    # Water Index: WI1 = r900 / r970
    # Water Index: WI2 = r1600 / r820
    # Moisture Stress Index: MSI = r1599 / r819
    # Ratio Vegetation Index: RVI = r887 / r678
    # Green Ratio Vegetation Index: GRVI = r865/r550
    # Green Red Ratio Vegetation Index: GR = r550/r650
    # Green Blue Ratio Vegetation Index: GB = r550/r485
    # VI8 = r998 / r713
    # Water Band Index: WBI = wl_970 / wl_900
# Model 2a in Vegetation Index
def calculate_vi_model2a(band_a, band_b, band_c, band_d):
```

```
    vi_model2a = (band_a - band_b) / (band_a + band_b)
    return vi_model2a
    # Normalized Phaeophytinization Index: NPQI = (r415 - r435) / (r415 + r435)
    # Photochemical Reflectance Index 1: PRI1 = (r528 - r567) / (r528 + r567)
    # Normalized Pigment Chlorophyll Index: NPCI = (r680 - r430) / (r680 + r430)
    # Lichtenthaler Index 1: Lic1 = (r800 - r680) / (r800 + r680)
    # Visible Atmospherically Resistant Index: VARI = (r550 - r670) / (r550 + r670)
    # Normalized Difference Water Index: NDWI = (r800 - r1600) / (r800 + r1600)
    # Normalized Difference Water Index 2: NDWI2 = (r857 - r1241) / (r857 + r1241)
    # Depth Water Index: DWI = (r816 - r2218) / (r816 + r2218)
    # Hyperspectral Fire Detection Index: HFDI = (r2430 - r2060) / (r2430 + r2060)
    # VI7 = (r998 - r713) / (r998 + r713)
    # Normalized Difference Vegetation Index red-edge 1: NDVIre1 = (r833 - r699) / (r833 +
r699)
    # Normalized Difference Vegetation Index red-edge 1: NDVIre1n = (r865 - r699) / (r865 +
r699)
    # Normalized Difference Vegetation Index red-edge 2: NDVIre2 = (r833 - r729) / (r833 +
r729)
    # Normalized Difference Vegetation Index red-edge 2: NDVIre2n = (r865 - r729) / (r865 +
r729)
    # Normalized Difference Vegetation Index red-edge 3: NDVIre3 = (r833 - r780) / (r833 +
r780)
    # Normalized Difference Vegetation Index red-edge 3: NDVIre3n = (r865 - r780) / (r865 +
r780)
    # Normalized Difference red-edge 1: NDre1 = (r729 - r699) / (r729 + r699)
    # Normalized Difference red-edge 2: NDre2 = (r780 - r699) / (r780 + r699)
    # Leaf Water Vegetation Index 1: LWVI1 = (r1099 - r988) / (r1099 + r988)
    # Leaf Water Vegetation Index 2: LWVI2 = (r1099 - r1207) / (r1099 + r1205)
    # Normalized Difference Infrared Index: NDII = (r823 - r1646) / (r823 + r1646)
# Model 2b in Vegetation Index
def calculate_vi_model2b(band_a, band_b, band_c, band_d):
    vi_model2b = (band_a - band_b) / (band_a + band_c)
    return vi_model2b
    # Structure Intensive Pigment Index: SIPI = (r800 - r450) / (r800 + r650)
    # Meris Terrestrial Chlorophyll Index: MTCI = (r865 - r717) / (r865 - r650)
    # Leaf Chlorophyll Index: LCI = (r855 - r708) / (r855 + r679)
# Model 2c in Vegetation Index
def calculate_vi_model2c(band_a, band_b, band_c, band_d):
    vi_model2c = (band_a - band_b) / (band_c - band_b)
    return vi_model2c
    # Mangrove Vegetation Index: MVI = (r842 - r561) / (r1610 - r561)
# Model 2d in Vegetation Index
def calculate_vi_model2d(band_a, band_b, band_c, band_d):
    vi_model2d = (band_a - band_b) / (band_c + band_d)
    return vi_model2d
    # Vogelmann Index 2: Vog2 = (r734 - r747) / (r715 + r726)
    # Vogelmann Index 3: Vog3 = (r734 - r747) / (r715 + r720)
```

```
    # Disease Water Stress Index: DWSI = (r801 - r546) / (r1656 + r879)
# Model 2e in Vegetation Index
def calculate_vi_model2e(band_a, band_b, band_c, band_d):
    vi_model2e = (band_a ** 2- band_b ** 2) / (band_a ** 2 + band_b ** 2)
    return vi_model2e
    # VI5 = (r513 ** 2 - r504 **2) / (r513 ** 2 + r504 ** 2)
# Model 2f in Vegetation Index
def calculate_vi_model2f(band_a, band_b, band_c, band_d):
    vi_model2f = (band_a- band_b) / (band_c - band_b)
    return vi_model2f
    # Simple Ratio red-edge 1: SRre1 = (r729 - r441) / (r699 - r441)
    # Simple Ratio red-edge 2: SRre2 = (r780 - r441) / (r699 - r441)
    # Structure Independent Pigment Index: SIPI1 = (r445 - r800) / (r670 + r800)
# Model 3a in Vegetation Index
def calculate_vi_model3a(band_a, band_b, band_c, band_d):
    vi_model3a = (band_a / band_b) / ((band_a / band_b)**0.5)
    return vi_model3a
    # Renormalized Difference Vegetation Index: RDVI = (r800 / r670) / ((r800 / r670)**0.5)
    # Renormalized Difference Vegetation Index: RDVI2 = (r865 / r670) / ((r865 / r670)**0.5)
    # Red Difference Vegetation Index With Red Edge: RDVIREG = (r865 - r717) / ((r865 +
r717) ** 0.5)
# Model 3b in Vegetation Index
def calculate_vi_model3b(band_a, band_b, band_c, band_d):
    vi_model3b = (band_a / (band_b - 1)) / ((band_a / (band_b + 1))**0.5)
    return vi_model3b
    # Modified Simple Ratio: MSR = (r865 / (r660 - 1))/(r865 / (r660 + 1)) ** 0.5
    # Modified Simple Ratio With Red Edge: MSRREG = (r865 / (r717 - 1))/(r865 / (r717 +
1)) ** 0.5
# Model 4 in Vegetation Index
def calculate_vi_model4(band_a, band_b, band_c, band_d):
    vi_model4 = ((band_a / band_b) - 1) / (((band_a / band_b) + 1)**0.5)
    return vi_model4
    # Modified Simple Ratio Index: MSR2 = ((r800 / r670) - 1) / (((r800 / r670) + 1)**0.5)
# Model 5a in Vegetation Index
def calculate_vi_model5a(band_a, band_b, band_c, band_d):
    vi_model5a = (1 + 0.16) * (band_a - band_b) / (band_a + band_b + 0.16)
    return vi_model5a
    # Optimized Soil-Adjusted Vegetation Index: OSAVI = (1 + 0.16) * (r800 - r670) / (r800 +
r670 + 0.16)
    # Soil-Adjusted Vegetation Index: SAVI = (1 + 0.16) * (r887 - r678) / (r887 + r678 + 0.16)
    # Optimized Soil-adjusted Vegetation Index With Red Edge: OSAVIREG = (1 + 0.16) *
(r865 - r717) / (r865 + r717 + 0.16)
# Model 5b in Vegetation Index
def calculate_vi_model5b(band_a, band_b, band_c, band_d):
    vi_model5b = 1.5 * (band_a - band_b) / (band_a + band_b + 0.5)
    return vi_model5b
    # Green Soil Adjusted Vegetation Index: GSAVI = 1.5 * (r800 - r560) / (r800 + r560 + 0.5)
```

```
# Model 6 in Vegetation Index
def calculate_vi_model6(band_a, band_b, band_c, band_d):
    vi_model6 = ((band_a - band_b) - 0.2 * (band_a - band_c)) * (band_c / band_b)
    return vi_model6
    # Modified Chlorophyll Absorption in Reflectance Index 1: MCARI1 = ((r700 - r670) - 0.2
* (r700 - r550)) * (r700 / r670)
# Model 7 in Vegetation Index
def calculate_vi_model7(band_a, band_b, band_c, band_d):
    vi_model7 = 1.2 * (2.5 * (band_a - band_b) - 1.3 * (band_a - band_c))
    return vi_model7
    # Modified Chlorophyll Absorption in Reflectance Index 2: MCARI2 = 1.2 * (2.5 * (r800 -
r670) - 1.3 * (r800 - r550))
# Model 8 in Vegetation Index
def calculate_vi_model8(band_a, band_b, band_c, band_d):
    vi_model8 = 1.5 * (2.5 * (band_a - band_b) - 1.3 * (band_a - band_c)) / ((((2 * band_a +
1) ** 2) - (6 * band_a - 5 * (band_b ** 0.5)) - 0.5) ** 0.5)
    return vi_model8
    # Modified Chlorophyll Absorption in Reflectance Index 3: MCARI3 = 1.5 * (2.5 * (r800 -
r670) - 1.3 * (r800 - r550)) / ((((2 * r800 + 1) ** 2) - (6 * r800 - 5 * (r670 ** 0.5)) - 0.5) ** 0.5)
# Model 9 in Vegetation Index
def calculate_vi_model9(band_a, band_b, band_c, band_d):
    vi_model9 = 3 * ((band_a - band_b) - 0.2 * (band_a - band_c) * (band_a / band_b))
    return vi_model9
    # Transformed CARI: TCARI = 3 * ((r700 - r670) - 0.2 * (r700 - r550) * (r700 / r670))
# Model 10 in Vegetation Index
def calculate_vi_model10(band_a, band_b, band_c, band_d):
    vi_model10 = 0.5 * (120 * (band_a - band_b) - 200 * (band_c - band_b))
    return vi_model10
    # Triangular Vegetation Index: TVI = 0.5 * (120 * (r750 - r550) - 200 * (r670 - r550))
# Model 11 in Vegetation Index
def calculate_vi_model11(band_a, band_b, band_c, band_d):
    vi_model11 = 1.2 * (1.2 * (band_a - band_b) - 2.5 * (band_c - band_b))
    return vi_model11
    # Modified Triangular Vegetation Index 1: MTVI1 = 1.2 * (1.2 * (r800 - r550) - 2.5 * (r670 -
r550))
# Model 12 in Vegetation Index
def calculate_vi_model12(band_a, band_b, band_c, band_d):
    vi_model12 = (1.5 * (1.2 * (band_a - band_b) - 2.5 * (band_c - band_b))) / ((((2 * band_a
+ 1) ** 2 - (6 * band_a - (5 * (band_c ** 0.5)))) - 0.5) ** 0.5)
    return vi_model12
    # Modified Triangular Vegetation Index 2: MTVI2 = 1.5 * (1.2 * (r800 - r550) - 2.5 * (r670 -
r550)) / ((((2 * r800 + 1) ** 2 - (6 * r800 - (5 * (r670 ** 0.5)))) - 0.5) ** 0.5)
# Model 13 in Vegetation Index
def calculate_vi_model13(band_a, band_b, band_c, band_d):
    vi_model13 = 0.5 * (2 * band_a + 1 - (((2 * band_a + 1) ** 2) - 8 * (band_a - band_b)) **
0.5)
    return vi_model13
```

```
    # Improved SAVI with self-adjustment factor L: MSAVI = 0.5 * (2 * r800 + 1 - (((2 * r800 +
1) ** 2) - 8 * (r800 - r670)) ** 0.5)
# Model 14 in Vegetation Index
def calculate_vi_model14(band_a, band_b, band_c, band_d):
    vi_model14 = 2.5 * ((band_a - band_b) / (band_a + 2.4 * band_b + 1))
    return vi_model14
    # Enhanced Vegetation Index 2: EVI2 = 2.5 * ((r800 - r670) / (r800 + 2.4 * r670 + 1))
# Model 15 in Vegetation Index
def calculate_vi_model15(band_a, band_b, band_c, band_d):
    vi_model15 = ((band_a - band_b)/(band_a + band_b)) - ((band_a - band_c)/(band_a +
band_c))
    return vi_model15
    # Combine Mangrove Recognition Index (CMRI = NDVI - NDWI): CMRI = ((r865 -
r660)/(r865 + r660)) - ((r857 - r1241)/(r857 + r1241))
# Model 16 in Vegetation Index
def calculate_vi_model16(band_a, band_b, band_c, band_d):
    vi_model16 = ((band_a + 1.5 * band_b) - band_c) / (band_a - band_d)
    return vi_model16
    # Temperature Condition Index: TCI = ((r887 + 1.5 * r524) - r678) / (r887 - r701)
# Model 17 in Vegetation Index
def calculate_vi_model17(band_a, band_b, band_c, band_d):
    vi_model17 = (band_a - band_b) / (band_a + band_b + 0.01)
    return vi_model17
    # Normalized Red Green Difference Vegetation Index: NDIG = (r650 - r560)/(r650 + r560
+ 0.01)
    # Normalized Red Blue Difference Vegetation Index: NDIB = (r650 - r485)/(r650 + r485 +
0.01)
# Model 18 in Vegetation Index
def calculate_vi_model18(band_a, band_b, band_c, band_d):
    vi_model18 = 1.5 * (band_a - band_b) / (band_a + band_b + 0.5)
    return vi_model18
    # Soil-adjusted Vegetation Index With Green: SAVIGRE = 1.5 * (r865 - r560) / (r865 +
r560 + 0.5)
# Model 19 in Vegetation Index
def calculate_vi_model19(band_a, band_b, band_c, band_d):
    vi_model19 = (band_a - band_b) / (band_a + band_b - band_c)
    return vi_model19
    # Visible Atmospherically Resistant Index: VARI2 = (r560 - r650) / (r560 + r650 - r485)
# Model 20 in Vegetation Index
def calculate_vi_model20(band_a, band_b, band_c, band_d):
    vi_model20 = (band_a - band_b + 1.7 * (band_c - band_d)) /(band_a + band_b - 1.7 *
(band_c - band_d))
    return vi_model20
    # Green Atmospherically Resistant Index: GARI = (r865 - r560 + 1.7 * (r485 - r650))
/(r865 + r560 - 1.7 * (r485 - r650))
# Model 21 in Vegetation Index
def calculate_vi_model21(band_a, band_b, band_c, band_d):
```

```
    vi_model21 = (band_a) / (0.666 * band_b + 0.334 * band_c)
    return vi_model21
    # Carbon Dioxide Continuum Interpolated Band Ratio: CO2-CIBR = (r2010) / (0.666 *
r1990 + 0.334 * r2040)
# Model 22 in Vegetation Index
def calculate_vi_model22(band_a, band_b, band_c, band_d):
    vi_model22 = band_a / (band_b + band_c)
    return vi_model22
    # VI1 = r712 / (r998 + r693)
# Model 23 in Vegetation Index
def calculate_vi_model23(band_a, band_b, band_c, band_d):
    vi_model23 = (band_a - band_b) / band_c
    return vi_model23
    # VI3 = (r708 - r693) / r758
    # Plant Senescence Reflectance Index: PSRI = (r660 - r554) / (r729)
# Model 24 in Vegetation Index
def calculate_vi_model24(band_a, band_b, band_c, band_d):
    vi_model24 = (1 / band_a) - (1 / band_b)
    return vi_model24
    # VI6 = (1 / r1000) - (1 / r713)
    # Anthocyanin Reflectance Index 1: ARI1 =  (1 / r554) - (1 / r699)
    # Carotenoid Reflectance Index 1: CRI1 =  (1 / r507) - (1 / r546)
    # Carotenoid Reflectance Index 2: CRI2 =  (1 / r507) - (1 / r699)
# Model 25 in Vegetation Index
def calculate_vi_model25(band_a, band_b, band_c, band_d):
    vi_model25 = (band_a / band_b) - 1
    return vi_model25
    # Chlorophyll Index red-edge: Clre = (r780 / r699) - 1
# Model 26 in Vegetation Index
def calculate_vi_model26(band_a, band_b, band_c, band_d):
    vi_model26 = (band_a - band_b) / (band_a + band_b - 2 * band_c)
    return vi_model26
    # Normalized Difference red-edge 1 modified: NDre1m = (r729 - r699) / (r729 + r699 - 2 *
r441)
    # Normalized Difference red-edge 2 modified: NDre2m = (r780 - r699) / (r780 + r699 - 2 *
r441)
# Model 27 in Vegetation Index
def calculate_vi_model27(band_a, band_b, band_c, band_d):
    vi_model27 = ((band_a / band_b) - 1 ) / ((band_a / band_b) + 1) ** 0.5
    return vi_model27
    # Modified Simple Ratio red-edge: MSRre = ((r833 / r699) - 1 ) / ((r833 / r699) + 1) ** 0.5
    # Modified Simple Ratio red-edge narrow: MSRren = ((r865 / r699) - 1 ) / ((r865 / r699) +
1) ** 0.5
# Model 28 in Vegetation Index
def calculate_vi_model28(band_a, band_b, band_c, band_d):
    vi_model28 = (band_a - (band_b - (band_c - band_b))) / (band_a + (band_b - (band_c -
band_b)))
```

```
    return vi_model28
    # Atmospherically Resistant Vegetation Index: ARVI = (r801 - (r679 - (r449 - r679))) /
(r801 + (r679 - (r449 - r679)))
# Model 29 in Vegetation Index
def calculate_vi_model29(band_a, band_b, band_c, band_d):
    vi_model29 = (band_a - band_b) / (band_a + band_b - 2 * band_c)
    return vi_model29
    # Modified Red Edge Normalized Difference Vegetation Index: MRENDVI = (r749 - r708)
/ (r749 + r708 - 2 * r441)
# Model 30 in Vegetation Index
def calculate_vi_model30(band_a, band_b, band_c, band_d):
    vi_model30 = (np.log(1/band_a) - np.log(1/band_b)) / (np.log(1/band_a) +
np.log(1/band_b))
    return vi_model30
    # Normalized Difference Nitrogen Index: NDNI =  (log(1/r1512) - log(1/r1677)) /
(log(1/r1512) + log(1/r1677))
    # Normalized Difference Lignin Index: NDLI =  (log(1/r1755) - log(1/r1677)) /
(log(1/r1755) + log(1/r1677))
# Model 31 in Vegetation Index
def calculate_vi_model31(band_a, band_b, band_c, band_d):
    vi_model31 = 0.5 * (band_a + band_b) - band_c
    return vi_model31
    # Cellulose Absorption Index: CAI =  0.5 * (r1993 + r2206) - r2102
# Model 32 in Vegetation Index
def calculate_vi_model32(band_a, band_b, band_c, band_d):
    vi_model32 = 100 * ((band_a - band_b) + (band_a - band_c))
    return vi_model32
    # Lignin Cellulose Absorption Index: LCAI =  100 * ((r2206 - r2159) + (r2206 - r2335))
# Model 33 in Vegetation Index
def calculate_vi_model33(band_a, band_b, band_c, band_d):
    vi_model33 = band_a * ((1 / band_b) - (1 / band_c))
    return vi_model33
    # Anthocyanin Reflectance Index 2: ARI2 =  r801 * ((1 / r554) - (1 / r699))
# Model 34 in Vegetation Index
def calculate_vi_model34(band_a, band_b, band_c, band_d):
    vi_model34 = (band_a - (band_b - band_c)) / (band_a + (band_b - band_c))
    return vi_model34
    # Normalized Multi-band Drought Index: NMDI = (r855 - (r1636 - r2127)) / (r855 + (r1636
- r2127))
def select_model(vi, band_a, band_b, band_c, band_d):
    model1 = ["G", "SRPI", "Lic2", "Ctr1", "Ctr2", "Vog1", "GM1", "GM2", "ZM", "FRI1",
"FRI2", "SR", "WI1", "WI2", "MSI", "RVI", "GRVI", "GR", "GB", "P1", "P2", "VI8","WBI"]
    model2a = ["NPQI", "PRI1", "PRI2", "NPCI", "Lic1", "VARI", "NDWI", "NDWI2", "DWI",
"HFDI", "VI7", "NDVIre1", "NDVIre1n", "NDVIre2", "NDVIre2n", "NDVIre3", "NDVIre3n",
"NDre1", "NDre2","LWVI1","LWVI2","NDII"]
    model2b = ["SIPI", "MTCI", "LCI"]
    model2c = ["MVI"]
```

```
model2d = ["Vog2", "Vog3","DWSI"]
model2e = ["VI5"]
model2f = ["SRre1","SRre2","SIPI1"]
model3a = ["RDVI", "RDVI2", "RDVIREG"]
model3b = ["MSR", "MSRREG"]
model4 = ["MSR2"]
model5a = ["OSAVI", "SAVI", "OSAVIREG"]
model5b = ["GSAVI"]
model6 = ["MCARI1"]
model7 = ["MCARI2"]
model8 = ["MCARI3"]
model9 = ["TCARI"]
model10 = ["TVI"]
model11 = ["MTVI1"]
model12 = ["MTVI2"]
model13 = ["MSAVI"]
model14 = ["EVI2"]
model15 = ["CMRI"]
model16 = ["TCI"]
model17 = ["NDIG", "NDIB"]
model18 = ["SAVIGRE"]
model19 = ["VARI2"]
model20 = ["GARI"]
model21 = ["CO2-CIBR"]
model22 = ["VI1"]
model23 = ["VI3", "PSRI"]
model24 = ["VI6","ARI1","CRI1","CRI2"]
model25 = ["Clre"]
model26 = ["NDre1m", "NDre2m"]
model27 = ["MSRre", "MSRren"]
model28 = ["ARVI"]
model29 = ["MRENDVI"]
model30 = ["NDNI", "NDLI"]
model31 = ["CAI"]
model32 = ["LCAI"]
model33 = ["ARI2"]
model34 = ["NMDI"]

if vi in model1:
   veg_index_values = calculate_vi_model1(band_a, band_b, band_c, band_d)
elif vi in model2a:
   veg_index_values = calculate_vi_model2a(band_a, band_b, band_c, band_d)
elif vi in model2b:
   veg_index_values = calculate_vi_model2b(band_a, band_b, band_c, band_d)
elif vi in model2c:
   veg_index_values = calculate_vi_model2c(band_a, band_b, band_c, band_d)
elif vi in model2d:
```

```
    veg_index_values = calculate_vi_model2d(band_a, band_b, band_c, band_d)
elif vi in model2e:
    veg_index_values = calculate_vi_model2e(band_a, band_b, band_c, band_d)
elif vi in model2f:
    veg_index_values = calculate_vi_model2f(band_a, band_b, band_c, band_d)
elif vi in model3a:
    veg_index_values = calculate_vi_model3a(band_a, band_b, band_c, band_d)
elif vi in model3b:
    veg_index_values = calculate_vi_model3b(band_a, band_b, band_c, band_d)
elif vi in model4:
    veg_index_values = calculate_vi_model4(band_a, band_b, band_c, band_d)
elif vi in model5a:
    veg_index_values = calculate_vi_model5a(band_a, band_b, band_c, band_d)
elif vi in model5b:
    veg_index_values = calculate_vi_model5b(band_a, band_b, band_c, band_d)
elif vi in model6:
    veg_index_values = calculate_vi_model6(band_a, band_b, band_c, band_d)
elif vi in model7:
    veg_index_values = calculate_vi_model7(band_a, band_b, band_c, band_d)
elif vi in model8:
    veg_index_values = calculate_vi_model8(band_a, band_b, band_c, band_d)
elif vi in model9:
    veg_index_values = calculate_vi_model9(band_a, band_b, band_c, band_d)
elif vi in model10:
    veg_index_values = calculate_vi_model10(band_a, band_b, band_c, band_d)
elif vi in model11:
    veg_index_values = calculate_vi_model11(band_a, band_b, band_c, band_d)
elif vi in model12:
    veg_index_values = calculate_vi_model12(band_a, band_b, band_c, band_d)
elif vi in model13:
    veg_index_values = calculate_vi_model13(band_a, band_b, band_c, band_d)
elif vi in model14:
    veg_index_values = calculate_vi_model14(band_a, band_b, band_c, band_d)
elif vi in model15:
    veg_index_values = calculate_vi_model15(band_a, band_b, band_c, band_d)
elif vi in model16:
    veg_index_values = calculate_vi_model16(band_a, band_b, band_c, band_d)
elif vi in model17:
    veg_index_values = calculate_vi_model17(band_a, band_b, band_c, band_d)
elif vi in model18:
    veg_index_values = calculate_vi_model18(band_a, band_b, band_c, band_d)
elif vi in model19:
    veg_index_values = calculate_vi_model19(band_a, band_b, band_c, band_d)
elif vi in model20:
    veg_index_values = calculate_vi_model20(band_a, band_b, band_c, band_d)
elif vi in model21:
    veg_index_values = calculate_vi_model21(band_a, band_b, band_c, band_d)
```

```
    elif vi in model22:
        veg_index_values = calculate_vi_model22(band_a, band_b, band_c, band_d)
    elif vi in model23:
        veg_index_values = calculate_vi_model23(band_a, band_b, band_c, band_d)
    elif vi in model24:
        veg_index_values = calculate_vi_model24(band_a, band_b, band_c, band_d)
    elif vi in model25:
        veg_index_values = calculate_vi_model25(band_a, band_b, band_c, band_d)
    elif vi in model26:
        veg_index_values = calculate_vi_model26(band_a, band_b, band_c, band_d)
    elif vi in model27:
        veg_index_values = calculate_vi_model27(band_a, band_b, band_c, band_d)
    elif vi in model28:
        veg_index_values = calculate_vi_model28(band_a, band_b, band_c, band_d)
    elif vi in model29:
        veg_index_values = calculate_vi_model29(band_a, band_b, band_c, band_d)
    elif vi in model30:
        veg_index_values = calculate_vi_model30(band_a, band_b, band_c, band_d)
    elif vi in model31:
        veg_index_values = calculate_vi_model31(band_a, band_b, band_c, band_d)
    elif vi in model32:
        veg_index_values = calculate_vi_model32(band_a, band_b, band_c, band_d)
    elif vi in model33:
        veg_index_values = calculate_vi_model33(band_a, band_b, band_c, band_d)
    elif vi in model34:
        veg_index_values = calculate_vi_model34(band_a, band_b, band_c, band_d)
    return veg_index_values
#### Dictionaries of vegetation indices bands
# Classed bands to calculate vegetatio index
vi_classed_band_dict = {
    "NDVI": ("Red", "NIR"),
    "NBR": ("NIR", "SWIR 2"),
    "NDMI": ("NIR", "SWIR 1"),
    "DVI": ("Red", "NIR"),
    "DVIGRE": ("Green", "NIR"),
    "DVIRED": ("Red Edge", "NIR"),
    "CIREDGE": ("Red Edge", "NIR"),
    "CIGREEN": ("Green", "NIR"),
    "IPVI": ("Red", "NIR"),
    "NIRV": ("Red", "NIR"),
    "MNLI": ("NIR", "Red"),
    "NLI": ("NIR", "Red"),
    "WDRVI": ("NIR", "Red"),
    "NDRE": ("Red Edge", "NIR"),
    "BAI": ("Red Edge", "NIR"),
    "SVI": ("Red Edge", "Red"),
    "MRESR": ("Red Edge", "NIR"),
```

```
}

vi_classed_band_dict2 = {
    "TBDVI": ("Red", "NIR", "SWIR 1"),
    "EVI": ("Blue", "Red", "NIR"),
    "EXG2": ("Blue", "Green", "Red"),
    "NRI": ("Blue", "Green", "Red"),
    "NGI": ("Blue", "Green", "Red"),
    "GNDVI": ("Green", "Red Edge", "NIR"),
    "ENDVI": ("Red Edge", "Green", "Blue"),
    "MRGBVI": ("Red Edge", "Green", "Blue"),
    "NREI": ("Green", "Red Edge", "NIR"),
    "EXG": ("Red", "Green", "Blue"),
    "EXB": ("Red", "Green", "Blue"),
    "EXR": ("Red", "Green", "Blue"),
    "RGR": ("Red", "Green", "Blue"),
    "BGR": ("Red", "Green", "Blue"),
    "NGRDI": ("Red", "Green", "Blue"),
    "NGBDI": ("Red", "Green", "Blue"),
    "MGRVI": ("Red", "Green", "Blue"),
    "RGBVI": ("Red", "Green", "Blue"),
    "GLI": ("Red", "Green", "Blue"),
    "CIVE": ("Red", "Green", "Blue"),
    "EXGR": ("Red", "Green", "Blue"),
    "IRGBVI": ("Red", "Green", "Blue"),
    "REP": ("Red", "Red Edge", "NIR"),
}
# Fixed bands to calculate vegetation index
vi_fixed_band_dict = {
    "Vog1": (37, 35, 0, 0),
    "ZM": (38, 34, 0, 0),
    "Vog2": (37, 38, 35, 36),
    "Vog3": (37, 38, 35, 35),
    "MCARI1": (33, 30, 16, 0),
    "TCARI": (33, 30, 16, 0),
    "P1": (2, 189, 0, 0),
    "P2": (3, 190, 0, 0),
    "CO2-CIBR": (134, 133, 135, 0),
    "VI3": (34, 32, 39, 0),
    "VI3": (12, 10, 0, 0),
}
# Variable bands to calculate vegetation index
vi_variable_band_dict = {
    "G": (17, 31, 0, 0),
    "SRPI": (1, 31, 0, 0),
    "Lic2": (2, 32, 0, 0),
    "Ctr1": (33, 1, 0, 0),
```

```
"Ctr2": (33, 39, 0, 0),
"GM1": (38, 17, 0, 0),
"GM2": (38, 33, 0, 0),
"FRI1": (37, 43, 0, 0),
"FRI2": (32, 22, 0, 0),
"SR": (43, 30, 0, 0),
"WI1": (52, 59, 0, 0),
"WI2": (112, 45, 0, 0),
"NPQI": (112, 45, 0, 0),
"PRI1": (14, 19, 0, 0),
"NPCI": (31, 1, 0, 0),
"Lic1": (43, 31, 0, 0),
"VARI": (16, 30, 0, 0),
"NDWI": (43, 112, 0, 0),
"NDWI2": (48, 88, 0, 0),
"DWI": (44, 156, 0, 0),
"SIPI": (43, 3, 28, 0),
"RDVI": (43, 30, 0, 0),
"MSR2": (43, 30, 0, 0),
"OSAVI": (43, 30, 0, 0),
"MCARI2": (43, 30, 16, 0),
"MCARI3": (43, 30, 16, 0),
"TVI": (38, 16, 30, 0),
"MTVI1": (43, 16, 30, 0),
"MTVI2": (43, 16, 30, 0),
"MSAVI": (43, 30, 0, 0),
"EVI2": (43, 30, 0, 0),
"MSI": (112, 45, 0, 0),
"MVI": (47, 18, 113, 0),
"CMRI": (49, 29, 88, 0),
"SAVI": (51, 31, 0, 0),
"RVI": (51, 31, 0, 0),
"TCI": (51, 13, 31, 33),
"GRVI": (49, 16, 0, 0),
"GR": (16, 28, 0, 0),
"GB": (16, 8, 0, 0),
"MTCI": (49, 35, 28, 0),
"MVI": (47, 18, 113, 0),
"RDVI2": (49, 30, 0, 0),
"RDVIREG": (49, 35, 0, 0),
"MSR": (49, 29, 0, 0),
"MSRREG": (49, 35, 0, 0),
"MSR2": (43, 30, 0, 0),
"OSAVIREG": (49, 35, 0, 0),
"NDIG": (28, 18, 0, 0),
"NDIB": (28, 8, 0, 0),
"SAVIGRE": (49, 18, 0, 0),
```

```
    "VARI2": (18, 28, 0, 0),
    "GARI": (49, 18, 8, 28),
    "GSAVI": (43, 18, 0, 0),
    "HFDI": (185, 137, 0, 0),
    "VI7": (65, 34, 0, 0),
    "VI1": (34, 65, 32, 0),
    "VI6": (65, 34, 0, 0),
    "VI8": (65, 34, 0, 0),
    "NDVIre1": (46, 33, 0, 0),
    "NDVIre1n": (49, 33, 0, 0),
    "NDVIre2": (46, 36, 0, 0),
    "NDVIre2n": (49, 36, 0, 0),
    "NDVIre3": (46, 41, 0, 0),
    "NDVIre3n": (49, 41, 0, 0),
    "NDre1": (36, 33, 0, 0),
    "NDre2": (41, 33, 0, 0),
    "LCI": (48, 34, 31, 0),
    "PSRI": (29, 17, 36, 0),
    "CIre": (41, 33, 0, 0),
    "NDre1m": (36, 33, 2, 0),
    "NDre2m": (41, 33, 2, 0),
    "SRre1": (36, 2, 33, 0),
    "SRre2": (36, 2, 33, 0),
    "MSRre": (46, 33, 0, 0),
    "MSRren": (49, 33, 0, 0),
    "SIPI1": (2, 43, 30, 0),
    "WBI": (59, 52, 0, 0),
    "LWVI1": (75, 64, 0, 0),
    "LWVI2": (75, 85, 0, 0),
    "NDII": (45, 117, 0, 0),
    "DWSI": (43, 16, 118, 50),
    "ARI1": (17, 33, 0, 0),
    "CRI1": (11, 16, 0, 0),
    "CRI2": (11, 33, 0, 0),
    "ARVI": (43, 31, 3, 0),
    "MRENDVI": (38, 34, 2, 0),
    "NDNI": (104, 120, 0, 0),
    "NDLI": (128, 120, 0, 0),
    "CAI": (133, 155, 142, 0),
    "LCAI": (155, 149, 172, 0),
    "ARI2": (43, 17, 33, 0),
    "NMDI": (48, 116, 145, 0),
}
#### Read the excel file
# Read the Excel file
excel_file = working_dir + "CulebraPointsCBI.xlsx"
points = pd.read_excel(excel_file)
```

```
# Initialize lists to store results
cb_results_lst = 0
cb2_results_lst = 0
fb_results_lst = 0
vb_results_lst = 0
rb_results_lst = 0
### FOR CLASSED BANDS
#### Combination of bands of CLASSED BANDS
def bands_combinations(tiff_file, band_lst, vi_classed_band_dict):
    for i in vi_classed_band_dict:
        print(i)
    vi_name = input("Insert the index name: ")
    combination_lst = []
    band_names = vi_classed_band_dict[vi_name]
    with rasterio.open(tiff_file) as src:
        for band_a in band_lst:
            if band_a[1] == band_names[0]:
                band_ax = band_a[0]
                for band_b in band_lst:
                    if band_b[1] == band_names[1]:
                        band_bx = band_b[0]
                        combination_lst.append((band_ax, band_bx))
    for i in combination_lst:
        print(i)
    return combination_lst, vi_name

def bands_combinations2(tiff_file, band_lst, vi_classed_band_dict2):
    for i in vi_classed_band_dict2:
        print(i)
    vi_name = input("Insert the index name: ")
    combination_lst2 = []
    band_names = vi_classed_band_dict2[vi_name]
    with rasterio.open(tiff_file) as src:
        for band_a in band_lst:
            if band_a[1] == band_names[0]:
                band_ax = band_a[0]
                for band_b in band_lst:
                    if band_b[1] == band_names[1]:
                        band_bx = band_b[0]
                        for band_c in band_lst:
                            if band_c[1] == band_names[2]:
                                band_cx = band_c[0]
                                combination_lst2.append((band_ax, band_bx, band_cx))
    for i in combination_lst2:
        print(i)
    return combination_lst2, vi_name
#### Calculate vegetation index values for CLASSED BANDS
```

```
def get_vi_cb_image(tiff_file, vi_name, band_a, band_b):
    with rasterio.open(tiff_file) as dataset:
        band_1 = dataset.read(band_a)
        band_2 = dataset.read(band_b)
        if vi_name == "NDVI":
            vi_values = calculate_ndvi(band_1, band_2)
        elif vi_name == "NBR":
            vi_values = calculate_nbr(band_1, band_2)
        elif vi_name == "NDMI":
            vi_values = calculate_ndmi(band_1, band_2)
        elif vi_name == "DVI":
            vi_values = calculate_dvi(band_1, band_2)
        elif vi_name == "DVIGRE":
            vi_values = calculate_dvigre(band_1, band_2)
        elif vi_name == "DVIRED":
            vi_values = calculate_dvired(band_1, band_2)
        elif vi_name == "CIREDGE":
            vi_values = calculate_ciredge(band_1, band_2)
        elif vi_name == "CIGREEN":
            vi_values = calculate_cigreen(band_1, band_2)
        elif vi_name == "IPVI":
            vi_values = calculate_ipvi(band_1, band_2)
        elif vi_name == "NIRV":
            vi_values = calculate_nirv(band_1, band_2)
        elif vi_name == "MNLI":
            vi_values = calculate_mnli(band_1, band_2)
        elif vi_name == "NLI":
            vi_values = calculate_nli(band_1, band_2)
        elif vi_name == "WDRVI":
            vi_values = calculate_wdrvi(band_1, band_2)
        elif vi_name == "NDRE":
            vi_values = calculate_ndre(band_1, band_2)
        elif vi_name == "BAI":
            vi_values = calculate_bai(band_1, band_2)
        elif vi_name == "SVI":
            vi_values = calculate_svi(band_1, band_2)
        elif vi_name == "MRESR":
            vi_values = calculate_mresr(band_1, band_2)
        else:
            print("Insert other vegetation index name")
    return vi_values, dataset

def get_vi_cb_at_points(vi_values, dataset, points):
    veg_index_values = []
    for _, row in points.iterrows():
        name, x, y = row['Parcela'], row['Coord_X'], row['Coord_Y']
        row_idx, col_idx = rasterio.transform.rowcol(dataset.transform, x, y)
```

```
        veg_index_value = vi_values[row_idx, col_idx]
        veg_index_values.append((name, veg_index_value))
    return veg_index_values

def get_cb_comparative_points(tiff_file, band_lst, vi_classed_band_dict, points):
    cb_results_lst = []
    combination_lst, vi_name = bands_combinations(tiff_file, band_lst,
vi_classed_band_dict)
    for paired_bands in combination_lst:
        band_a = paired_bands[0]
        band_b = paired_bands[1]
        vi_values, dataset = get_vi_cb_image(tiff_file, vi_name, band_a, band_b)
        veg_index_values = get_vi_cb_at_points(vi_values, dataset, points)
        cb_results_lst.append((vi_name, band_a, band_b, veg_index_values))
    return cb_results_lst
def get_vi_cb2_image(tiff_file, vi_name, band_a, band_b, band_c):
    with rasterio.open(tiff_file) as dataset:
        band_1 = dataset.read(band_a)
        band_2 = dataset.read(band_b)
        band_3 = dataset.read(band_c)
        if vi_name == "TBDVI":
            vi_values = calculate_tbdvi(band_1, band_2, band_3)
        elif vi_name == "EVI":
            vi_values = calculate_evi(band_1, band_2, band_3)
        elif vi_name == "EXG2":
            vi_values = calculate_exg2(band_1, band_2, band_3)
        elif vi_name == "NRI":
            vi_values = calculate_nri(band_1, band_2, band_3)
        elif vi_name == "NGI":
            vi_values = calculate_ngi(band_1, band_2, band_3)
        elif vi_name == "GNDVI":
            vi_values = calculate_gndvi(band_1, band_2, band_3)
        elif vi_name == "ENDVI":
            vi_values = calculate_endvi(band_1, band_2, band_3)
        elif vi_name == "MRGBVI":
            vi_values = calculate_mrgbvi(band_1, band_2, band_3)
        elif vi_name == "NREI":
            vi_values = calculate_nrei(band_1, band_2, band_3)
        elif vi_name == "EXG":
            vi_values = calculate_exg(band_1, band_2, band_3)
        elif vi_name == "EXB":
            vi_values = calculate_exb(band_1, band_2, band_3)
        elif vi_name == "EXR":
            vi_values = calculate_exr(band_1, band_2, band_3)
        elif vi_name == "RGR":
            vi_values = calculate_rgr(band_1, band_2, band_3)
        elif vi_name == "BGR":
```

```
        vi_values = calculate_bgr(band_1, band_2, band_3)
    elif vi_name == "NGRDI":
        vi_values = calculate_ngrdi(band_1, band_2, band_3)
    elif vi_name == "NGBDI":
        vi_values = calculate_ngbdi(band_1, band_2, band_3)
    elif vi_name == "MGRVI":
        vi_values = calculate_mgrvi(band_1, band_2, band_3)
    elif vi_name == "RGBVI":
        vi_values = calculate_rgbvi(band_1, band_2, band_3)
    elif vi_name == "GLI":
        vi_values = calculate_gli(band_1, band_2, band_3)
    elif vi_name == "CIVE":
        vi_values = calculate_cive(band_1, band_2, band_3)
    elif vi_name == "EXGR":
        vi_values = calculate_exgr(band_1, band_2, band_3)
    elif vi_name == "IRGBVI":
        vi_values = calculate_irgbvi(band_1, band_2, band_3)
    elif vi_name == "REP":
        vi_values = calculate_rep(band_1, band_2, band_3)
    else:
        print("Insert other vegetation index name")
  return vi_values, dataset

def get_cb2_comparative_points(tiff_file, band_lst, vi_classed_band_dict2, points):
  cb2_results_lst = []
  combination_lst2, vi_name = bands_combinations2(tiff_file, band_lst,
vi_classed_band_dict2)
  for paired_bands in combination_lst2:
    band_a = paired_bands[0]
    band_b = paired_bands[1]
    band_c = paired_bands[2]
    vi_values, dataset = get_vi_cb2_image(tiff_file, vi_name, band_a, band_b, band_c)
    veg_index_values = get_vi_cb_at_points(vi_values, dataset, points)
    cb2_results_lst.append((vi_name, band_a, band_b, band_c, veg_index_values))
  return cb2_results_lst
#### Extract results of wavelength and vegetation index of CLASSED BANDS
cb_results_lst = get_cb_comparative_points(tiff_file, band_lst, vi_classed_band_dict,
points)
for i in cb_results_lst:
  print(i)
cb2_results_lst = get_cb2_comparative_points(tiff_file, band_lst, vi_classed_band_dict2,
points)
for i in cb2_results_lst:
  print(i)
### FOR FIXED BANDS
#### Calculate vegetation index values for FIXED BANDS
def get_vi_fb_image(tiff_file, vi_fixed_band_dict):
```

```
    vi_list = []
    for vi in vi_fixed_band_dict:
        band = vi_fixed_band_dict[vi]
        band = tuple(1 if b == 0 else b for b in band)
        with rasterio.open(tiff_file) as dataset:
            band_a = dataset.read(band[0])
            band_b = dataset.read(band[1])
            band_c = dataset.read(band[2])
            band_d = dataset.read(band[3])

        veg_index_values = select_model(vi, band_a, band_b, band_c, band_d)
        vi_list.append((veg_index_values, dataset))
    return vi_list

def get_vi_fb_at_points(veg_index, dataset, points):
    veg_index_values = []
    for _, row in points.iterrows():
        name, x, y = row['Parcela'], row['Coord_X'], row['Coord_Y']
        row_idx, col_idx = rasterio.transform.rowcol(dataset.transform, x, y)
        veg_index_value = veg_index[row_idx, col_idx]
        veg_index_values.append((name, veg_index_value))
    return veg_index_values

def get_fb_comparative_points(tiff_file, vi_fixed_band_dict, points):
    fb_results_lst = []

    vi_list = get_vi_fb_image(tiff_file, vi_fixed_band_dict)

    iv_keys = []
    for key in vi_fixed_band_dict:
        iv_keys.append(key)
    cnt = 0

    for tup in vi_list:
        veg_index = tup[0]
        dataset = tup[1]
        veg_index_values = get_vi_fb_at_points(veg_index, dataset, points)

        band_tup = vi_fixed_band_dict[iv_keys[cnt]]
        fb_results_lst.append((iv_keys[cnt], band_tup[0], band_tup[1], band_tup[2],
band_tup[3], veg_index_values))
        cnt += 1
    return fb_results_lst
#### Extract results of wavelength and vegetations index of FIXED BANDS
fb_results_lst = get_fb_comparative_points(tiff_file, vi_fixed_band_dict, points)
for i in fb_results_lst:
    print(i)
```

FOR VARIABLE BANDS

Combination of bands of VARIABLE BANDS

```
import itertools

def get_vb_combination_bands(vi_variable_band_dict):
    vi_combination_lst = []

    for key, val_tup in vi_variable_band_dict.items():
        total_neighborhood = [[] for _ in range(len(val_tup))]  # Create a list of empty lists for each value in the tuple
        for idx, val in enumerate(val_tup):
            if val != 0:
                band_neighborhood = [val + i for i in range(-2, 3)]  # Generate values from val-2 to val+2
            else:
                band_neighborhood = [val]  # If the value is zero, keep it as zero in all combinations
            total_neighborhood[idx] = band_neighborhood

        # Generate all possible combinations from the neighborhoods
        combinations = list(itertools.product(*total_neighborhood))

        # Add the key to each combination and filter out combinations with negative values
        for combination in combinations:
            if all(x >= 0 for x in combination):
                vi_combination_lst.append((key, *combination))

    return vi_combination_lst
```

Calculate vegetation index values for VARIABLE BANDS

```
def get_vi_vb_image(tiff_file, vi_variable_band_dict):
    vi_list = []

    vb_combination_band = get_vb_combination_bands(vi_variable_band_dict)
    for val_tup in vb_combination_band:
        val_tup = tuple(1 if b == 0 else b for b in val_tup)
        with rasterio.open(tiff_file) as dataset:
            band_a = dataset.read(val_tup[1])
            band_b = dataset.read(val_tup[2])
            band_c = dataset.read(val_tup[3])
            band_d = dataset.read(val_tup[4])

        veg_index_values = select_model(val_tup[0], band_a, band_b, band_c, band_d)
        vi_list.append((veg_index_values, dataset))
    return vi_list, vb_combination_band

def get_vi_vb_at_points(veg_index, dataset, points):
    veg_index_values = []
```

```
    for _, row in points.iterrows():
        name, x, y = row['Parcela'], row['Coord_X'], row['Coord_Y']
        row_idx, col_idx = rasterio.transform.rowcol(dataset.transform, x, y)
        veg_index_value = veg_index[row_idx, col_idx]
        veg_index_values.append((name, veg_index_value))
    return veg_index_values

def get_vb_comparative_points(tiff_file, vi_variable_band_dict, points):
    vb_results_lst = []

    vi_list, vb_combination_band = get_vi_vb_image(tiff_file, vi_variable_band_dict)

    count = 0

    for tup in vi_list:
        veg_index = tup[0]
        dataset = tup[1]
        veg_index_values = get_vi_vb_at_points(veg_index, dataset, points)

        band_tup = vb_combination_band[count]
        vb_results_lst.append((band_tup[0], band_tup[1], band_tup[2], band_tup[3],
band_tup[4],veg_index_values))
        count += 1
    return vb_results_lst
####  Extract results of wavelength and vegetation index of VARIABLE BANDS
vb_results_lst = get_vb_comparative_points(tiff_file, vi_variable_band_dict, points)
# for i in vb_results_lst:
#     print(i)
### FOR RAW BANDS
#### Calculate vegetation index values for RAW BANDS
def get_rb_image(tiff_file, band_number):
    with rasterio.open(tiff_file) as dataset:
        band_values = dataset.read(band_number)
    return band_values, dataset

def get_rb_at_points(band_values, dataset, points):
    band_values_lst = []
    for _, row in points.iterrows():
        name, x, y = row['Parcela'], row['Coord_X'], row['Coord_Y']
        row_idx, col_idx = rasterio.transform.rowcol(dataset.transform, x, y)
        band_value = band_values[row_idx, col_idx]
        band_values_lst.append((name, band_value))
    return band_values_lst

def get_rb_comparative_points(tiff_file, band_lst, points):
    rb_results_lst = []
```

```
    for band_number in range(1,192):
        band_values, dataset = get_rb_image(tiff_file, band_number)
        band_values_lst = get_rb_at_points(band_values, dataset, points)
        rb_results_lst.append((band_lst[band_number-1][1], band_number,
band_lst[band_number-1][2], band_values_lst))

    return rb_results_lst
#### Extract results of wavelength and vegetation index of RAW BANDS
rb_results_lst = get_rb_comparative_points(tiff_file, band_lst, points)
# for i in rb_results_lst:
#     print(i)
### SAVE INDICES VALUES
#### Save vegetation indices values in an excel file (.xlsx)
def save_xlsx(input_file, results_lst):
    # Creamos un diccionario para almacenar los datos
    data_dict = {}

    for elm in results_lst:
        if results_lst == cb_results_lst:
            col_name = f"{elm[0]}_{elm[1]}_{elm[2]}"
            type_name = "classed_bands"
        elif results_lst == cb2_results_lst:
            col_name = f"{elm[0]}_{elm[1]}_{elm[2]}_{elm[3]}"
            type_name = "classed_bands"
        elif results_lst == fb_results_lst:
            col_name = f"{elm[0]}_{elm[1]}_{elm[2]}_{elm[3]}_{elm[4]}"
            type_name = "fixed_bands"
        elif results_lst == vb_results_lst:
            col_name = f"{elm[0]}_{elm[1]}_{elm[2]}_{elm[3]}_{elm[4]}"
            type_name = "variable_bands"
        elif results_lst == rb_results_lst:
            col_name = f"{elm[0]}_{elm[1]}_{elm[2]:.0f}nm"
            type_name = "raw_bands"
        data_dict[col_name] = [value for point, value in elm[len(elm)-1] ]

    # Convertimos el diccionario en un DataFrame
    df = pd.DataFrame(data_dict)

    ### PARA DATAFRAMES CON MÁS DE 16000 COLUMNAS ###
    # Si el DataFrame tiene más de 16000 columnas, dividirlo en partes
    max_columns = 16000
    num_parts = (df.shape[1] // max_columns) + 1

    for part in range(num_parts):
        start_col = part * max_columns
        end_col = start_col + max_columns
        df_part = df.iloc[:, start_col:end_col]
```

```
        # Define the output file name for each part
        if type_name == "classed_bands":
            output_file = input_file[:-5] + f"_hyp_{type_name}_{results_lst[0][0]}_p{part+1}.xlsx"
        else:
            output_file = input_file[:-5] + f"_hyp_{type_name}_p{part+1}.xlsx"

        # Copia el archivo original al nuevo archivo
        shutil.copyfile(input_file, output_file)

        # Abre el nuevo archivo
        wb = openpyxl.load_workbook(output_file)
        sheet = wb.active

        # Encuentra la última columna con datos en la hoja existente
        last_col = sheet.max_column

        # Escribe los datos del DataFrame en las columnas nuevas a partir de la última
columna existente
        for col_idx, col_name in enumerate(df_part.columns, start=last_col + 1):
            sheet.cell(row=1, column=col_idx, value=col_name)
            for row_idx, value in enumerate(df_part[col_name], start=2):
                sheet.cell(row=row_idx, column=col_idx, value=value)

        # Guarda el archivo con las nuevas columnas
        wb.save(output_file)

    # # Copia el archivo original al nuevo archivo
    # if type_name == "classed_bands":
    #     output_file = input_file[:-5] + "_hyp_" + type_name + "_" + results_lst[0][0] + ".xlsx"
    # else:
    #     output_file = input_file[:-5] + "_hyp_" + type_name + ".xlsx"
    # shutil.copyfile(input_file, output_file)

    # # Abre el nuevo archivo
    # wb = openpyxl.load_workbook(output_file)
    # sheet = wb.active

    # # Encuentra la última columna con datos en la hoja existente
    # last_col = sheet.max_column

    # # Escribe los datos del DataFrame en las columnas nuevas a partir de la última
columna existente
    # for col_idx, col_name in enumerate(df.columns, start=last_col + 1):
    #     sheet.cell(row=1, column=col_idx, value=col_name)
    #     for row_idx, value in enumerate(df[col_name], start=2):
    #         sheet.cell(row=row_idx, column=col_idx, value=value)
```

```
    # # Guarda el archivo con las nuevas columnas
    # wb.save(output_file)
    return output_file

## Options to save file
# save_xlsx(excel_file, cb_results_lst)
save_xlsx(excel_file, cb2_results_lst)
# save_xlsx(excel_file, fb_results_lst)
# save_xlsx(excel_file, vb_results_lst)
# save_xlsx(excel_file, rb_results_lst)
```

A5.2. Python script for calculating vegetation indices from SENTINEL-2 multispectral imagery aligned with CBI plots

```
# Calculate indices from MULTISPECTRAL image
#### Import libraries and read multispectral image (.tiff)
from math import log
import numpy as np
import pandas as pd
import rasterio
from rasterio.plot import show
from rasterio.transform import rowcol
import matplotlib.pyplot as plt
from pyproj import Proj, transform
import openpyxl
import shutil

# Path to the .tiff file
working_dir = "C:/Users/User/OneDrive - UVa/1_ASIGNATURAS/TFM/1_DataProcessing/"
tiff_file = working_dir + "2_SatellitalImages/1_MLT/S2_post_clip.tif"
#### Open multispectral image and classify wavelengths
# Sentinel 2 bands
band_lst = [
    (1, "Blue", "B2", 450, 520),
    (2, "Green", "B3", 540, 570),
    (3, "Red", "B4", 650, 680),
    (4, "Red Edge", "B5", 690, 710),
    (5, "Red Edge", "B6", 730, 740),
    (6, "Red Edge", "B7", 770, 790),
    (7, "NIR", "B8", 780, 900),
    (8, "NIR", "B8A", 850, 870),
    (9, "SWIR 1", "B11", 1560, 1650),
    (10, "SWIR 2", "B12", 2100, 2280),
]

# Display band information for the 10 bands assumed to be in your TIFF file
print(f"{'Band':<5} {'Name':<25} {'Wavelength (nm)':<15}")
print("="*50)
for band in band_lst:
    print(f"{band[2]:<5} {band[1]:<25} {band[3]} - {band[4]:<15}")
#### Vegetation Indices Equations
# Normalized Difference Vegetation Index: NDVI
def calculate_ndvi(red, nir):
    ndvi = (nir - red) / (nir + red)
    return ndvi
# Normalized Burn Ratio: NBR
def calculate_nbr(nir, swir2):
    nbr = (nir - swir2) / (nir + swir2)
```

```
    return nbr
# Normalized Difference Moisture Index: NDMI
def calculate_ndmi(nir, swir1):
    ndmi = (nir - swir1) / (nir + swir1)
    return ndmi
# Difference Vegetation Index: DVI
def calculate_dvi(red, nir):
    dvi = nir - red
    return dvi
# Green Difference Vegetation Index: DVIGRE o GDVI
def calculate_dvigre(green, nir):
    dvigre = nir - green
    return dvigre
# Red Difference Vegetation Index: DVIRED
def calculate_dvired(redge, nir):
    dvired = nir - redge
    return dvired
# Chlorophyll Index With Red Edge: CIREDGE
def calculate_ciredge(redge, nir):
    ciredge = (nir / redge) - 1
    return ciredge
# Chlorophyll Index With Green: CIGREEN
def calculate_cigreen(green, nir):
    cigreen = (nir / green) - 1
    return cigreen
# Infrared Percentage Vegetation Index: IPVI
def calculate_ipvi(red, nir):
    ipvi = nir / (nir + red)
    return ipvi
# Near-Infrared Reflectance of Vegetation: NIRV
def calculate_nirv(red, nir):
    nirv = nir * ((nir - red) / (nir + red))
    return nirv
# Modified Non-Linear Index: MNLI
def calculate_mnli(nir, red):
    mnli = 1.5 * (nir ** 2 - red) / (nir ** 2 + red + 0.5)
    return mnli
# Non-Linear Index: NLI
def calculate_nli(nir, red):
    nli = (nir ** 2 - red) / (nir ** 2 + red)
    return nli
# Wide Dynamic Range Vegetation Index: WDRVI
def calculate_wdrvi(nir, red):
    wdrvi = (0.2 * nir - red) / (0.2 * nir + red)
    return wdrvi
# Normalized Difference Red Edge Index: NDRE
def calculate_ndre(redge, nir):
```

```
    ndre = (nir - redge) / (nir + redge)
    return ndre
# Burn Area Index: BAI
def calculate_bai(redge, nir):
    bai = 1 / (((redge - 0.1) ** 2) + ((nir - 0.06) ** 2))
    return bai
# Structural Vegetation Index: SVI
def calculate_svi(redge, red):
    svi = (redge - red) / (redge + red)
    return svi
# Modified Red-Edge Simple Ratio: MRESR
def calculate_mresr(redge, nir):
    mresr = nir / redge
    return mresr
# Three-Band Difference Vegetation Index: TBDVI
def calculate_tbdvi(red, nir, swir1):
    tbdvi = nir - (red - swir1) / 2
    return tbdvi
# Enhanced Vegetation Index: EVI
def calculate_evi(blue, red, nir):
    evi = 2.5 * ((nir - red)/(nir + 6 * red - 7.5 * blue + 1))
    return evi
# Excess Green Index: EXG2
def calculate_exg2(blue, green, red):
    exg2 = 2 * green - red - blue
    return exg2
# Red Light Normalized Value: NRI
def calculate_nri(blue, green, red):
    nri = red / (red + green + blue)
    return nri
# Green Light Normalized Value: NGI
def calculate_ngi(blue, green, red):
    ngi = green / (red + green + blue)
    return ngi
# Green Normalized Difference Vegetation Index: GNDVI
def calculate_gndvi(green, redge, nir):
    gndvi = (nir - green) / (nir + redge)
    return gndvi
# Enhances Normalized Difference Vegetation Index: ENDVI
def calculate_endvi(redge, green, blue):
    endvi = (redge + green - 2 * blue) / (redge + green + 2 * blue)
    return endvi
# Modified Red Green- Blue Vegetation Index: MRGBVI
def calculate_mrgbvi(redge, green, blue):
    mrgbvi = (redge + 2 * green - 2 * blue) / (redge + 2 * green + 2 * blue)
    return mrgbvi
# Nitrogen Reflectance Index: NREI
```

```
def calculate_nrei(green, redge, nir):
    nrei = redge / (redge + nir + green)
    return nrei
# Red Edge Position Index: REP
def calculate_rep(red, redge, nir):
    rep = 700 + 40 * ((red + nir)/(2 - redge))
    return rep
###############################################
def normalized_band (red, green, blue):
    R = red / (red + green + blue)
    G = green / (red + green + blue)
    B = blue / (red + green + blue)
    return R, G, B
###############################################
# Excess Green Index: EXG
def calculate_exg(red, green, blue):
    R,G,B = normalized_band(red, green, blue)
    exg = 2 * G - R - B
    return exg
# Excess Blue Index: EXB
def calculate_exb(red, green, blue):
    R,G,B = normalized_band(red, green, blue)
    exb = 1.4 * R - G
    return exb
# Excess Red Index: EXR
def calculate_exr(red, green, blue):
    R,G,B = normalized_band(red, green, blue)
    exr = 1.4 * B - G
    return exr
# Red / Green Ratio: RGR
def calculate_rgr(red, green, blue):
    R,G,B = normalized_band(red, green, blue)
    rgr = R / G
    return rgr
# Blue / Green Ratio: BGR
def calculate_bgr(red, green, blue):
    R,G,B = normalized_band(red, green, blue)
    bgr = B / G
    return bgr
# Normalized Green-Red Difference Index: NGRDI
def calculate_ngrdi(red, green, blue):
    R,G,B = normalized_band(red, green, blue)
    ngrdi = (G - R) / (G + R)
    return ngrdi
# Normalized Green-Blue Difference Index: NGBDI
def calculate_ngbdi(red, green, blue):
    R,G,B = normalized_band(red, green, blue)
```

```
    ngbdi = (G - B) / (G + B)
    return ngbdi
# Modified Green-Red Vegetation Index: MGRVI
def calculate_mgrvi(red, green, blue):
    R,G,B = normalized_band(red, green, blue)
    mgrvi = (G**2 - R**2) / (G**2 + R**2)
    return mgrvi
# Red Green- Blue Vegetation Index: RGBVI
def calculate_rgbvi(red, green, blue):
    R,G,B = normalized_band(red, green, blue)
    rgbvi = (G**2 - R * B) / (G**2 + R * B)
    return rgbvi
# Green Leaf Index: GLI
def calculate_gli(red, green, blue):
    R,G,B = normalized_band(red, green, blue)
    gli = (2*G - R - B) / (2*G + R + B)
    return gli
# Color Index of Vegetation Extraction: CIVE
def calculate_cive(red, green, blue):
    R,G,B = normalized_band(red, green, blue)
    cive = 0.441*R - 0.881*G + 0.385*R + 18.78745
    return cive
# Excess Green Minus Excess Red Index: ExGR
def calculate_exgr(red, green, blue):
    exg = calculate_exg(red, green, blue)
    exr = calculate_exr(red, green, blue)
    exgr = exg - exr
    return exgr
# Improved Red Green- Blue Vegetation Index: IRGBVI
def calculate_irgbvi(red, green, blue):
    R,G,B = normalized_band(red, green, blue)
    irgbvi = (5*G**2 - 2*R**2 - 5*B**2) / (5*G**2 + 2*R**2 + 5*B**2)
    return irgbvi
#### Dictionaries of vegetation indices bands
# Classed bands to calculate vegetatio index
vi_classed_band_dict = {
    "NDVI": ("Red", "NIR"),
    "NBR": ("NIR", "SWIR 2"),
    "NDMI": ("NIR", "SWIR 1"),
    "DVI": ("Red", "NIR"),
    "DVIGRE": ("Green", "NIR"),
    "DVIRED": ("Red Edge", "NIR"),
    "CIREDGE": ("Red Edge", "NIR"),
    "CIGREEN": ("Green", "NIR"),
    "IPVI": ("Red", "NIR"),
    "NIRV": ("Red", "NIR"),
    "MNLI": ("NIR", "Red"),
```

```
    "NLI": ("NIR", "Red"),
    "WDRVI": ("NIR", "Red"),
    "NDRE": ("Red Edge", "NIR"),
    "BAI": ("Red Edge", "NIR"),
    "SVI": ("Red Edge", "Red"),
    "MRESR": ("Red Edge", "NIR"),
}

vi_classed_band_dict2 = {
    "TBDVI": ("Red", "NIR", "SWIR 1"),
    "EVI": ("Blue", "Red", "NIR"),
    "EXG2": ("Blue", "Green", "Red"),
    "NRI": ("Blue", "Green", "Red"),
    "NGI": ("Blue", "Green", "Red"),
    "GNDVI": ("Green", "Red Edge", "NIR"),
    "ENDVI": ("Red Edge", "Green", "Blue"),
    "MRGBVI": ("Red Edge", "Green", "Blue"),
    "NREI": ("Green", "Red Edge", "NIR"),
    "EXG": ("Red", "Green", "Blue"),
    "EXB": ("Red", "Green", "Blue"),
    "EXR": ("Red", "Green", "Blue"),
    "RGR": ("Red", "Green", "Blue"),
    "BGR": ("Red", "Green", "Blue"),
    "NGRDI": ("Red", "Green", "Blue"),
    "NGBDI": ("Red", "Green", "Blue"),
    "MGRVI": ("Red", "Green", "Blue"),
    "RGBVI": ("Red", "Green", "Blue"),
    "GLI": ("Red", "Green", "Blue"),
    "CIVE": ("Red", "Green", "Blue"),
    "EXGR": ("Red", "Green", "Blue"),
    "IRGBVI": ("Red", "Green", "Blue"),
    "REP": ("Red", "Red Edge", "NIR"),
}
#### Read the excel file
# Read the Excel file
excel_file = working_dir + "CulebraPointsCBI.xlsx"
points = pd.read_excel(excel_file)
# Initialize lists to store results
cb_results_lst = 0
cb2_results_lst = 0
cb3_results_lst = 0
fb_results_lst = 0
vb_results_lst = 0
### FOR CLASSED BANDS
#### Combination of bands of CLASSED BANDS
def bands_combinations(tiff_file, band_lst, vi_classed_band_dict):
    for i in vi_classed_band_dict:
```

```
        print(i)
    vi_name = input("Insert the index name: ")
    combination_lst = []
    band_names = vi_classed_band_dict[vi_name]
    with rasterio.open(tiff_file) as src:
        for band_a in band_lst:
            if band_a[1] == band_names[0]:
                band_ax = band_a[0]
                for band_b in band_lst:
                    if band_b[1] == band_names[1]:
                        band_bx = band_b[0]
                        combination_lst.append((band_ax, band_bx))
    for i in combination_lst:
        print(i)
    return combination_lst, vi_name

def bands_combinations2(tiff_file, band_lst, vi_classed_band_dict2):
    for i in vi_classed_band_dict2:
        print(i)
    vi_name = input("Insert the index name: ")
    combination_lst2 = []
    band_names = vi_classed_band_dict2[vi_name]
    with rasterio.open(tiff_file) as src:
        for band_a in band_lst:
            if band_a[1] == band_names[0]:
                band_ax = band_a[0]
                for band_b in band_lst:
                    if band_b[1] == band_names[1]:
                        band_bx = band_b[0]
                        for band_c in band_lst:
                            if band_c[1] == band_names[2]:
                                band_cx = band_c[0]
                                combination_lst2.append((band_ax, band_bx, band_cx))
    for i in combination_lst2:
        print(i)
    return combination_lst2, vi_name
#### Calculate vegetation index values for CLASSED BANDS
def get_vi_cb_image(tiff_file, vi_name, band_a, band_b):
    with rasterio.open(tiff_file) as dataset:
        band_1 = dataset.read(band_a)
        band_2 = dataset.read(band_b)
        if vi_name == "NDVI":
            vi_values = calculate_ndvi(band_1, band_2)
        elif vi_name == "NBR":
            vi_values = calculate_nbr(band_1, band_2)
        elif vi_name == "NDMI":
            vi_values = calculate_ndmi(band_1, band_2)
```

```
    elif vi_name == "DVI":
        vi_values = calculate_dvi(band_1, band_2)
    elif vi_name == "DVIGRE":
        vi_values = calculate_dvigre(band_1, band_2)
    elif vi_name == "DVIRED":
        vi_values = calculate_dvired(band_1, band_2)
    elif vi_name == "CIREDGE":
        vi_values = calculate_ciredge(band_1, band_2)
    elif vi_name == "CIGREEN":
        vi_values = calculate_cigreen(band_1, band_2)
    elif vi_name == "IPVI":
        vi_values = calculate_ipvi(band_1, band_2)
    elif vi_name == "NIRV":
        vi_values = calculate_nirv(band_1, band_2)
    elif vi_name == "MNLI":
        vi_values = calculate_mnli(band_1, band_2)
    elif vi_name == "NLI":
        vi_values = calculate_nli(band_1, band_2)
    elif vi_name == "WDRVI":
        vi_values = calculate_wdrvi(band_1, band_2)
    elif vi_name == "NDRE":
        vi_values = calculate_ndre(band_1, band_2)
    elif vi_name == "BAI":
        vi_values = calculate_bai(band_1, band_2)
    elif vi_name == "SVI":
        vi_values = calculate_svi(band_1, band_2)
    elif vi_name == "MRESR":
        vi_values = calculate_mresr(band_1, band_2)
    else:
        print("Insert other vegetation index name")
  return vi_values, dataset

def get_vi_cb_at_points(vi_values, dataset, points):
  veg_index_values = []
  for _, row in points.iterrows():
    name, x, y = row['Parcela'], row['Coord_X'], row['Coord_Y']
    row_idx, col_idx = rasterio.transform.rowcol(dataset.transform, x, y)
    veg_index_value = vi_values[row_idx, col_idx]
    veg_index_values.append((name, veg_index_value))
  return veg_index_values

def get_cb_comparative_points(tiff_file, band_lst, vi_classed_band_dict, points):
  cb_results_lst = []
  combination_lst, vi_name = bands_combinations(tiff_file, band_lst,
vi_classed_band_dict)
  for paired_bands in combination_lst:
    band_a = paired_bands[0]
```

```
            band_b = paired_bands[1]
            vi_values, dataset = get_vi_cb_image(tiff_file, vi_name, band_a, band_b)
            veg_index_values = get_vi_cb_at_points(vi_values, dataset, points)
            cb_results_lst.append((vi_name, band_a, band_b, veg_index_values))
    return cb_results_lst
def get_vi_cb2_image(tiff_file, vi_name, band_a, band_b, band_c):
    with rasterio.open(tiff_file) as dataset:
        band_1 = dataset.read(band_a)
        band_2 = dataset.read(band_b)
        band_3 = dataset.read(band_c)
        if vi_name == "TBDVI":
            vi_values = calculate_tbdvi(band_1, band_2, band_3)
        elif vi_name == "EVI":
            vi_values = calculate_evi(band_1, band_2, band_3)
        elif vi_name == "EXG2":
            vi_values = calculate_exg2(band_1, band_2, band_3)
        elif vi_name == "NRI":
            vi_values = calculate_nri(band_1, band_2, band_3)
        elif vi_name == "NGI":
            vi_values = calculate_ngi(band_1, band_2, band_3)
        elif vi_name == "GNDVI":
            vi_values = calculate_gndvi(band_1, band_2, band_3)
        elif vi_name == "ENDVI":
            vi_values = calculate_endvi(band_1, band_2, band_3)
        elif vi_name == "MRGBVI":
            vi_values = calculate_mrgbvi(band_1, band_2, band_3)
        elif vi_name == "NREI":
            vi_values = calculate_nrei(band_1, band_2, band_3)
        elif vi_name == "EXG":
            vi_values = calculate_exg(band_1, band_2, band_3)
        elif vi_name == "EXB":
            vi_values = calculate_exb(band_1, band_2, band_3)
        elif vi_name == "EXR":
            vi_values = calculate_exr(band_1, band_2, band_3)
        elif vi_name == "RGR":
            vi_values = calculate_rgr(band_1, band_2, band_3)
        elif vi_name == "BGR":
            vi_values = calculate_bgr(band_1, band_2, band_3)
        elif vi_name == "NGRDI":
            vi_values = calculate_ngrdi(band_1, band_2, band_3)
        elif vi_name == "NGBDI":
            vi_values = calculate_ngbdi(band_1, band_2, band_3)
        elif vi_name == "MGRVI":
            vi_values = calculate_mgrvi(band_1, band_2, band_3)
        elif vi_name == "RGBVI":
            vi_values = calculate_rgbvi(band_1, band_2, band_3)
        elif vi_name == "GLI":
```

```
        vi_values = calculate_gli(band_1, band_2, band_3)
    elif vi_name == "CIVE":
        vi_values = calculate_cive(band_1, band_2, band_3)
    elif vi_name == "EXGR":
        vi_values = calculate_exgr(band_1, band_2, band_3)
    elif vi_name == "IRGBVI":
        vi_values = calculate_irgbvi(band_1, band_2, band_3)
    elif vi_name == "REP":
        vi_values = calculate_rep(band_1, band_2, band_3)
    else:
        print("Insert other vegetation index name")
  return vi_values, dataset

def get_cb2_comparative_points(tiff_file, band_lst, vi_classed_band_dict2, points):
  cb2_results_lst = []
  combination_lst2, vi_name = bands_combinations2(tiff_file, band_lst,
vi_classed_band_dict2)
  for paired_bands in combination_lst2:
    band_a = paired_bands[0]
    band_b = paired_bands[1]
    band_c = paired_bands[2]
    vi_values, dataset = get_vi_cb2_image(tiff_file, vi_name, band_a, band_b, band_c)
    veg_index_values = get_vi_cb_at_points(vi_values, dataset, points)
    cb2_results_lst.append((vi_name, band_a, band_b, band_c, veg_index_values))
  return cb2_results_lst
#### Extract results of wavelength and vegetation index of CLASSED BANDS
cb_results_lst = get_cb_comparative_points(tiff_file, band_lst, vi_classed_band_dict,
points)
for i in cb_results_lst:
  print(i)
cb2_results_lst = get_cb2_comparative_points(tiff_file, band_lst, vi_classed_band_dict2,
points)
for i in cb2_results_lst:
  print(i)
### FOR RAW BANDS
#### Calculate vegetation index values for RAW BANDS
def get_rb_image(tiff_file, band_number):
  with rasterio.open(tiff_file) as dataset:
    band_values = dataset.read(band_number)
  return band_values, dataset

def get_rb_at_points(band_values, dataset, points):
  band_values_lst = []
  for _, row in points.iterrows():
    name, x, y = row['Parcela'], row['Coord_X'], row['Coord_Y']
    row_idx, col_idx = rasterio.transform.rowcol(dataset.transform, x, y)
    band_value = band_values[row_idx, col_idx]
```

```
        band_values_lst.append((name, band_value))
    return band_values_lst

def get_rb_comparative_points(tiff_file, band_lst, points):
    rb_results_lst = []

    for band_number in range(1,11):
        band_values, dataset = get_rb_image(tiff_file, band_number)
        band_values_lst = get_rb_at_points(band_values, dataset, points)
        rb_results_lst.append((band_lst[band_number-1][1], band_number,
band_lst[band_number-1][3], band_lst[band_number-1][4], band_values_lst))

    return rb_results_lst
```

Extract results of wavelength and vegetation index of RAW BANDS

```
rb_results_lst = get_rb_comparative_points(tiff_file, band_lst, points)
for i in rb_results_lst:
    print(i)
```

SAVE INDICES VALUES

Save vegetation indices values in an excel file (.xlsx)

```
def save_xlsx(input_file, results_lst):
    # Creamos un diccionario para almacenar los datos
    data_dict = {}

    for elm in results_lst:
        if results_lst == cb_results_lst:
            col_name = f"{elm[0]}_{elm[1]}_{elm[2]}"
            type_name = "classed_bands"
        elif results_lst == cb2_results_lst:
            col_name = f"{elm[0]}_{elm[1]}_{elm[2]}_{elm[3]}"
            type_name = "classed_bands"
        elif results_lst == cb3_results_lst:
            col_name = f"{elm[0]}_{elm[1]}_{elm[2]}_{elm[3]}_{elm[4]}"
            type_name = "classed_bands"
        elif results_lst == rb_results_lst:
            col_name = f"{elm[0]}_{elm[1]}_{elm[2]}-{elm[3]}nm"
            type_name = "raw_bands"
        data_dict[col_name] = [value for point, value in elm[len(elm)-1] ]

    # Convertimos el diccionario en un DataFrame
    df = pd.DataFrame(data_dict)

    # Copia el archivo original al nuevo archivo
    if type_name == "classed_bands":
        output_file = input_file[:-5] + "_mlt_" + type_name + "_" + results_lst[0][0] + ".xlsx"
    else:
        output_file = input_file[:-5] + "_mlt_" + type_name + ".xlsx"
    shutil.copyfile(input_file, output_file)
```

```
    # Abre el nuevo archivo
    wb = openpyxl.load_workbook(output_file)
    sheet = wb.active

    # Encuentra la última columna con datos en la hoja existente
    last_col = sheet.max_column

    # Escribe los datos del DataFrame en las columnas nuevas a partir de la última columna
existente
    for col_idx, col_name in enumerate(df.columns, start=last_col + 1):
        sheet.cell(row=1, column=col_idx, value=col_name)
        for row_idx, value in enumerate(df[col_name], start=2):
            sheet.cell(row=row_idx, column=col_idx, value=value)

    # Guarda el archivo con las nuevas columnas
    wb.save(output_file)
    return output_file
## Options to save file
# save_xlsx(excel_file, cb_results_lst)
save_xlsx(excel_file, cb2_results_lst)
# save_xlsx(excel_file, cb3_results_lst)
# save_xlsx(excel_file, fb_results_lst)
# save_xlsx(excel_file, vb_results_lst)
# save_xlsx(excel_file, rb_results_lst)
```

A5.3. R Script for computing Pearson correlation coefficients from the CBI-Vegetation Index dataset

Load libraries

```
# install.packages("readxl")
library(readxl)
library(dplyr)
library(writexl)
library(ggplot2)
```

Load Data

```
# Leer los datos desde el archivo Excel
wd <- "C:/Users/User/OneDrive - UVa/1_ASIGNATURAS/TFM/1_DataProcessing/"

# Desactivar código: Ctrl + Shift + C
# data_file <- paste0(wd, "CulebraPointsCBIvgbj_mlt_classed_bands_TBDVI.xlsx")
data_file <- paste0(wd, "CulebraPointsCBI_hyp_variable_bands.xlsx")
# data_file <- paste0(wd, "CulebraPointsCBIvgbj_hyp_fixed_bands.xlsx")
# data_file <- paste0(wd, "CulebraPointsCBIpnvb_mlt_raw_bands.xlsx")
# data_file <- paste0(wd, "CulebraPointsCBI_hyp_classed_bands_TBDVI_p2_ok.xlsx")

sheet <- "Hoja1"  # Nombre de la hoja de cálculo

data <- read_excel(data_file, sheet = sheet)
```

Check data

```
# Function to convert data types
convert_columns <- function(data, factor_cols) {
  data[factor_cols] <- lapply(data[factor_cols], as.factor)
  return(data)
}

# Columns to convert to numeric and to factor
factor_cols <- c('Parcela','Ecosistema','Estado_de')

# Apply the conversion function
sig_data <- convert_columns(data, factor_cols)
# Ensure that phenotype_data is a data.frame
sig_data <- as.data.frame(sig_data)
# Check the structure of the modified data
# head(sig_data)
# str(sig_data)
```

Subset

```
#### FOR CBI_vegeta #####
# # Subset the data to select variables starting from column 8
# sig_data <- sig_data %>%
#   select(1:5, 7, 8, 6, everything())
#
# sig_data_vars <- sig_data[, 8:ncol(sig_data)]
# str(sig_data_vars)
```

```
#### FOR CBI_Suelo #####
# Subset the data to select variables starting from column 8
sig_data <- sig_data %>%
  select(1:5, 6, 8, 7, everything())

sig_data_vars <- sig_data[, 8:ncol(sig_data)]

#### FOR CBI_prom #####
# sig_data_vars <- sig_data[, 8:ncol(sig_data)]
```

Pearson correlation

```
### VEGETACIÓN ###
# # Calculate Pearson correlations based on normality -- "CBI_Suelo", "CBI_vegeta", "
CBI_Promed"
# pearson_corr <- sapply(sig_data_vars[-which(names(sig_data_vars) == "CBI_vegeta
")],
#                        function(x) cor(x, sig_data_vars$CBI_vegeta, method = "pearson"))
#
# # Create a dataframe for correlation results
# pearson_corr_df <- data.frame(Variable = names(pearson_corr), Correlation = pears
on_corr)
#
# # Sort the results by correlation
# result_corr_df <- pearson_corr_df %>% arrange(desc(Correlation))
# output_name <- "pearson_corr_veg.xlsx"
# # View the correlation results
# print(result_corr_df)

### SUELO ###
# Calculate Pearson correlations based on normality -- "CBI_Suelo", "CBI_vegeta", "C
BI_Promed"
pearson_corr <- sapply(sig_data_vars[-which(names(sig_data_vars) == "CBI_Suelo")
],
                       function(x) cor(x, sig_data_vars$CBI_Suelo, method = "pearson"))

# Create a dataframe for correlation results
pearson_corr_df <- data.frame(Variable = names(pearson_corr), Correlation = pearso
n_corr)

# Sort the results by correlation
result_corr_df <- pearson_corr_df %>% arrange(desc(Correlation))
output_name <- "pearson_corr_suelo.xlsx"
# View the correlation results
print(result_corr_df)

### PROMEDIO ###
# # Calculate Pearson correlations based on normality -- "CBI_Suelo", "CBI_vegeta", "
CBI_Promed"
# pearson_corr <- sapply(sig_data_vars[-which(names(sig_data_vars) == "CBI_Prome
d")],
#                        function(x) cor(x, sig_data_vars$CBI_Promed, method = "pearson"))
#
# # Create a dataframe for correlation results
```

```
# pearson_corr_df <- data.frame(Variable = names(pearson_corr), Correlation = pears
on_corr)
#
# # Sort the results by correlation
# result_corr_df <- pearson_corr_df %>% arrange(desc(Correlation))
# output_name <- "pearson_corr_prom.xlsx"
# # View the correlation results
# print(result_corr_df)
```

Create an output file

```
# Write the results to an Excel file
data_file_subst <- substr(data_file, 1, nchar(data_file) - 5)
output_file <- paste(data_file_subst, output_name, sep = "_")
write_xlsx(result_corr_df, output_file)
```

Graph scatterplot

```
# Specify the indices for the two variables you want to plot
# x_index <- 1  # column for the x-axis
# y_index <- 101  # column for the y-axis

# Create the scatterplot using ggplot2
# ggplot(sig_data_vars, aes(x = sig_data_vars[[x_index]],
#                          y = sig_data_vars[[y_index]])) +
#   geom_point() +
#   labs(x = colnames(sig_data_vars)[x_index],
#        y = colnames(sig_data_vars)[y_index],
#        title = paste("Scatterplot of",
#                      colnames(sig_data_vars)[x_index],
#                      "vs",
#                      colnames(sig_data_vars)[y_index])) +
#   theme_minimal()
```